THE NEOTECTONICS, UPLIFT, AND ACCOMMODATION OF DEFORMATION OF THE TALKEETNA MOUNTAINS, SOUTH-CENTRAL ALASKA

By

Demi C. Mixon

RECOMMENDED:

Dr. James Beget

Dr. Elisabeth Nadin

Dr. Catherine Hanks
Advisory Committee Chair

Dr. Paul McCarthy
Chair, Department of Geosciences

APPROVED:

Dr. Paul Layer
Dean, College of Natural Science and Mathematics

Dr. John Eichelberger
Dean of the Graduate School

24 June 2016
Date

THE NEOTECTONICS, UPLIFT, AND ACCOMMODATION OF DEFORMATION OF THE TALKEETNA MOUNTAINS, SOUTH-CENTRAL ALASKA

A

THESIS

Presented to the Faculty

of the University of Alaska Fairbanks

in Partial Fulfillment of the Requirements

for the Degree of

MASTER OF SCIENCE

By

Demi C. Mixon, B.S.

Fairbanks, Alaska

August 2016

Abstract

South-central Alaska is home to many tectonic structures and mountain ranges that have experienced active uplift and deformation within the past 5 to 10 Ma. The Talkeetna Mountains are located above the area of flat-slab subduction of the Yakutat microplate. I hypothesize that the Talkeetna Mountains have been uplifted as a result of this underlying flat-slab subduction and that areas of the Talkeetna Mountains are neotectonically active.

The Talkeetna Mountains are deforming heterogeneously across four different structural domains defined by differences in geomorphic patterns, seismicity, dominant fault types, and the orientation of horizontal maximum stress (SHmax). A strain partitioning structure divides the northern and southern domains, and is observed by a change in SHmax orientation from E-W in southern domains to NW-SE in the northern domain. The strain partition is accommodated by a crustal break along the Talkeetna thrust fault, which is expressed at the surface as a wide zone of deformation.

Apatite fission-track analysis suggests two distinct periods of uplift: one dated from 45 to 30 Ma and another from approximately 10 Ma to present, with uplift rates of 0.14 mm/yr and 0.24 mm/yr, respectively. The first phase of uplift coincides with a time of significant plate reorganization in the north Pacific which resulted in translation of terranes northwestward. The second phase of uplift correlates with Neogene accretion of the Yakutat microplate. I propose that the majority of Neogene deformation and uplift in the Talkeetna Mountains is due to far-field deformation in the upper plate above the subducting slab. Variations in both composition of the crust and depth to the downgoing slab resulted in strain partitioning and northwest-directed

compression in the northern Talkeetna Mountains and northwest compression and warping in the southern Talkeetna Mountains.

Dedication and Acknowledgements

I would first like to recognize my original advisor, Dr. Wesley Wallce, for his encouragement and constructive advice for my research and in my studies. This thesis project is dedicated to him as I would not have been exposed to the field of neotectonics had it not been for his introduction, teaching, and guidance.

I would like to thank Dr. Catherine Hanks for becoming my advisor this past year, and for supporting and encouraging me to produce my best work in my thesis studies as well as in my professional career. Also, I would like to thank my other committee members, Dr. Elisabeth Nadin and Dr. Jim Beget for their guidance and expertise in subject areas that were new to me.

I am grateful to my two field assistants, Carlisle Doria and James Shinas, who helped me haul multiple pounds of rock samples across the tundra of the Talkeenta Mountains, and who provided me with company, assurance, and many good laughs during my time in the field. Thank you for making sure I made it across those trecherous talus slopes alive.

I would like to express my appreciation to the Alaska Space Grant Program fellowship which provided me with plentiful resources for conducting field work and thermochronology analysis. Additionaly, I extend my thanks to other funding agencies that financially supported my thesis work which included the Geological Society of America Graduate Student Research Grant Program. I would like to thank Paul O'Sullivan with GeoSeps for valuable help on apatite thermochronology. Finally, I would like to express gratitude for the continual support from my family, friends, and colleagues at the University of Alaska Fairbanks.

Table of Contents

Page

Signature Page i
Title Page iii
Abstract v
Dedication and Acknowledgements vii
Table of Contents ix
List of Figures xiii
List of Tables xv
List of Appendices xv
CHAPTER 1: INTRODUCTION xv
1.1 Overview 1
1.2 Hypothesis 2
1.3 Significance 2
CHAPTER 2: REGIONAL TECTONICS AND GEOLOGIC SETTING 5
2.1 Tectonic Framework of South-central Alaska 5
2.1.1 Flat-slab Subduction of the Yakutat Microplate 8
2.2 Geologic Setting of the Talkeetna Mountains 12
2.2.1 Wrangellia and Peninsular Terranes 13
2.2.2 The Kahiltna Basin 14
2.2.3 The Kahiltna Basin and Wrangellia Terrane Boundary 15
2.3 Bounding Faults 17
2.3.1 Denali Fault 17
2.3.2 Castle Mountain Fault 17
2.4 Bounding Sedimentary Basins 18
2.4.1 The Susitna River Basin 18
2.4.2 The Copper River Basin 19
2.4.3 The Matanuska Valley-Talkeetna Mountains Basin 19
CHAPTER 3: METHODOLOGY AND DATA 21
3.1 Methods 21
3.1.1 Geomorphic Reconnaissance 21
3.1.1.1 Topographic Analysis 21

3.1.1.2 Drainage Patterns 22
3.1.2 Geomorphic Indices 25
3.1.2.1 Hypsometric Integral (HI) 25
3.1.2.2 Drainage Basin Asymmetry Factor (AF) 27
3.1.2.3 Valley Floor Width-to-Height Ratio (Vf) 29
3.1.2.4 Longitudinal Stream Profiles and Stream-Length (SL) Gradient Index 31
3.1.2.5 Index of Relative Active Tectonics (IRAT) Map 32
3.1.3 Apatite Fission-Track Thermochronology (AFT) 33
3.1.3.1 AFT Sampling Strategy 34
3.1.3.2 HeFTy Modeling 34
3.1.4 Glacial Isostasy 36
3.2 Data 39
3.2.1 Digital Elevation Models (DEMs) 39
3.2.2 Earthquake Hypocenters 39
3.2.3 ArcGIS Geological Maps 42
3.2.4 ArcGIS National Hydrology Dataset (NHD) 42
3.2.5 ArcGIS Late Wisconsin Glacial Extent Map 42
3.2.6 Apatite Fission-Track Thermochronology (AFT) 43
CHAPTER 4: RESULTS 45
4.1 Geomorphic Reconnaissance 45
4.1.1 Topographic Analysis 45
4.1.2 Drainage Patterns 46
4.2 Geomorphic Indices 47
4.2.1 Hypsometric Integral (HI) 48
4.2.2 Drainage Basin Asymmetry Factor (AF) 50
4.2.3 Valley Floor Width-to-Height Ratio (Vf) 52
4.2.4 Index of Relative Active Tectonics (IRAT) Map 54
4.2.5 Stream-Length Gradient Index (SL) 54
4.2.6 Susitna River Longitudinal Stream Profile 57
4.3 Apatite Fission-Track Thermochronology (AFT) 60
4.3.1 AFT Age Results 60
4.3.2 HeFTy Modeling Results 61
4.3.3 Distribution of Other Published Thermochronology Data 64
4.4 Glacial Isostasy 65

4.5 Structural Analysis 65
CHAPTER 5: ANALYSIS AND DISCUSSION 69
5.1 Structural Domains of the Talkeetna Mountains 69
5.1.1 Domain 1 69
5.1.2 Domain 2 72
5.1.3 Domain 3 73
5.1.4 Domain 4 74
5.2 Heterogeneous Deformation 74
5.2.1 Change in Scale of Deformation 75
5.2.2 Change in SHmax Orientation 77
5.3 Timing and Causes of Uplift and Deformation 78
5.3.1 Effect of Glacial Isostasy 78
5.3.2 Tectonic Causes of Uplift and Deformation 79
5.3.2.1 First Period of Rapid Uplift (45 to 30 Ma) 79
5.3.2.2 Second Period of Rapid Uplift (10 Ma to Present) 80
5.4 The Susitna River: Geomorphic Evidence for Neotectonic Activity 83
5.5 Sources of Uncertainty in this Analysis 84
CHAPTER 6: CONCLUSION 87
REFERENCES 89

List of Figures

Page

Figure 1. Tectonics of Southern Alaska 3
Figure 2. Digital Elevation Model of south-central Alaska 4
Figure 3. Geologic map of south-central Alaska 7
Figure 4 Vp tomographic cross sections through south-central Alaska 10
Figure 5. Color-scaled DEM of the Talkeetna Mountains 23
Figure 6. Drainage networks in the Talkeetna Mountains 24
Figure 7. Calculation of the hypsometric curve (HC) 26
Figure 8. Calculation of basin asymmetry factor (AF) 28
Figure 9. Calculation of the valley floor width-to-height (Vf) ratio 30
Figure 10. Calculation of stream length gradient index (SL) 32
Figure 11. Locations of thermochronology sample and cooling ages in the Talkeetna Mountains 35
Figure 12. Glacial extent in the Talkeetna Mountains during Late Wisconsin time 38
Figure 13. Earthquakes > *M1.5* in the Talkeenta Mountains from 1994 – 2014 40
Figure 14. Earthquake focal mechanisms in the Talkeetna Mountains 41
Figure 15. Valley profiles A-E of the Susitna River 47
Figure 16. Hypsometric Integral (HI) map 48
Figure 17. Basin asymmetry (AF) map 50
Figure 18. Valley floor width-to-height (Vf) ratio map 52
Figure 19. Index of relative active tectonics (IRAT) map 54
Figure 20. Stream length gradient index map 55
Figure 21. Longitudinal stream profile and SL for the Susitna River 57
Figure 22a. HeFTy model and track length distribution sample DCM01 (032-01) 61
Figure 22b. HeFTy model and track length distribution sample DCM02 (032-02) 61
Figure 22c. HeFTy model and track length distribution sample DCM03 (032-03) 62
Figure 22d. HeFTy model and track length distribution sample DCM05 (032-04) 62
Figure 22e. HeFTy model and track length distribution sample DCM06 (032-05) 63
Figure 23. Theoretical glacial profile and the reconstructed ice sheet thickness 65
Figure 24. Structural domains of the Talkeetna Mountains 68

List of Tables

Page

Table 1 11
Table 2 59
Table 3 74

List of Appendices

Page

Appendix A 94
Appendix B 95

CHAPTER 1: INTRODUCTION

1.1 Overview

South-central Alaska is home to many tectonic structures and mountain ranges that have experienced active uplift and deformation within the past 5 to 10 Ma (Armstrong et al., 2007; Benowitz et al., 2007; Chapman et al., 2008; Eberhart-Phillips et al., 2006; Fitzgerald et al., 1995; Haeussler, 2008; O'Sullivan and Currie, 1996; Plafker et al., 1992; Ridgway and Flesch, 2007). Major structures in south-central Alaska include the right-lateral Denali and Castle Mountain faults, the arcuate Alaska Range (including the Tordrillo Mountains, Denali, and the Hayes Range), the southern Chugach Mountains, and the St. Elias Mountains (Figure 1). Each of these features has been extensively studied with some inferred to be currently active, while others have had evidence of uplift and or deformation since 23 Ma.

Major contributing factors to deformation and uplift in south-central Alaska are the flat-slab subduction of the Yakutat microplate beneath southern Alaska and the associated movement along transpressional fault systems like the Denali and Castle Mountain faults (Chapman et al., 2008; Eberhart-Phillips et al., 2006; Finzel et al., 2011; Freymueller et al., 2008; Haeussler et al., 2008). Haeussler (2008) suggested that the subducting Yakutat microplate has been a driving mechanism for far-field deformation throughout Alaska since 25 Ma based on regional evidence.

In comparison to surrounding structures in south-central Alaska, very little is known about the uplift and deformation of the Talkeetna Mountains, which are located just south of the central Alaska Range and are bounded by the Denali and Castle Mountain faults (Figure 1). The objective of this thesis is to determine whether the Talkeetna Mountains are undergoing active uplift and deformation, and if so, to document the age of uplift and identify local areas that are

potentially accommodating active uplift. This information places the Talkeetna Mountains into the regional tectonic and neotectonic framework of south-central Alaska.

1.2 Hypothesis

Flat-slab subduction of the Yakutat microplate extends north through south-central Alaska directly beneath the Talkeetna Mountains (Figure 1). I hypothesize that the Talkeetna Mountains have been uplifted primarily as a result of buoyancy and/or flexure associated with flat-slab subduction of the Yakutat microplate, and that the Talkeetna Mountains are actively deforming due to continued activity on these structures.

1.3 Significance

Project results will contribute to the understanding of the consequences of flat-slab subduction on the overriding plate, both in Alaska and other areas with similar tectonic settings, such as the southwest Japan, Cascadia, and Andean margins (Gutscher and Peacock, 2009).

In addition, although the Talkeetna Mountains are seismically active, there has been little research on the neotectonic activity in the area or the potential seismic hazard to nearby communities and infrastructure or proposed infrastructure. For example, a proposed hydroelectric dam site is located near previously mapped faults within the Talkeetna Mountains along the Susitna River (Figure 2). This project will identify areas of possible neotectonic activity so that future work can establish whether there is a significant seismic hazard to nearby communities and hydroelectric projects.

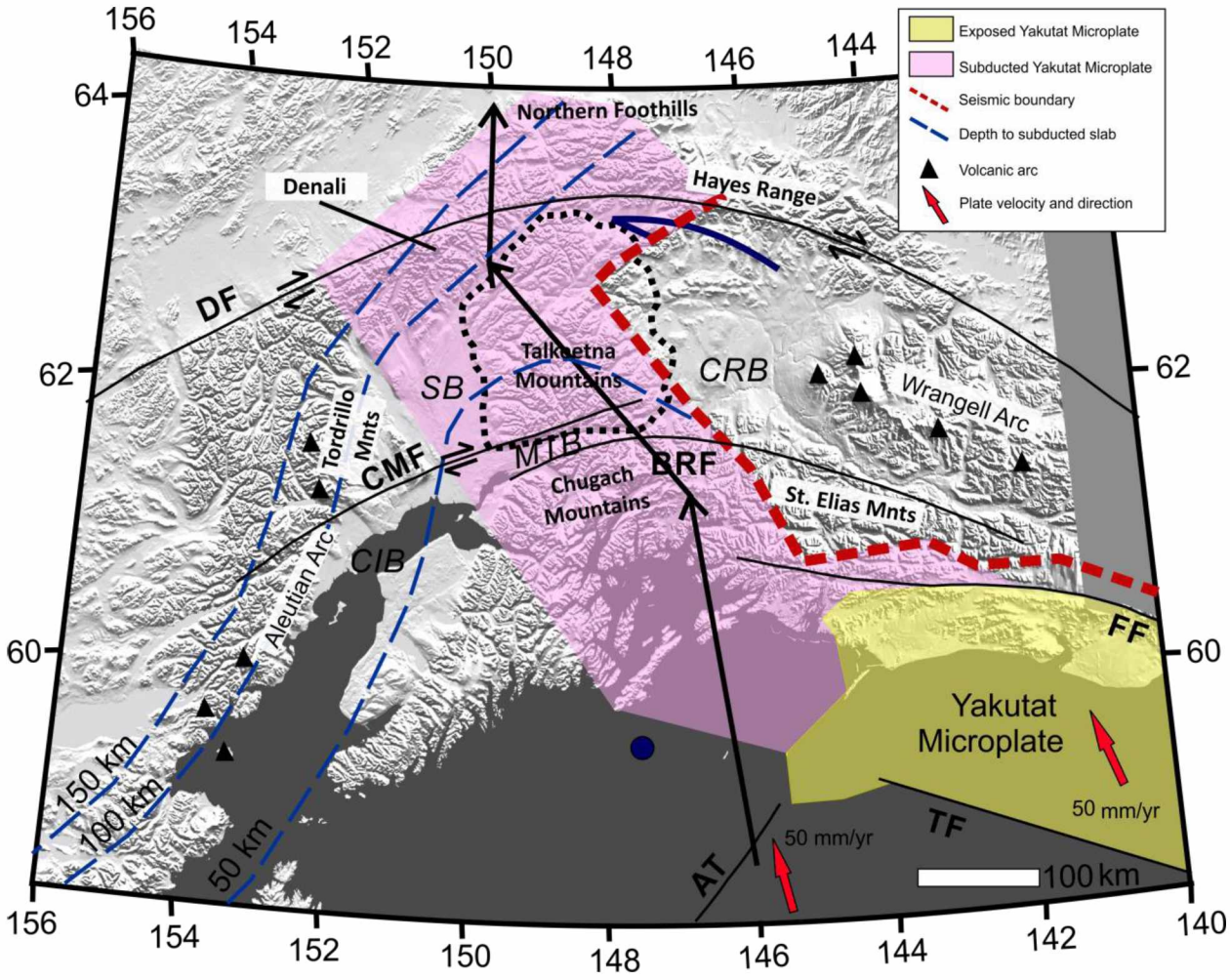

Figure 1. Tectonics of Southern Alaska. Talkeetna Mountains are outlined by bold dashed black line. Surrounding basins are labeled as *CIB,* Cook Inlet Basin; *SB*, Susitna River Basin; *CRB*, Copper River Basin; and *MTB*, Matanuska Valley – Talkeetna Mountains Basin. Faults: *DF*, Denali Fault; *CMF*, Castle Mountain fault; *BRF*, Border Ranges Fault; *FF*, Fairweather Fault; *TF*, Transition Fault; *AT*, Aleutian Megathrust. Counterclockwise rotation of the Southern Alaska Block beneath the Denali Fault is represented by the arcuate dark blue arrow; the pole of rotation is represented by the large dark blue dot in the south of Prince William Sound. Long black arrows from south to north are from Eberhart-Phillips et al. (2006) and represent an interpreted path of the subducting Yakutat slab. The suggested time at which the slab was beneath the area of the Talkeetna Mountains is around 9.4 Ma (Eberhart-Phillips et al., 2006). Modified from Eberhart-Phillips et al., 2006; Fuis et al., 2008; Haeussler, 2008.

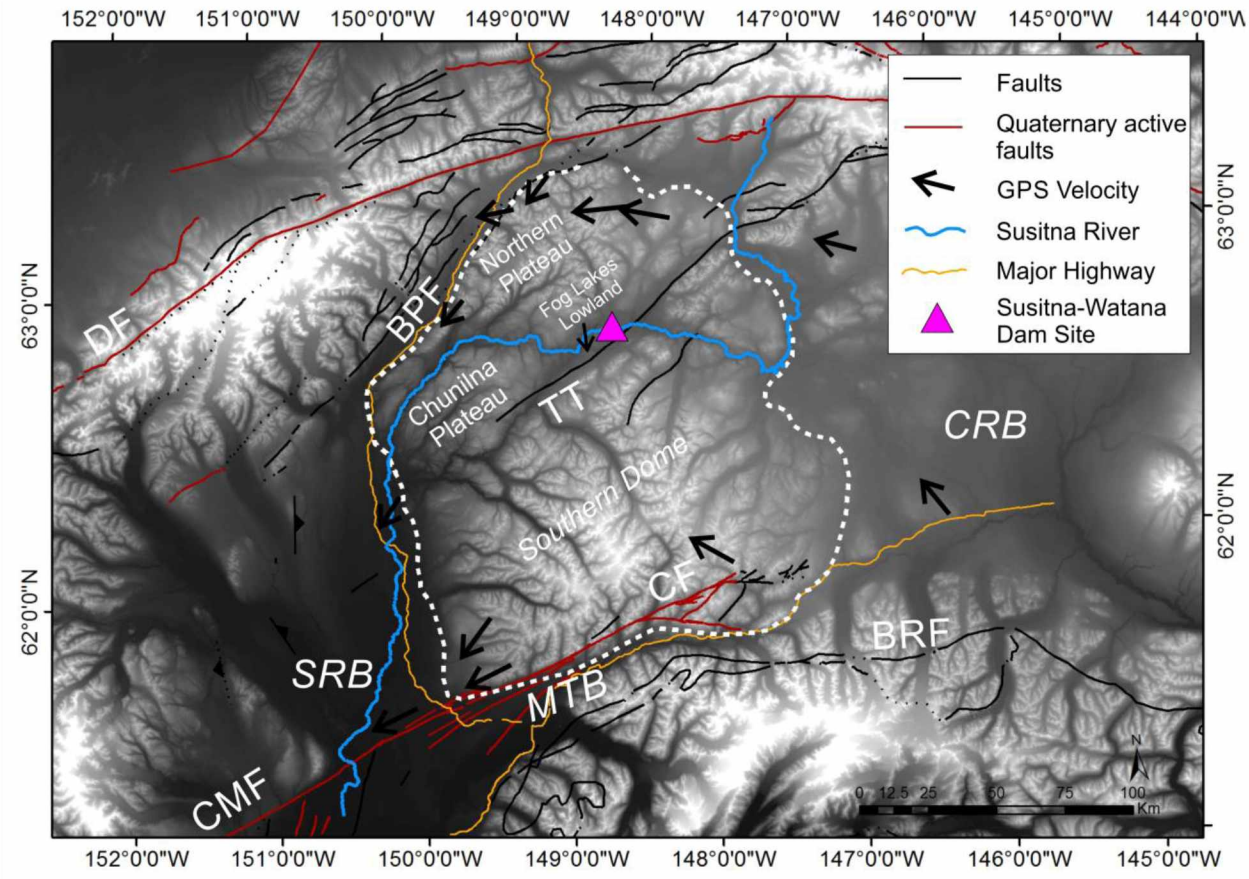

Figure 2. Digital Elevation Model of south-central Alaska showing major features surrounding the Talkeetna Mountains, GPS velocities, and the location of the proposed Susitna-Watana Dame site. The Talkeetna Mountains are outlined by the white dashed line. Surrounding basins are: *CIB,* Cook Inlet Basin; *SRB*, Susitna River Basin; *CRB*, Copper River Basin; and *MTB*, Matanuska Valley – Talkeetna Mountains Basin. Faults: *DF,* Denali Fault (right-lateral); *CMF*, Castle Mountain fault (oblique right-lateral with north side up); *CF,* Caribou Fault; *BRF*, Border Ranges Fault (right-lateral); *TT*, Talkeetna Thrust Fault. Red faults represent those with Quaternary activity after Khoeler et al., 2012. Major topographic features in the Talkeetna Mountains that are discussed in text are labeled in black.

CHAPTER 2: REGIONAL TECTONICS AND GEOLOGIC SETTING

2.1 Tectonic Framework of South-central Alaska

South-central Alaska is a part of a dynamic, actively deforming continental margin. It is characterized by an active subduction zone to the south, the active Aleutian and Wrangell volcanic arcs, extensive right-lateral strike-slip fault systems (the Denali, Castle Mountain, and Border Ranges faults), and allochthonous terranes that accreted during the Mesozoic-Cenozoic time (Wrangellia and Peninsular terranes; Plafker and Berg, 1994; Figure 1).

The physiography of south-central Alaska is unique, in that most structures follow an arcuate trend; this is seen in the Alaska Range, Chugach-St. Elias Mountains, and the Denali, Castle Mountain, and Border Ranges fault systems (Figure 1). The hinge of this arcuate trend is referred to as the oroclinal hinge. The eastern boundary of the Talkeetna Mountains boarders the western edge of the oroclinal hinge (Glen, 2004; Haeussler, 2008). Additionally, the Southern Alaska Block (SOAK), or block south of the Denali fault, is rotating counterclockwise contributing to tectonic escape of terranes to the west along dextral fault systems and is driven by the northwest collision of the Yakutat microplate (Freymueller et al., 2008; Haeussler, 2008: Figure 1).

Modern interpretations of the tectonic development of south-central Alaska use the terrane accretion model where allochthonous terranes, or crustal blocks, have been transported northward with subducting oceanic crust (Coney et al., 1980). Terranes that are too buoyant or thick to subduct accrete to the North American margin, resulting in fault-bounded terranes that have no geologic affinity to their adjacent surroundings (Coney et al., 1980; Plafker and Berg, 1994). South-central Alaska is mostly composed of three composite allocthonous terranes (from

north to south): the Yukon composite terrane, the Wrangellia composite terrane, and the Southern margin composite terrane (Trop and Ridgway, 2007; Figure 3).

The Yukon composite terrane is north of the Denali fault and is composed of the Yukon-Tanana and Stikine terranes, which are highly metamorphosed and deformed (Nokleberg et al., 1994; Figure 3). These terranes were probably accreted to the margin by the Middle Jurassic time and represent a complex geologic and tectonic history as a collapsed passive continental margin that has experienced extensive thrusting and structural imbrication (Monger and Nokleberg, 1996; Trop and Ridgway, 2007).

The Wrangellia composite terrane is south of the Yukon composite terrane. The Wrangellia composite terrane is composed of the Wrangellia, Peninsular, and Alexander terranes and is one of the largest composite terranes of the North American Cordillera, extending from western Alaska to southern British Columbia (Plafker and Berg, 1994). The Wrangellia and Yukon composite terranes are separated by the intervening Denali fault, arcuate Alaska Range, and the Kahiltna basin, a complexly deformed Jurassic-Cretaceous collisional basin (Trop and Ridgway, 2007; Figure 3). The Wrangellia composite terrane was accreted and transported northwest along the right-lateral strike-slip Denali fault and is thought to have reached its present location in Middle to Late Eocene time (Nokleberg et al., 1994; Trop et al., 2003).

South of the Wrangellia composite terrane lies the Southern margin composite terrane, which is composed of the Chugach and Prince William terranes (Plafker and Berg, 1994; Trop and Ridgway, 2007; Figure 3). It is separated from the Wrangellia composite terrane by the Border Ranges fault. The Border Ranges fault is a major high angle fault with a complex history. It was interpreted as a major crustal boundary that accommodated northward underthrusting of the oceanic crust beneath the Wrangellia composite terrane during Early Jurassic to Late Cretaceous

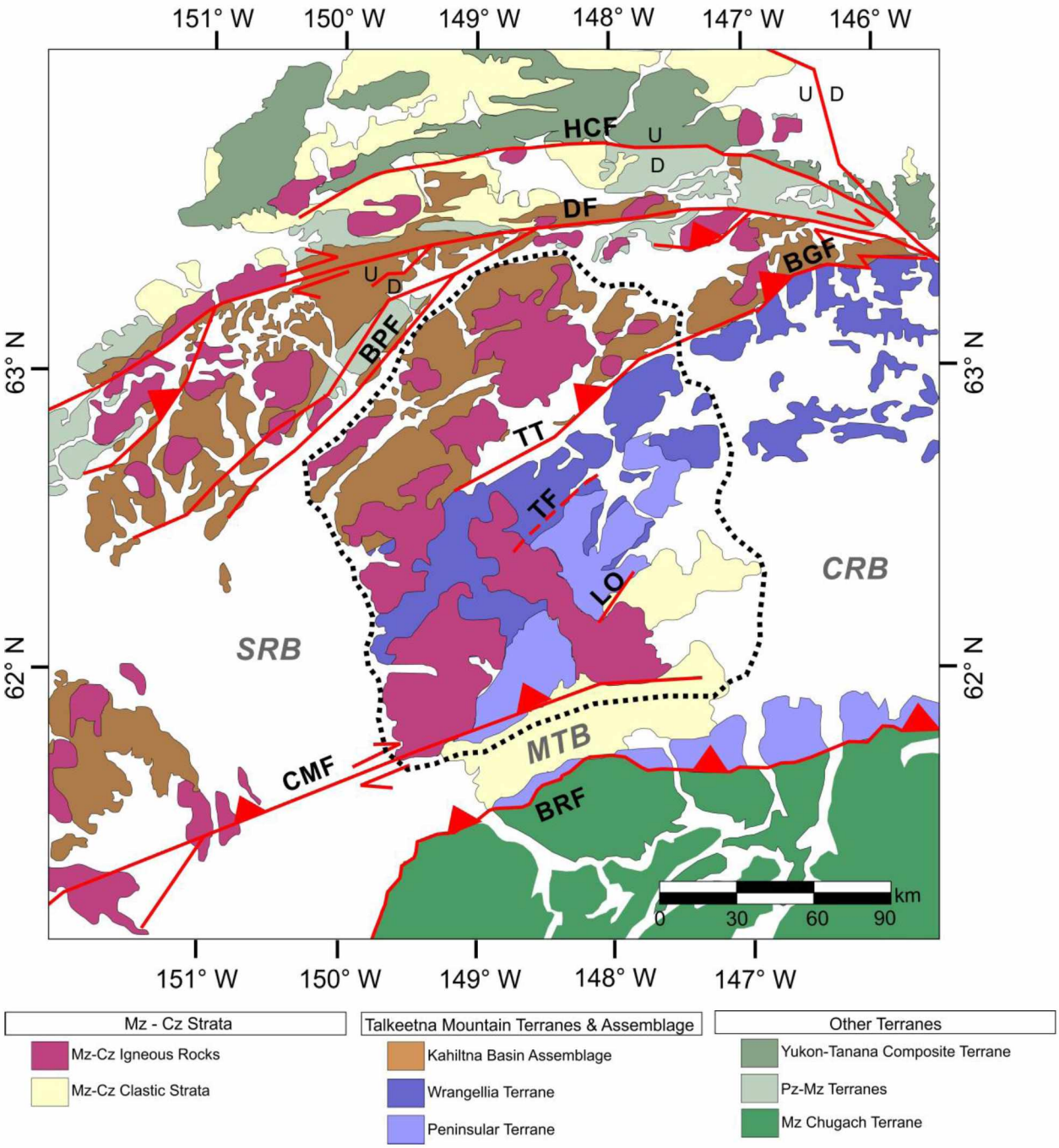

Figure 3. Geologic map of south-central Alaska showing major lithostratigraphic terranes, faults and basins. The Talkeetna Mountains are outlined by the black dashed line. Surrounding basins are *CIB,* Cook Inlet Basin; *SRB*, Susitna River Basin; *CRB*, Copper River Basin; and *MTB*, Matanuska Valley – Talkeetna Mountains Basin. Faults: HCF, Hines Creek Fault; BGF, Broxson Gulch Fault; DF, Denali Fault; BRF, Broad Pass Fault; CMF, Castle Mountain fault; BRF, Border Ranges Fault; TT, Talkeetna Thrust Fault; TF, Tsisi Creek Fault; LO, Little Oshetna Fault. Map modified from Hampton et al., 2010.

time (Trop and Ridgway, 2007). The Chugach and Prince William terranes are composed of rocks of subduction complex affinities (Plafker and Berg, 1994).

Faulted against the southern margin of the Prince William and Chugach terranes is the Yakutat terrane, also known as the Yakutat microplate (Figure 1). The Yakutat microplate is a present-day example of terrane accretion and is responsible for uplift and deformation in southern Alaska from Neogene to present day (Chapman et al., 2008; Haeussler et al., 2008; Plafker and Berg, 1994). The accretion of the relatively thick and buoyant Yakutat block is also acting as a driver for counterclockwise rotation of the crust south of the Denali fault and the tectonic 'escape' of crust to the west along dextral fault systems like the Denali and Castle Mountain faults (Freymueller et al., 2008; Haeussler et al., 2008). Since the Yakutat microplate is the major deformational driver in southern Alaska it will be explained in further detail.

2.1.1 Flat-slab Subduction of the Yakutat Microplate

The Yakutat microplate is an allochthonous oceanic plateau that is thick and buoyant. It is obliquely colliding with southern Alaska (Haeussler et al., 2008) and is moving northward at a rate of 50mm/yr (Elliott, 2011; Figure 1). The exact time of collision and initial subduction of the Yakutat microplate is not well defined, but its collision is thought to have initiated flat-slab subduction of the Pacific Plate under central Alaska. Previous studies and tectonic models have suggested that flat-slab subduction at the leading edge of the Yakutat block began around 25 Ma (Plafker and Berg, 1994). This age was based on the oldest lavas in the Wrangell volcanic field, which are interpreted as recording the initiation of arc magmatism above the Yakutat subduction zone around this time (Richter et al., 1990). During mid-Miocene time (~15 to 10 Ma), the thicker, more “continentalized" crust of the Yakutat began colliding with the continental margin.

The timing was inferred from the onset of glaciation, deposition of the Yakutaga formation, and the beginning of orogenesis in mid-late Miocene (Chapman et al., 2008; Plafker and Berg, 1994; Ridgway et al., 1996).

The Yakutat microplate is composed of two basement types that are divided by a high-angle structural boundary separating the exposed southeastern portion from the western subducted portion of the microplate (Chapman et al., 2008; Plafker et al., 1994). The exposed Yakutat microplate in southeastern Alaska has a thickness of 20 to 25 km, has a "continentalized" basement of metamorphosed flysch and accretionary mélange of a Late Mesozoic subduction complex, and is partially accreted to North America where it is colliding along the junction of the Queen Charlotte-Fairweather fault system and the Aleutian megathrust subduction zone (Bruhn et al., 2004; Chapman et al., 2008; Eberhart-Phillips et al., 2006; Plafker, 1987). Based on tomographic and seismic reflection and refraction studies, the western subducted portion of the Yakutat microplate is 11 to 22 km thick and the basement is inferred to be a Paleogene oceanic crust, possibly an oceanic plateau, that is descending at a, nearly horizontal angle (Eberhart-Phillips et al., 2006; Plafker, 1987; Wells and Coppersmith, 1994). Cross-sections through south-central Alaska based on P-wave velocity (Vp) tomographic studies show the nearly horizontal angle of flat-slab subduction of the Yakutat microplate, and the transition from west to east from normal to flat-slab subduction (Eberhart-Phillips et al., 2006; Figure 4).

The extent of the subducted Yakutat microplate is outlined in Figure 1 and has been determined by the width of the seismogenic zone, tomography, seismogram analysis, and 3-D hypocenter analysis (Eberhart-Phillips et al., 2006; Ferris et al., 2003; Fuis et al., 2008). The boundaries of the subducted slab correspond to the area of uplift of the Talkeetna Mountains, a lack of subduction-related arc magmatism in the Aleutian and Wrangell arcs, and a seismic boundary to

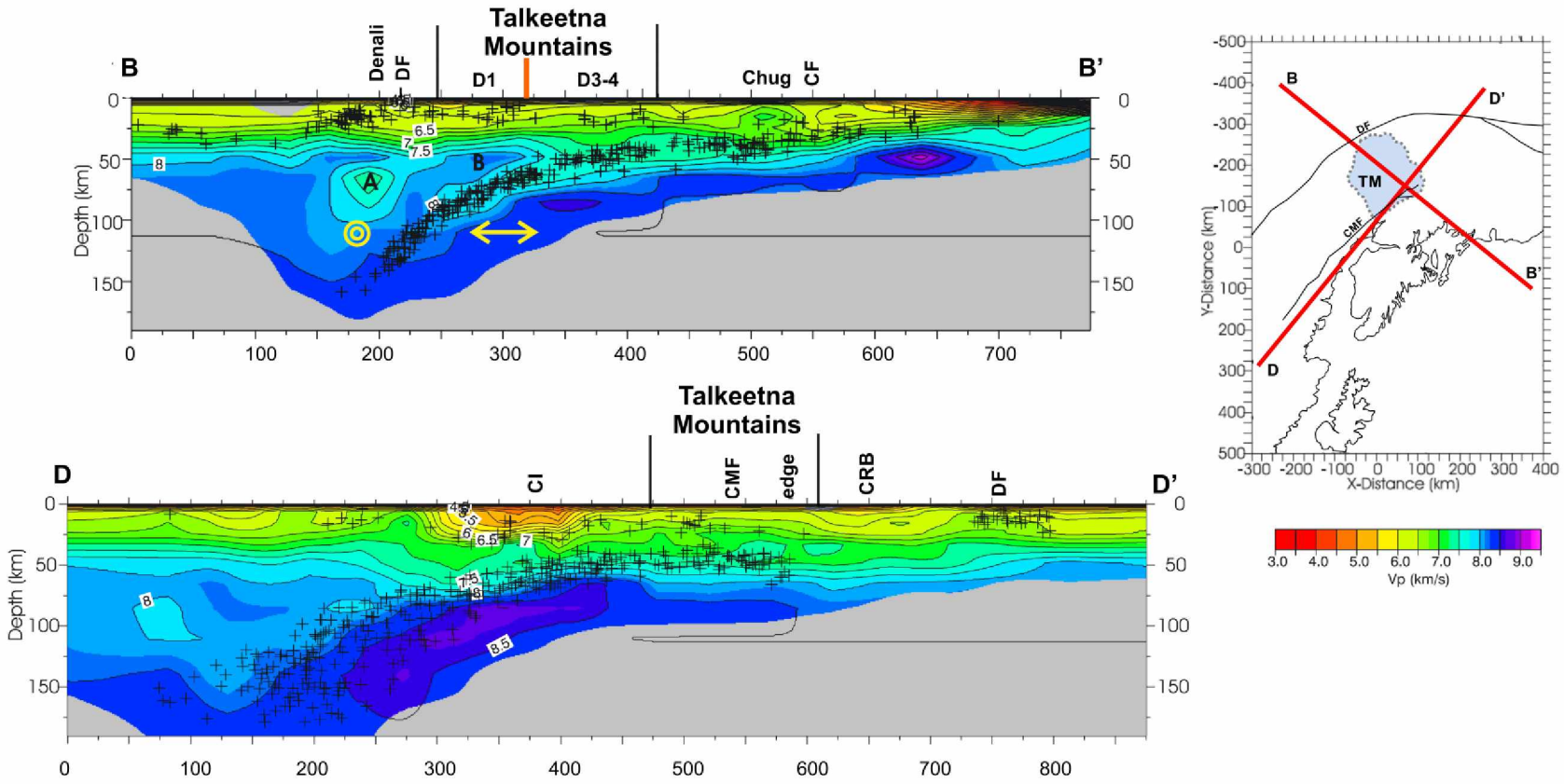

Figure 4. Vp tomographic cross sections through south-central Alaska from Figures 9 and 10 of Eberhart-Phillips et al. (2006). In cross sections, + symbols indicate earthquakes within 50 km of the cross section line. B-B' runs NW-SE through south-central Alaska and the Talkeetna Mountains (TM), highlighted in blue on the regional map to the right. The dip of the subducting Yakutat microplate is relatively shallow as far inboard as the southern Talkeetna Mountains. The boundary of the Talkeetna Mountains is shown by the vertical lines on both cross sections. The vertical orange line on section B-B' represents the position of the crustal break suggested by Glen et al. 2007a&b that coincides with the boundary between Domain 1 (D1) to the north, and Domains 3 and 4 (D 3-4) to the south (this study). D-D' runs SW-NE, parallel to the megathrust, the dip of the subduction zone is flatter to the east due to the nature of the Yakutat microplate. Crust of the overlying plate are within low velocities <7 km/s. DF, Denali fault; Chug, Chugach Mountains; CF, Contact fault; CI, Cook Inlet; CMF, Castle Mountain fault; edge, edge of Yakutat slab; CRB, Copper River Basin.

the east defined by the abrupt lack of seismicity (Figure 1). Eberhart-Phillips et al.'s (2006) geophysical examination of the subducting slab suggests a northward path for the subducting slab during the past 20 Ma based on cumulative plate motions (Figure 1 and 4). The interpreted path of the subducting buoyant Yakutat microplate places the flat-slab beneath the northern Talkeetna Mountains study area between approximately 15 and 9 Ma.

Recent work has at least partly attributed deformation, exhumation, and uplift around southern Alaska to the collision and flat-slab subduction of the Yakutat microplate. Haeussler (2008) identified far-field deformation seen in the Chugach – St. Elias Mountains, the Tordrillo Mountains, the Alaska Range, and the northern foothills fold-and-thrust belt as a consequence of the subduction and collision of the Yakutat microplate based on the timing of uplift and deformation observed in these areas (Figure 1; Table 1).

Table 1. Uplift ages of mountain ranges around south-central Alaska. Mountain ranges can be found in Figure 1. The Talkeetna Mountains are located at the center of these mountain ranges.

Mountain Ranges		Uplift Ages (Ma)	Data Type	Source
Alaska Range	Tordrillo Mountains	6 - 23	AFT, AHe	Haeussler and O'Sullivan, 2006 Haeussler et al., 2008
	Denali Mountain	5 - 6	AFT	Fitzgerald, 1995 Haeussler, 2008
	Hayes Range	2.8 - 5.1, 15.5 *Rapid exhumation @ 1.4	(U-Th)/He, AFT	Armstrong et al., 2007 Benowitz et al., 2007
Chugach-St. Elias Mountains		40 -3 *Rapid exhumation @ 40, 15, 4	AFT	O'Sullivan and Currie, 1996

The collision of the Yakutat microplate is also responsible for the counterclockwise rotation of the SOAK south of the Denali fault (Freymueller et al., 2008; Haeussler, 2008). Since the

microplate is composed of thick, buoyant crust that does not subduct, it is acting as a ram as it collides obliquely with southern Alaska, in the process translating terranes through the dextral fault system (Freymueller et al., 2008; Haeussler, 2008). Geodetic studies by Freymueller et al. (2008) documented active deformation rates using global positioning system (GPS) data collected from 1992 to 2007 throughout Alaska. The study found that GPS velocities support the concept of a counterclockwise rotating SOAK and suggest that the driving mechanism of rotation is the collision and subduction of the thick and buoyant Yakutat block in southern Alaska (Freymueller et al., 2008; Haeussler, 2008; Figure 1). In Freymueller et al. (2008), GPS velocities around the Talkeetna Mountains showed that sites just east of the mountains moved northwest and away from the trench, while sites near the northern Talkeetna Mountains moved west parallel to the Denali fault, and sites west of the mountains moved rapidly toward the trench to the south-southeast (Figure 2). This suggests that the Talkeetna Mountains are rotating counterclockwise. between the Denali and Border Ranges faults (Freymueller et al., 2008; Figure 2).

2.2 Geologic Setting of the Talkeetna Mountains

The Talkeetna Mountains are a major topographic high between the Susitna River basin to the west and the Copper River basin to the east, and are bounded by two dextral strike slip faults: the Denali fault to the north and Castle Mountain fault to the south (Figure 1 and 3). The Talkeetna Mountains consists of the Kahiltna basin assemblage and Wrangellia composite terrane (Figure 3).

2.2.1 Wrangellia and Peninsular Terranes

The Wrangellia composite terrane is composed of two accretionary terranes: the Wrangellia and Peninsular terranes (Figure 3). The Wrangellia terrane is exposed in the central Talkeetna Mountains, between the Kahiltna basin assemblage in the north and the Peninsular terrane in the south (Figure 3). The Wrangellia terrane includes Mississippian to Middle Triassic age metasedimentary rocks, including siliceous siltstone, chert, sandstone, and fossiliferous limestone (Nokleberg et al., 1994). These metasedimentary rocks are overlain by the Nikolai Greenstone flood basalt of Middle to Late Triassic age and by shallow marine sedimentary rocks of Triassic and Jurassic age (Nokleberg et al., 1985).

The Peninsular terrane is located south of the Wrangellia terrane (Figure 3) and consist of Paleozoic to Mesozoic metasedimentary rocks, Late Triassic to Early Jurassic Talkeetna volcanic arc rocks, and Early to Middle Jurassic granitoid batholiths (Nokleberg et al., 1985).

The Peninsular and Wrangellia terranes were amalgamated into the Wrangellia composite terrane starting in Late Paleozoic (Coney et al., 1980) based on the correlation of Late Paleozoic age metasedimentary and metavolcanic rocks within the Peninsular and Wrangellia terranes, as well as the Permian-age volcanic rocks and limestone of the Skolai arc, which overlay both terranes (Nokleberg et al., 1994). The Wrangellia and Peninsular terrane boundary is debated but is typically mapped through the Talkeetna Mountains along the northeast-trending Tsisi Creek fault, which is a major shear zone following the Tsisi Creek (Csejtey et al., 1978; Glen et al., 2007b; Figure 3).

Paleomagnetic studies of the Nikolai Greenstone, which are metamorphosed flood basalts produced as a consequence of the onset of rifting, place the Wrangellia and Peninsular terranes at least 30° south of their present latitude near the Late Triassic paleoequator (Nokleberg et al.,

1994). After rifting from the western North American margin at low paleolatitudes the terranes migrated toward the northwest continental margin were they collided and began accreting by mid-Cretaceous time, closing an ocean basin of unknown size between them (Nokleberg et al., 1985). The terranes were transported northwest along dextral fault systems like the Denali fault and were at or near their present position by Middle to Late Eocene time (45.5 to 36.8 Ma; Nokleberg et al., 1994; Trop et al., 2003). Terranes in the Talkeetna Mountains were overprinted by igneous rocks during the Mesozoic to Cenozoic (Figure 3). In the southeastern Talkeetna Mountains, granitic intrusions attributed to arc magmatism were emplaced from the Late Cretaceous to Paleocene (Trop et al., 2003). To the east of the plutonic intrusion is an Eocene northwest-trending igneous body of volcanic and intrusive rocks, attributed to slab-window magmatism (Trop et al., 2003).

2.2.2 The Kahiltna Basin

The Wrangellia composite terrane of the northern Talkeetna Mountains is separated from rocks of the Alaska Range by the Kahiltna basin (Figure 3). The Kahiltna basin in the Talkeetna Mountains is part of a much larger discontinuous belt of Jurassic to Cretaceous flysch basins inboard of the Wrangellia composite terrane, extending from southwestern Alaska to western British Columbia (Hampton et al., 2007; Wallace et al., 1989). The extensive flysch basin was deposited during the collision and accretion of the Wrangellia composite terrane to the Mesozoic continental margin and is commonly referred to as a major suture zone (Nokleberg et al., 1985; Trop and Ridgway, 2007; Wallace et al., 1989).

The flysch basin exposed in the northern Talkeetna Mountains consists of sediments shed northward from the accreting Wrangellia terrane (Hampton et al., 2007). The Kahiltna basin's

stratigraphic sequences record the deposition of pre- to post-collisional sediments overlying an Upper Triassic to Lower Jurassic volcanic basement (Glen et al., 2007a; Hampton et al., 2007). Glen et al. (2007a) inferred the Kahiltna basin crust to be transitional based on the weakly magnetic, low, and subdued gravity fields observed through magnetotelluric studies, and the Wrangellia crust to be mafic to ultramafic oceanic lower crust based on its dense, highly magnetic, and strong gravity readings. Over 45 Ma of continuous clastic sedimentation is preserved in the submarine fan strata of the flysch basin, as documented by thick units of synorogenic strata deposited from the Late Jurassic to Late Cretaceous (Hampton et al., 2010, 2007; Wallace et al., 1989).

The Kahiltna basin is intensely deformed into tight isoclinal folds and complex faults, and has a structural thickness of several thousand meters (Nokleberg et al., 1994). Because of the monotonous nature of the flysch, individual faults and shear zones are not easily detected (Hampton et al., 2007). This intense deformation occurred during the Late Cretaceous and Tertiary as the Wrangellia Composite Terrane was accreted and translated north along the western margin of North America (Plafker and Berg, 1994).

2.2.3 The Kahiltna Basin and Wrangellia Terrane Boundary

The boundary between the Kahiltna basin assemblage and the Wrangellia terrane has been mapped as the Talkeetna thrust fault (Figure 1 and 2). Csejtey (Csejtey et al., 1978; Csejtey 1982) described this structure as a southeast dipping Alpine nappe-like thrust. However, more recent geophysical studies and mapping in the area suggest that the Talkeetna fault dips slightly to the northwest, does not exist as a singular through-going fault, and that it is likely to be a series of high-angle, complex fault strands (Glen et al., 2007b; O'Neill et al., 2005, 2003). Where

the Talkeetna fault is exposed, it shows little offset and deformation, which was interpreted as evidence against an Alpine nappe-like thrust (Glen et al., 2007a, 2007b; O'Neill et al., 2005, 2003; Twelker et al., 2015).

Geophysical studies by Glen et al. (2007a, 2007b) suggested that there is a prominent vertical crustal break between the oceanic crust of the Wrangellia terrane and the transitional crust of the Kahiltna basin (Figure 4). This crustal break underlies the northeast trend of the previously mapped Talkeetna thrust fault. Glen et al. (2007a, 2007b; Figures 2 and 3) suggested that this deep crustal structure was an area of structural weakness that guided the development of overlying shallow crustal features (O'Neill et al., 2005). Consequently, the boundary between the Wrangellia terrane and the Kahiltna basin is not a singular fault but a wide zone of deformation overlying a major crustal break at depth.

Site-specific seismic hazard studies have been conducted along this boundary near the proposed site of the Susitna-Watana hydroelectric dam (Acres, 1982; AEA, 2015). Only structures that were within 15 miles of the dam site were evaluated for evidence of Quaternary faulting, the presence of significant shear zones, and the potential of reactivation of geologic structures. The study revealed an absence of deformation in Quaternary deposits and the lack of an extensive shear zone beneath the dam site and concluded that the structures in the area were not a seismic hazard to the project (Acres, 1982; AEA, 2015).

2.3 Bounding Faults

2.3.1 Denali Fault

The active right-lateral strike-slip Denali fault forms the northern boundary of the Talkeetna Mountains and extends over 2000 km from southeastern Alaska to the Bering Sea (Haeussler, 2008; Figure 1). The fault has been considered to have significantly aided in the northward transport of allochthonous terranes along the North American margin since the Late Cretaceous (Nokleberg et al., 1994; Plafker and Berg, 1994). The fault has been historically active; in 2002, an M7.9 earthquake ruptured most of the central part of the fault. The earthquake initiated along the Susitna Glacier thrust, a previously unknown northeast trending thrust fault splay off the Denali fault (Haeussler, 2008).

There are many indicators along the central Denali fault that suggest slip rates of several mm/yr (Haeussler, 2008); however, these rates are not homogeneous. The variation in observed slip rates suggests that slip rates decrease along the fault from east to west (Fletcher, 2002; Haeussler, 2008; Matmon et al., 2006). Slip rates on the eastern strand of the Denali fault are around 14 mm/yr. The central Denali fault has slip rates of about 10 mm/yr, and the western strand has slip rates of 9 mm/yr (Fletcher, 2002; Haeussler, 2008; Matmon et al., 2006).

2.3.2 Castle Mountain Fault

The Castle Mountain fault is an active east to northeast-trending fault that forms the southern boundary of the Talkeetna Mountains (Haeussler, 2008; Figure 1). The fault is a nearly vertical or steeply north-dipping right-lateral oblique-slip fault with north side up displacement (Detterman et al., 1996, 1974). The western Castle Mountain fault consists of a single fault trace,

whereas the eastern section of the fault includes a major splay known as the Caribou fault (Detterman et al., 1974; Grantz et al., 1966).

Displacement along the fault has been occurring since the end of the Mesozoic (Grantz et al., 1966). The 100-km eastern section lacks a Holocene scarp but is seismically active; the 62-km western section has a Holocene scarp but remains seismically quiet (Haeussler, 2008). Holocene offset on the western section in the Susitna lowlands includes displacement of river terraces, near-surface sediment, and sand ridges. These Holocene features show right-lateral and/or vertical offset across the fault trace (AEA, 2015). There have been four significant surface ruptures in the past 2700 years; the most recent earthquake was 650 years ago (Haeussler, 2008). Based on the offset of postglacial drainage in the Late Pleistocene – Holocene, the slip rate is 2-3mm/yr (Willis et al., 2007).

2.4 Bounding Sedimentary Basins

The Talkeetna Mountains are bordered by the Susitna basin to the west, the Copper River basin to the east, and the Matanuska Valley – Talkeetna Mountains basin to the south (Figure 1). Understanding the characteristics and stratigraphic record of sedimentary basins provides information about the timing of basin subsidence and uplift of surrounding mountain ranges. Unfortunately, little information is available on most of these surrounding basins other than a few stratigraphic studies and exploratory wells.

2.4.1 The Susitna River Basin

The Susitna River basin forms the western boundary of the Talkeetna Mountains. The 13,000-km^2 basin is a swampy lowland that is considered to be the northern extension of the Cook Inlet

basin to the south (Trop and Ridgway, 2007; Figure 1). Little information is known or published about the Susitna River basin, although three exploratory wells suggest that it is likely Tertiary in age (Haeussler, 2008). In the northwest corner of the basin, the youngest exposed strata in a north-south trending fault-cored fold is likely Plio-Pleistocene in age, based on palynology of exposed rocks (Haeussler, 2008; Willis and Bruhn, 2006). This fold is one of several in the basin and suggests that the dominant maximum stress orientation during folding was approximately east to west.

2.4.2 The Copper River Basin

The Holocene Copper River basin forms the eastern boundary of the Talkeetna Mountains (Figures 1 and 3). The 4500-km^2 basin is a fluvial lacustrine lowland between the Talkeetna and Wrangell Mountains. There are eleven exploratory wells drilled in the Copper River basin that encountered 580 m of Tertiary strata and up to 1715 m of Late Jurassic to Late Cretaceous strata (Trop and Ridgway, 2007). The Copper River basin has a thin accumulation of Tertiary age sediments (Brocher et al.,1994), which, according to Haeussler (2008), indicate that regional subsidence did not occur or that areas surrounding the basin were not experiencing exhumation during Tertiary time.

2.4.3 The Matanuska Valley-Talkeetna Mountains Basin

The southern margin of the Talkeetna Mountains is juxtaposed with the Matanuska Valley-Talkeetna Mountains basin, which is itself bisected by the Castle Mountain fault (Figures 1 and 3). This basin is 90 km long and 20 to 70 km wide and contains Mesozoic-Cenozoic strata

derived from the Talkeetna Mountains to the north and the Chugach Mountains to the south (Trop and Ridgway, 2007). This basin is interpreted to record episodes of volcanism and uplift in the Talkeetna Mountains associated with spreading ridge subduction from 54.5 to 50 Ma and oblique movement along the Castle Mountain fault from Eocene to Neogene time (Trop et al., 2003).

CHAPTER 3: METHODOLOGY AND DATA

The Talkeetna Mountains cover about 23,000 km^2 and are remote and very hard to access. Because of these limitations, conducting an investigation bearing on the neotectonics, uplift, and deformation of the mountain range was limited to the analysis of digital data through geospatial information systems like ArcGIS and site-specific field work for sample collection. A variety of data and methods were used for this thesis in an attempt to develop a broader understanding of the study area.

3.1 Methods

3.1.1 Geomorphic Reconnaissance

Geomorphology is the study of landscape features of the Earth and their relation to the geology of the area (Keller and Pinter, 2002). Geomorphology is based on the analysis of feature morphology through either qualitative or quantitative methods and has been heavily used in neotectonic studies around the world in a variety of tectonic settings (e.g., Bemis and Wallace, 2007; Jacques et al., 2014; Mahmood and Gloaguen, 2012). I used a variety of geomorphic methods to analyze the topography of the Talkeetna Mountains and identify areas of possible neotectonic activity.

3.1.1.1 Topographic Analysis

Variations in elevation distribution and topography can reflect uplift patterns and/or characteristics. I used ArcGIS to analyze the topography in the Talkeetna Mountains. After importing the digital elevation model (DEM), I chose an appropriate color scale in ArcMap to

enhance elevation patterns (Figure 5). In ArcGIS, I used the "interpolate line" tool to extract elevation data along multiple profiles in the Talkeetna Mountains. Profiles were chosen at the highest ridge elevations along the edges of drainage basins, in an attempt to keep old erosional surfaces that might remain. I then imported the profile data into Excel in order to generate profiles and manipulate vertical exaggeration when necessary to accentuate patterns.

3.1.1.2 Drainage Patterns

The shape and area, or morphometry, of a stream or river is highly sensitive to tectonic activity or changes in lithology and responds quickly to these changes (Keller and Pinter, 2002). Therefore, a drainage map can be used to identify anomalous drainage patterns resulting from geologic features or activity (Figure 6).

The erosional force of rivers or streams is highly effective at exploiting structural weaknesses in bedrock. This is seen in many places around the world where a stream has found the path of least resistance through a structurally weakened fault trace or surface. This forms a linear drainage pattern that can be seen in a drainage network map. I used a drainage network map of the Talkeetna Mountains to identify pronounced linear drainages that could be related to faults in the area.

Barbed drainages refer to an area along a stream where there is a sharp 90° or greater angle downstream and occurs in areas where uplift or faulting has resulted in stream capture. I identified areas with barbed drainages on a drainage network map to highlight areas of possible structural activity and compared them with the occurrence of linear drainages and faults mapped in the area.

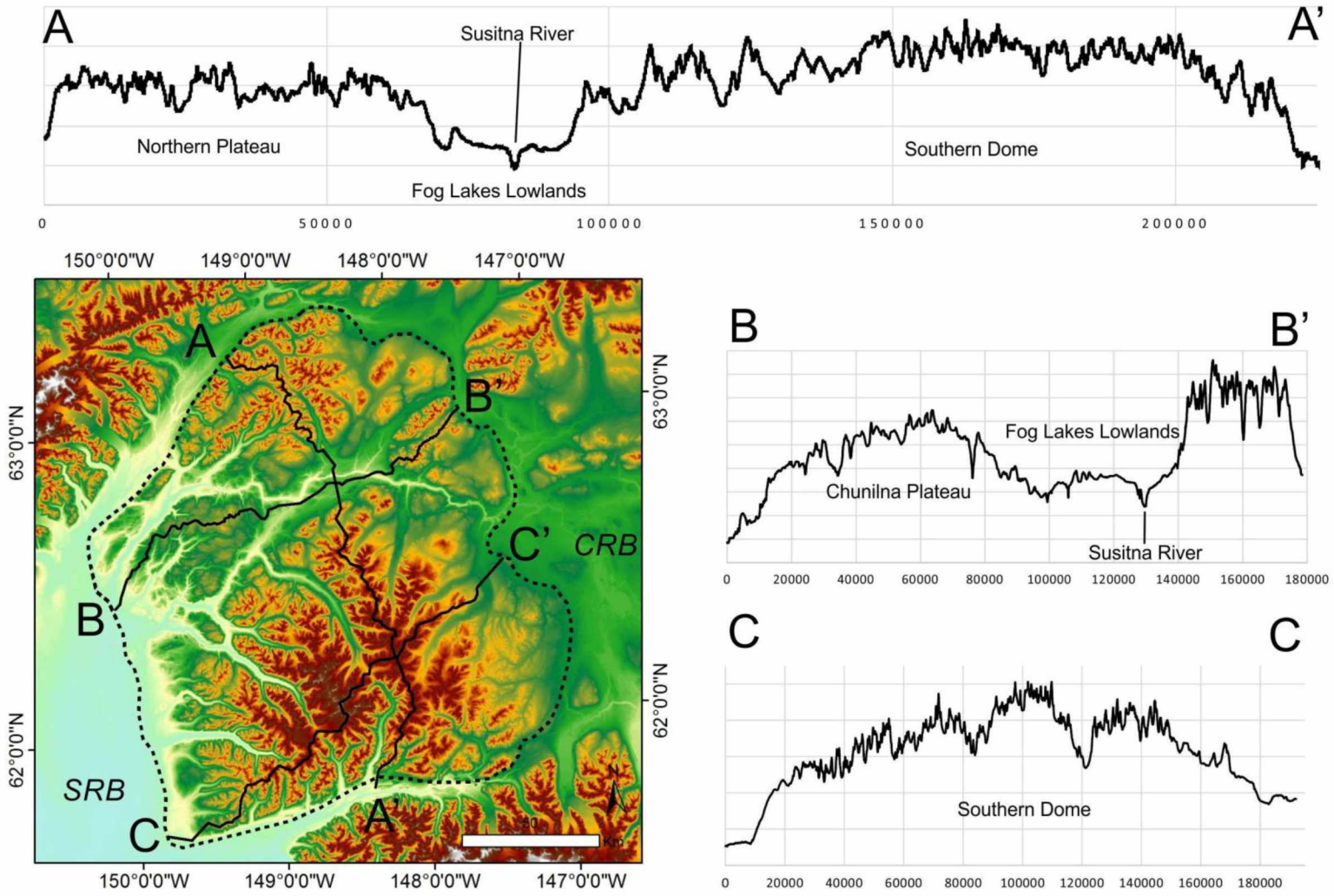

Figure 5. Color-scaled DEM of the Talkeetna Mountains used for analysis of elevation distribution and topography. The Talkeetna Mountains are outlined by the black dashed line; location of topographic profiles A-A', B-B' and C-C' are shown in solid black lines.

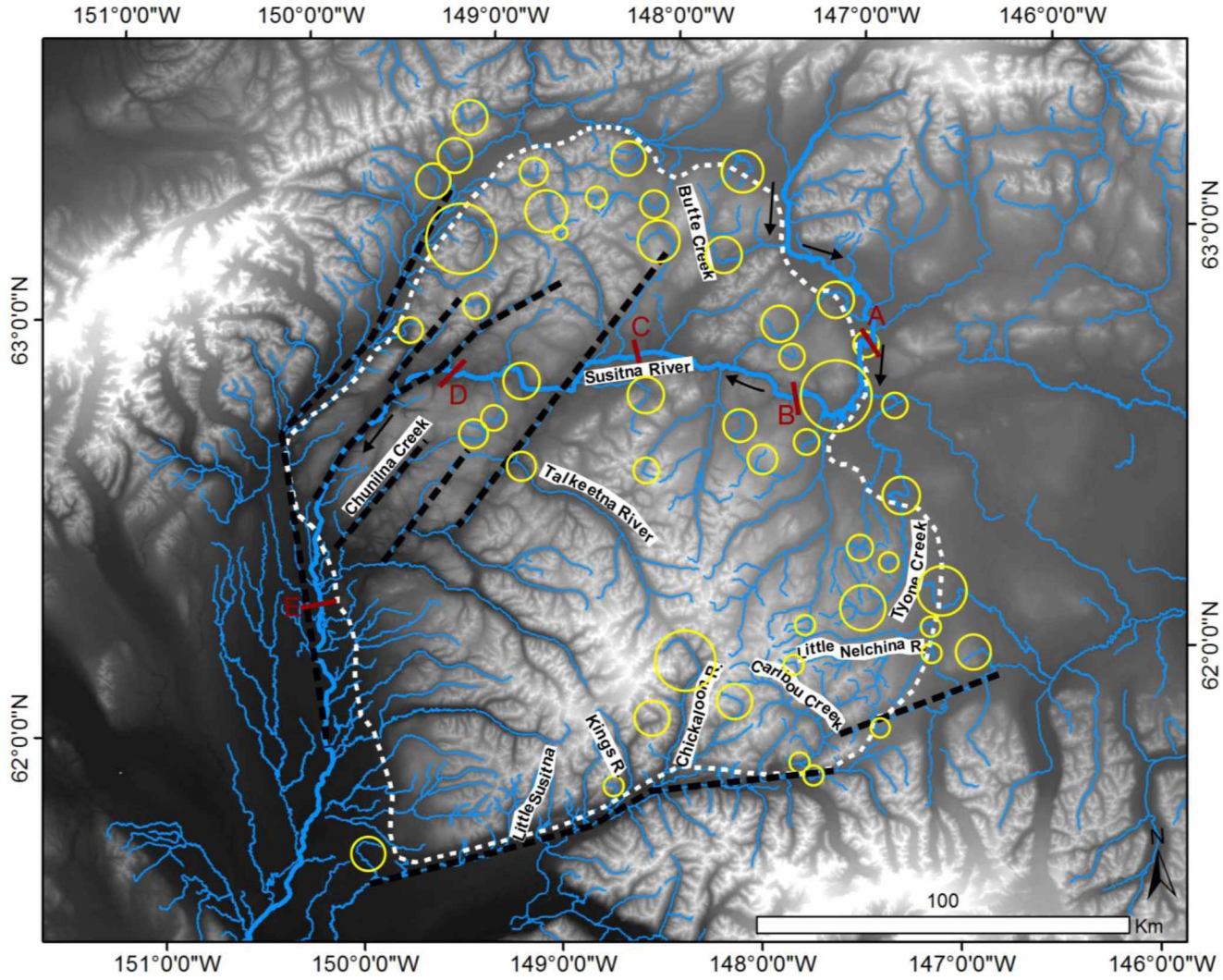

Figure 6. Drainage networks in the Talkeetna Mountains with drainage anomalies highlighted. The Talkeetna Mountains are outlined by the white dashed line. Blue lines represent drainages; areas where barbed drainages are observed are circled in yellow; linear drainages are shown by the black dashed lines. Red lines represent valley profiles A-E shown in Figure 14. The Susitna River is shown in bold, with black arrows representing flow direction along its path. Rivers referenced in text are labeled.

3.1.2 Geomorphic Indices

Geomorphic indices are tools that can be used to quantitatively or qualitatively define active tectonics. These indices rely on idealized models of landscape shape and evolution (Keller and Pinter, 2002). Geomorphic indices are particularly useful in large study areas that are hard to access, like the Talkeetna Mountains, because they allow for rapid evaluation of the landscape without lengthy field work.

Most of the geomorphic indices I used rely on hydrological information and are applied at the scale of individual drainage basins. Drainage basins are natural basins above select points on the main streams that formed as a result of the interaction of slope-wasting and channel deepening processes within the boundaries of the drainage divide. Consequently, each basin can be treated as an individual unit (Strahler, 1952). In this study, calculation of geomorphic indices were conducted in 170 drainage basins in the Talkeetna Mountains.

3.1.2.1 Hypsometric Integral (HI)

Hypsometry is a quantitative measure of the relationship between elevation and area of a drainage basin (Strahler, 1952). It is closely related to the erosional maturity of the basin and is therefore tied to the duration or intensity of erosion in the basin. The hypsometric curve and the hypsometric integral (HI) are products of hypsometric analysis. The hypsometric curve is a graphical representation of the proportion of total basin area against the proportion of total basin height (Keller and Pinter, 2002; Figure 7). The shape of the hypsometric curve represents the erosional maturity of the drainage basin, and the HI is defined as the area beneath the hypsometric curve (Keller and Pinter, 2002; Strahler, 1952; Figure 7).

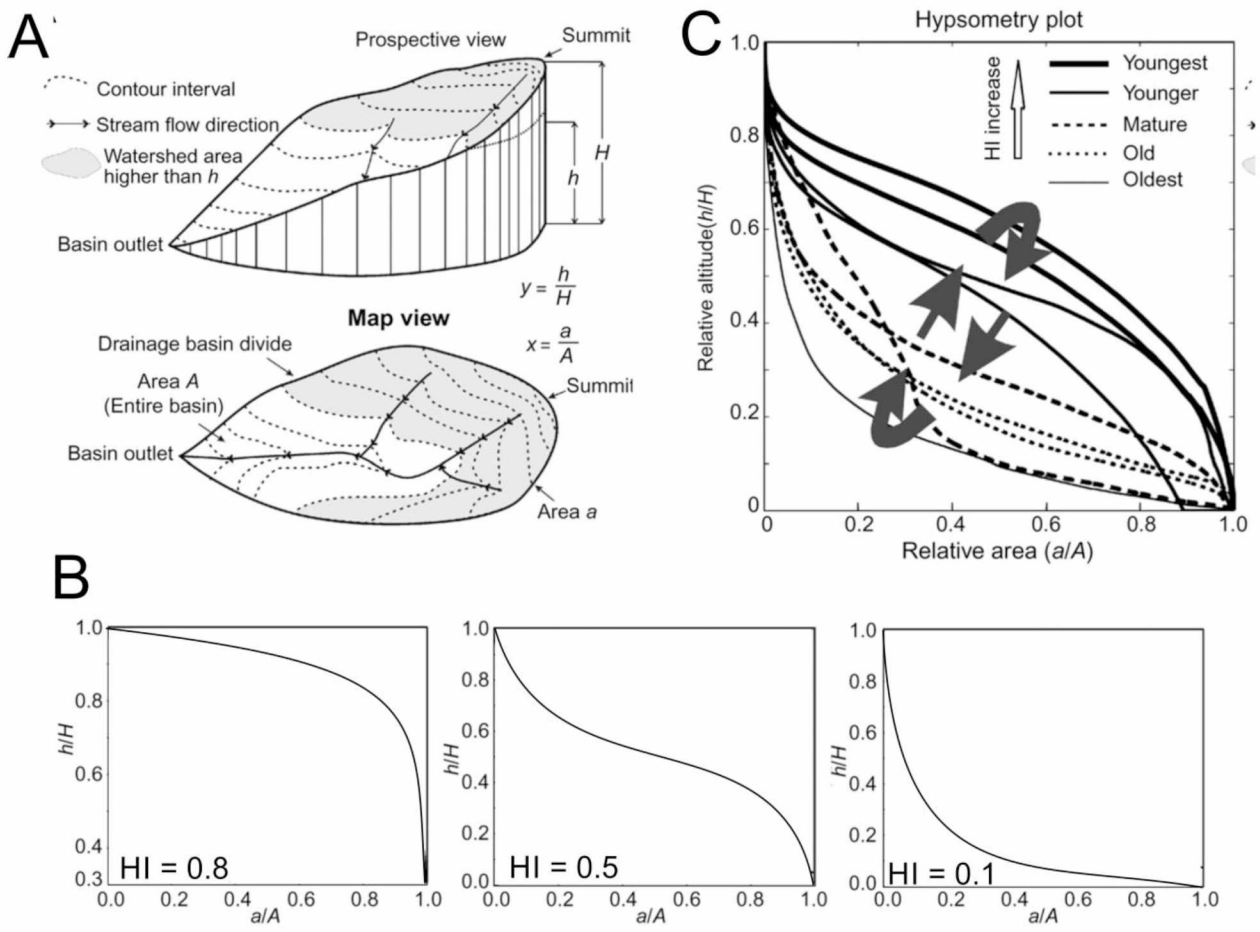

Figure 7. Calculation of the hypsometric curve (HC). The HC is a graphical representation of the maturity of a drainage basin and is based on the relationship between area and elevation in the basin. A) Prospective and map views of a drainage basin displaying what is being measured for calculations. B) Graphs showing idealized patterns (from left to right): a convex HC with a high hypsometric integral (HI) value representing a youthful topography associated with recent uplift; S-shaped HC with a moderate HI representing more mature basins, and a concave HC with a low HI value representing an old stage basin that has been tectonically inactive allowing erosion of previously uplifted topography. C) Graph displays the geomorphic cycle of hypsometric cycle of hypsometric curves from youthful to old stages. From Mahmood and Gloaguen, 2012.

Since producing 170 hypsometric curves and then finding the area beneath those curves would be time-consuming, an alternative equation can be used to calculate the HI (Keller and Pinter, 2002):

$$HI = (Elev_{mean} - Elev_{min})/(Elev_{max} - Elev_{min})$$

When the HI value is high, it means that most of the topography is at a higher elevation than the mean elevation, resembling a smooth uplifted surface that is incised deeply by rivers. Higher HI values indicate a basin that has a more youthful topography where streams are incised in valleys but erosion has not affected the uplands and is interpreted to reflect possible tectonic activity (Keller and Pinter, 2002; Mahmood and Gloaguen, 2012). Intermediate to low HI values indicate that the basin is more mature, has been more evenly dissected by rivers, and is less influenced by recent activity (Keller and Pinter, 2002; Mahmood and Gloaguen, 2012). Since hypsometric analysis is based on proportional values, it is an index that is independent of basin area; therefore, basins of different sizes can be compared across a study area (Keller and Pinter, 2002).

3.1.2.2 Drainage Basin Asymmetry Factor (AF)

The AF is defined as:

$$AF = 100\ (Ar/At),$$

where *Ar* is the area of the basin to the right of the trunk stream facing downstream, and *At* is the area of the total drainage basin (Figure 8; Keller and Pinter, 2002). When streams form in stable tectonic environments, AF equals about 50. If AF values are significantly greater than or less than 50, this implies a less stable tectonic environment where the stream has preferentially

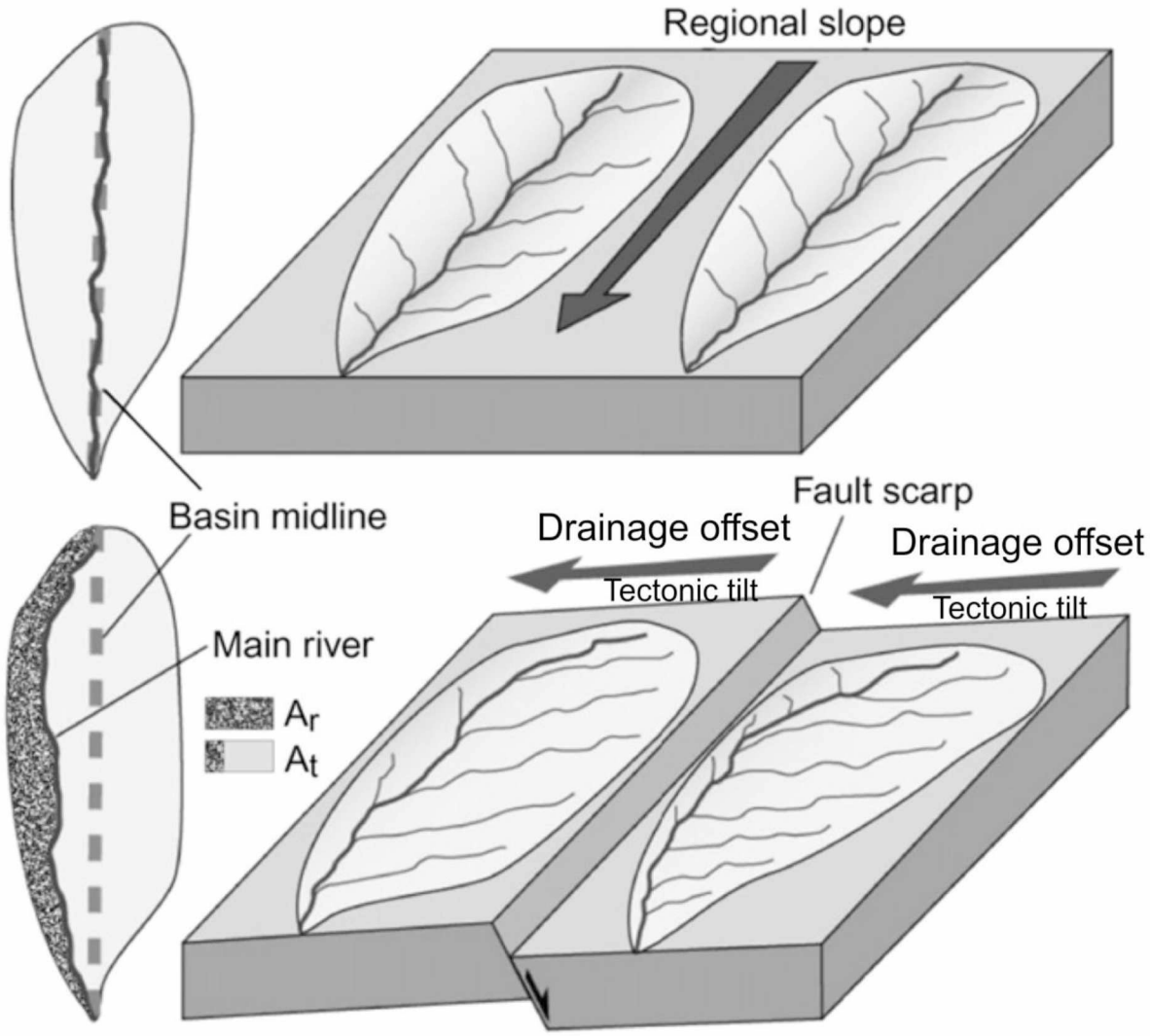

Figure 8. Calculation of basin asymmetry factor (AF). Differential uplift and lateral migration of the main river in a down-tilt direction can lead to development of asymmetrical drainage basins. A_r = area of the basin to the right (looking downstream), A_t = the total area of the drainage basin. From Keller and Pinter, 2002.

eroded one side of the basin. In order to simplify the AF values, I adjusted the equation based on Mahmood and Gloaguen (2012):

$$AF = |100\ (Ar/At)| - 50.$$

Using this adjusted AF equation, I evaluated values that were significantly different from zero for evidence of drainage asymmetry and observed an approximate tilt direction of the basin based on the direction of deviation of the main stream trunk. An AF map was generated for each drainage basin where the basins were color-scaled by AF value.

It is important to recognize that tectonic influence is not the only driving mechanism of AF. Asymmetry can be a consequence of bedrock structure, lithology, and climatically driven processes like glaciation as well as preferential erosion due to vegetation, wet versus dry slopes, and the location of precipitation (Curran et al., 2014; Poulos et al., 2012). In southern Alaska, more precipitation is experienced on the south facing slopes, which in turn experience more snow and periglacial processes (Poulos et al., 2012). This causes a deflection in drainage basins where more sedimentation occurs on the northern side of the valley, deflecting the river toward the southern side. This could be mistaken for tectonic control in some cases (Poulos et al., 2012).

3.1.2.3 Valley Floor Width-to-Height Ratio (Vf)

The valley floor width-to-height ratio (*Vf*) quantifies the shape of the valley and distinguishes between broad-floored valleys and deeply incised valleys (Figure 9; Keller and Pinter, 2002). The valley floor width-to-height ratio is defined as:

$$Vf = 2Vf_w/[(E_{ld} - E_{sc}) + (E_{rd} - E_{sc})],$$

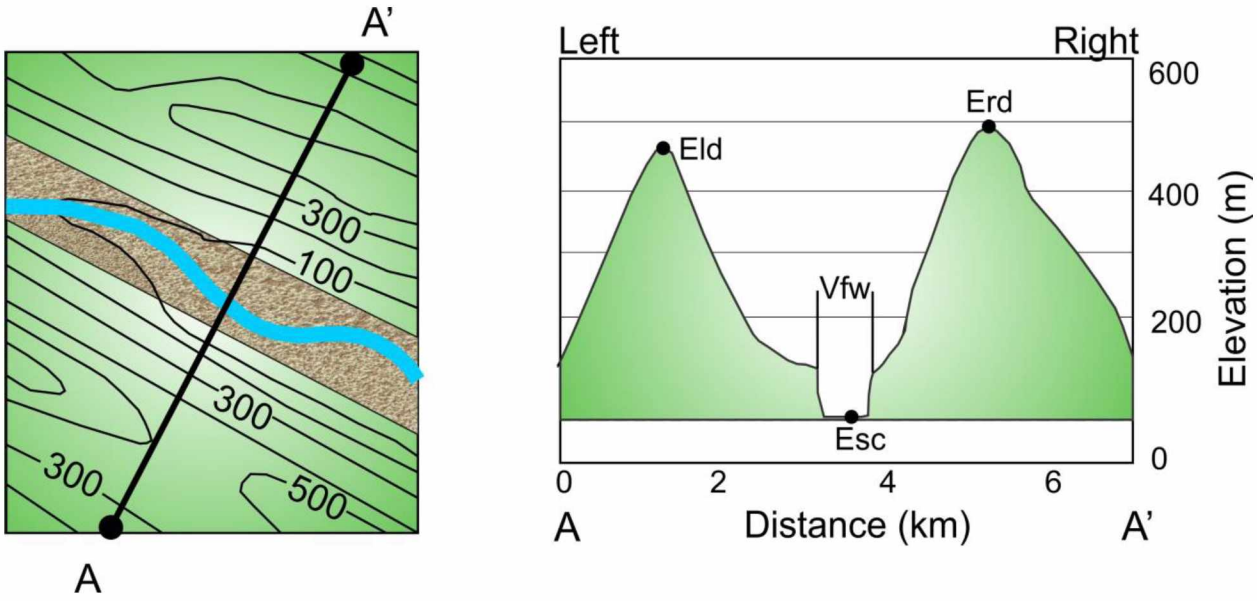

$$Vf = \frac{2Vfw}{(Eld - Esc) + (Erd - Esc)} = \frac{800m}{(450m - 50m) + (500m - 50m)}$$

$$= .094$$

Figure 9. Calculation of the valley floor width-to-height (Vf) ratio. Elevation values and valley floor widths are collected from the profile taken perpendicular to the river. Vf_w is the width of the valley floor; E_{ld} and E_{rd} are peak elevations to the left and right of the valley; and E_{sc} is the elevation of the valley floor. From Keller and Pinter, 2002.

where Vf_w is the width of the valley floor, E_{ld} and E_{rd} are peak elevations to the left and right of the valley, and E_{sc} is the elevation of the valley floor (Keller and Pinter, 2002).

Higher valley floor width-to-height ratio values (> 1) are associated with low uplift rates, which allow for streams to cut broad valley floors and are characteristic of areas of tectonic quiescence. Low valley floor width-to-height ratio values (values < 1) are associated with uplifted basins where rivers are actively incising into the valley floor and are characteristic of areas experiencing active uplift (Keller and Pinter, 2002).

3.1.2.4 Longitudinal Stream Profiles and Stream-Length (SL) Gradient Index

A longitudinal profile of a stream is a plot of elevation from the river headwaters downstream to the mouth of the river (Keller and Pinter, 2002). A typical longitudinal profile of a graded river, which is a river in a state of dynamic equilibrium (Keller and Pinter, 2002), displays a slight concave profile (Schumm et al., 2000). Deviations from the typical concave profile can be attributed to active tectonics or lithology (Hack, 1973). Deviations like convex upward warping or sharp upward jumps, called knickpoints, in elevation can be used as evidence of uplift and faults if lithology is ruled out as a cause.

The stream-length (SL) gradient index is calculated along particular reaches of the longitudinal profile of a stream and correlates to stream power (Keller and Pinter, 2002; Figure 10). The SL index is a tool that allows for the quantifying variations in gradient changes of a river profile. Changes in slope can be caused by active tectonic structures, and rivers are highly sensitive to this, causing a change from an equilibrium stream profile and resulting in anomalous SL values (Keller and Pinter, 2002). Since streams adjust quickly to deformation in an effort to reach equilibrium, deviations in their profile gradients are good indicators of recent tectonic activity (Keller and Pinter, 2002). The SL index is used to identify these areas of recent tectonic activity by identifying reaches of anomalously high SL values for certain rock types (Keller and Pinter, 2002). The SL index is defined as:

$$SL = (\Delta H/\Delta L)L,$$

where ΔH is the change in elevation, ΔL is the length of the particular reach, and L is the length of the entire river (Hack, 1973; Keller and Pinter, 2002).

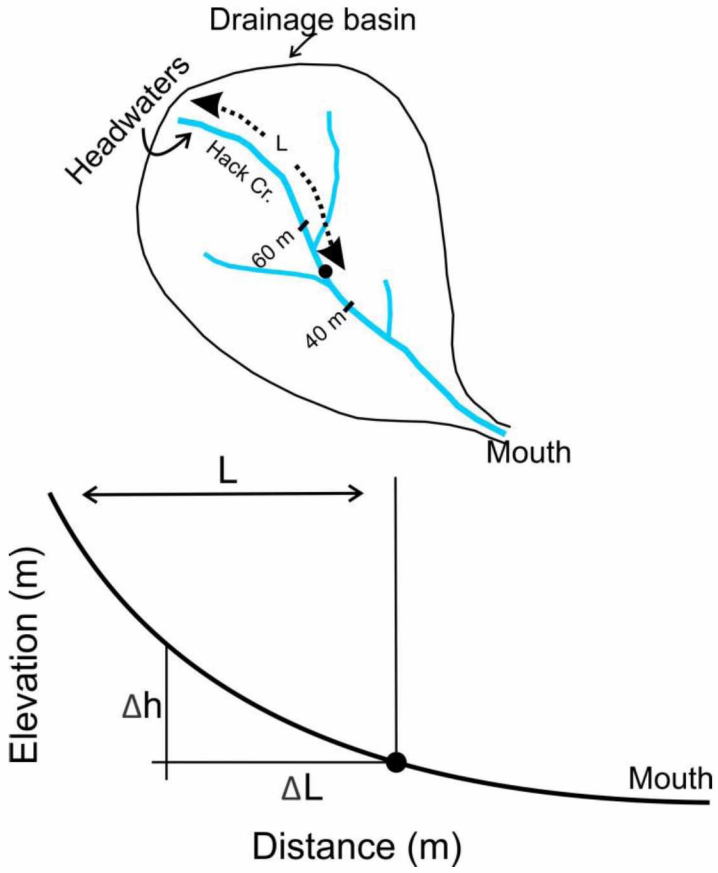

Figure 10. Calculation of stream length gradient index (SL) along a stream using a hypothetical creek as an example. ΔH is change in elevation, ΔL is the length of the particular reach, and L is the length of the entire river (Hack, 1973; Keller and Pinter, 2002).

3.1.2.5 Index of Relative Active Tectonics (IRAT) Map

When using geomorphic indices to evaluate the tectonic activity of an area, it is best if several indices are used in conjunction with one another (Keller and Pinter, 2002). This technique is described by Keller and Pinter (2002) and implemented in many neotectonic studies in areas experiencing active tectonics (El Hamdouni et al., 2008; Mahmood and Gloaguen, 2012; Silva et al., 2003). In this technique, I averaged values of each geomorphic index (HI, AF, valley floor width-to-height ratio) and then separated them into eight classes, with Class 1 being the most relatively active and Class 8 being the least.

3.1.3 Apatite Fission-Track Thermochronology (AFT)

Apatite fission-track thermochronology (AFT) is a widely used method to constrain low-temperature thermal histories for a variety of rock types that contain the mineral apatite. Apatite is a nearly ubiquitous mineral found in many crustal rock types (Donelick et al., 2005) and is a common detrital mineral in clastic rocks.

Apatite is a mineral that contains the radioactive trace elements uranium (U) and thorium (Donelick et al., 2005). When nuclear fission of ^{238}U takes place, it results in two repelling nuclei fragments that produce a damage trail as they repel each other (Donelick et al., 2005). This damage trail is referred to as a "fission track" and can be physically measured. Fission tracks can repair themselves through annealing partially to completely from ~60° to ~120°C. This window is called the partial annealing zone (PAZ) (Green et al., 1986; Laslett et al., 1987). As temperatures increase in the PAZ, the fission-track length decreases until it is completely healed or erased (Naeser, 1976). At temperatures less than ~60°C, fission tracks that form are retained (Ketcham et al., 1999). Since retention of fission tracks in apatite is extremely sensitive to temperature and to thermal annealing above ~120°C, they are used to document stages of cooling in the rock (Donelick et al., 2005).

The AFT has been used throughout Alaska to define the thermal and exhumation history of many structural and tectonic features surrounding the study area, including Denali (Fitzgerald et al., 1995; Plafker et al., 1992), the Tordrillo Mountains (Haeussler, 2008; Haeussler et al., 2008), the Hayes Range (Armstrong et al., 2007; Benowitz et al., 2007), and the Chugach-St. Elias Mountains (O'Sullivan and Currie, 1996).

3.1.3.1 AFT Sampling Strategy

Field work was conducted to collect samples for AFT from the Kahiltna basin along a northwest to southeast transect across an elliptical topographic high in the northwest Talkeetna Mountains (Figure 11). Elevation ranged from 1260 to 1456 m. A constant elevation profile is preferred; however, it was difficult to find outcrops suitable for apatite separation. Therefore, some deviation from constant elevation was required to accommodate this. Rock types were from the Kahiltna flysch sequence and ranged from fine-grained mudstone to conglomerate. Samples were sent to Paul O'Sullivan of GeoSeps, where rocks were crushed and apatites were separated using standard density and magnetic techniques, and AFT ages and lengths were measured following the method described by Donelick et al. (2005).

3.1.3.2 HeFTy Modeling

Paul O'Sullivan used HeFTy to model AFT data to produce time-temperature curves for each sample. A HeFTy model can predict a forward path using thermochronology data. In this study, I used the fission-track thermochronometric system to explore age evolution over time, based on annealing behaviors, parent-daughter decay relationships, and specific constraints, such as present-day surface temperature and depositional age. This data was combined in a statistical and algorithmic approach to generate possible time-temperature paths (Ketcham, 2005).

The HeFTy model used mineral properties and measurements from selected samples and a default of 0°C for present-day surface temperature. A modeled time-temperature path was fit to known stratigraphic ages and constraining fission-track data. All model paths were generated using a Monte Carlo scheme and displayed within a best fit model. Constraint boxes in HeFTy

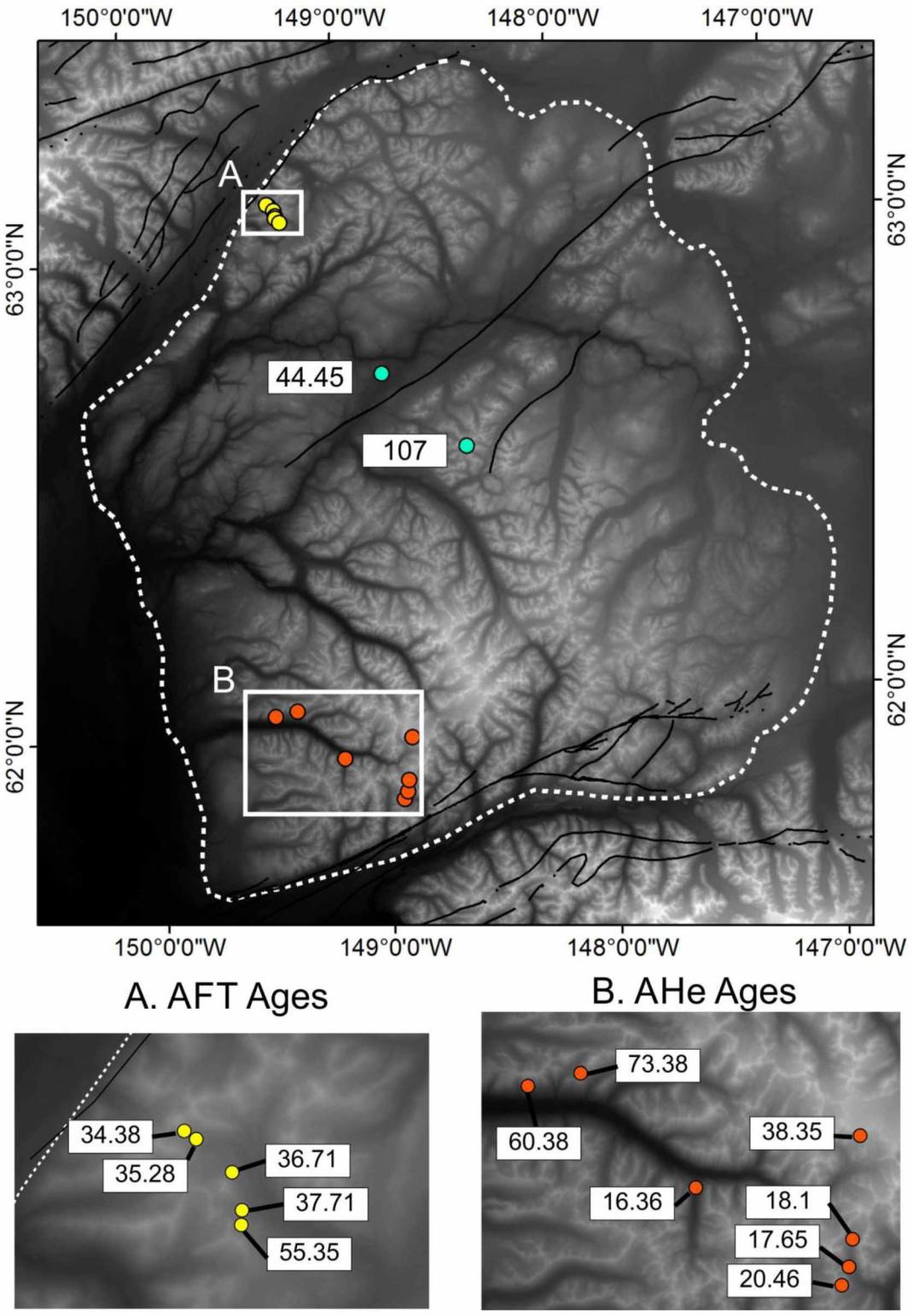

Figure 11. Locations of thermochronology sample and cooling ages in the Talkeetna Mountains. The Talkeetna Mountains are outlined by the white dashed line. Sample locations are color coded based on data source: yellow, AFT collected for this study; blue, AFT from Twelker et al., 2015; orange, apatite (U-TH)/He data from Hoffman and Armstrong, 2005.

models were based on fission-track length data and were added by Paul O'Sullivan, if there was a need for additional periods of stability, and were used to maximize the results of the model while running it in its purest form. I used the HeFTy inverse modeling results to compare uplift rates between samples and identified periods of significantly rapid cooling rates that may correlate to tectonic or structural events within the Talkeetna Mountains.

To compare my AFT results with apatite thermochronology in other areas of the Talkeetnas, I compiled data from two other sources (Figure 11): seven apatite (U-Th)/He ages from the southwestern Talkeetna Mountains near the Kashwitna River and north of the Castle Mountain fault (Hoffman and Armstrong, 2005), and two AFT ages from a recent mapping project in the Talkeetna Mountains C-4 quadrangle (Twelker et al., 2015).

3.1.4 Glacial Isostasy

The Talkeetna Mountains are located in an area of Alaska that experienced significant glaciation during the Pleistocene. Isostatic rebound, or isostatic adjustment, can produce uplift and exhumation in mountain ranges as the top load is removed from the crust during deglaciation. One of the causes of uplift over time in the Talkeetna Mountains in addition to neotectonic uplift may have been glacial isostasy.

To determine the amount of glacial isostatic adjustment experienced in the Talkeetna Mountains after the Last Glacial Maximum in the Late Wisconsin period, I first determined the approximate thickness of the ice sheet that covered the Talkeetna Mountains and then used that to determine the amount of vertical adjustment that would be expected after the ice melted. I used the classic

calculation by Nye (1952) for the height of an ice sheet over distance from the terminus to create a theoretical glacial profile:

$$h = (2T_bL/\rho_i g)^{1/2} \rightarrow h = 4.7(L)^{1/2},$$

where T_b is the basal shear stress experienced on the bedrock surface due to the glacier, ρ_i is the density of ice, g is the acceleration due to gravity, L is the distance from glacier terminus, and h is the total depth measured perpendicular to the surface (Nye, 1952). This calculation allowed me to generate a theoretical glacial profile over a distance that I specified.

To determine if the theoretical ice sheet profile matched the actual ice sheet profile over the Talkeetna Mountains during the Late Wisconsin period (21,000–25,000 thousand years ago) I reconstructed a profile using ArcGIS. This was done using a paleo glacier map of the extent of the ice sheet at this time in conjunction with a DEM of south-central Alaska (Figure 12). Elevation points at the edges of the ice sheet were collected and used to generate an approximate elevation contour map over the ice sheet. Using the generated elevation contours of the ice sheet, a profile was created from the terminus to the highest elevation and compared to the theoretical ice sheet profile to yield an approximate maximum thickness.

Once the thickness was determined, I calculated the asthenosphere displacement to approximate the amount of vertical offset that would have occurred upon rebound using the following equation (Middleton and Wilcock, 1994):

$$h_a = h_i\rho_i/\rho_a,$$

where h_a is the displacement of the asthenosphere, h_i is the thickness of ice sheet, ρ_i is the density of ice, which equals 917 kg/m^3, and ρ_a is the density of asthenosphere, which is 3300 kg/m^3.

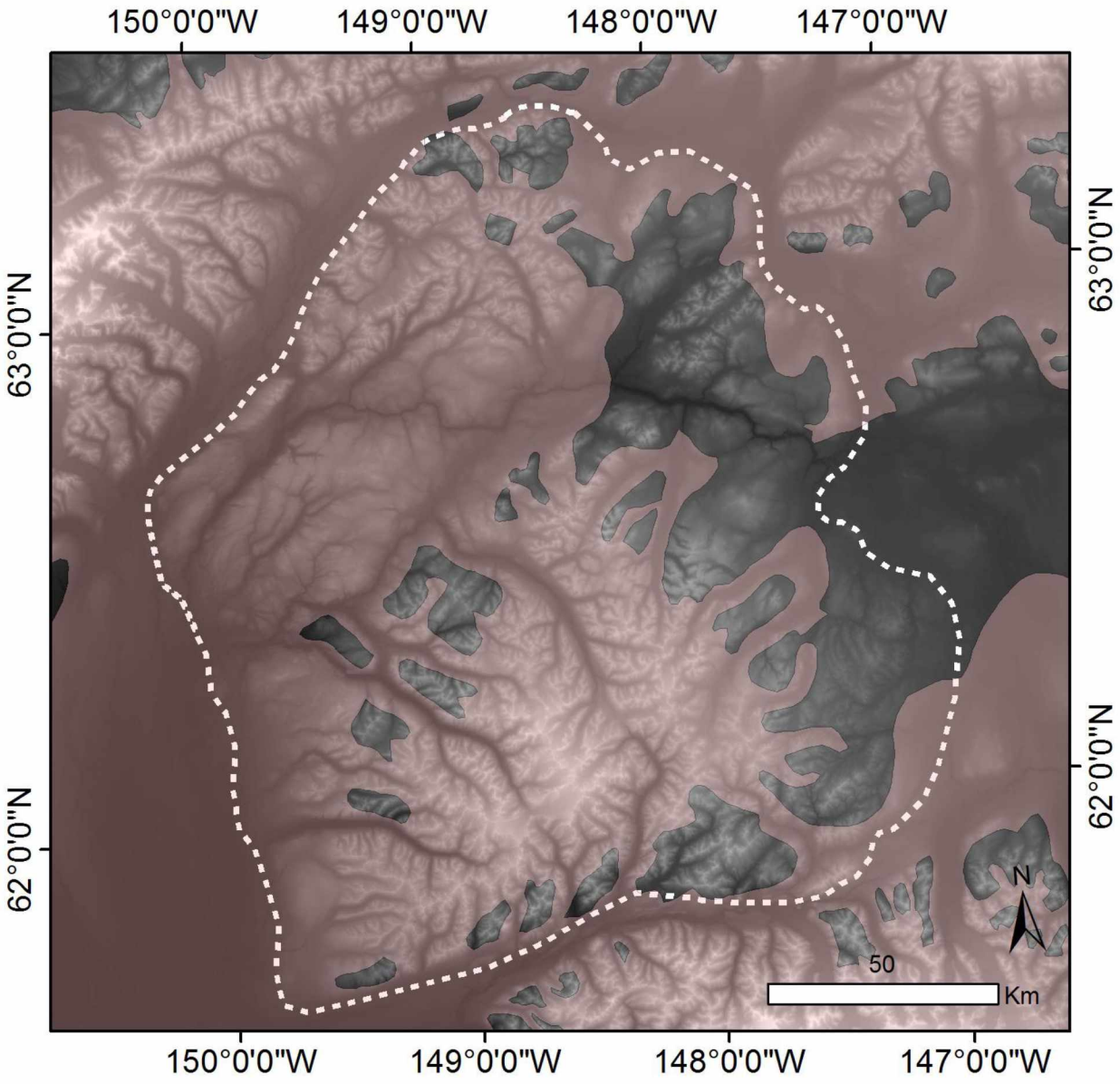

Figure 12. Glacial extent in the Talkeetna Mountains during Late Wisconsin time (25,000 – 21, 000 ca.). The Talkeetna Mountains are outlined by the white dashed line. The extent of the ice sheet is represented by the transparent pink color. From the Alaska PaleoGlacier Atlas, Manley and Koffman, 2002.

3.2 Data

3.2.1 Digital Elevation Models (DEMs)

The vast majority of my analyses uses DEMs. I obtained a 30 m resolution DEM from Anthony Arendt (Figure 2; personal communication, 2014). The bare earth DEM was clipped to include the Talkeetna Mountains and portions of the surrounding Copper River and Susitna River basins, the Alaska Range, and the Chugach Mountains. This DEM was derived from airborne interferometric synthetic aperture radar (IFSAR) data obtained in 2010 as a part of the Geographic Information Network of Alaska's (GINA) Alaska Mapped initiative. The DEM was projected into ArcMap using the North American Datum 1983 UTM Zone 6 projection coordinate system. I extracted elevation data from the DEM using ArcMap tools in order to analyze various characteristics including elevation, relief, topography, geomorphic indices and tectonic indicators.

3.2.2 Earthquake Hypocenters

Earthquake hypocenters and focal mechanisms were obtained from Natasha Ruppert (personal communication, 2014) who compiled a list of hypocenters within my area using the following parameters: depth from 0 to 25 km, all magnitudes, and magnitudes greater than 1.5 (Figure 13). There is a variable margin of error associated with the locations, including the station distribution and number of wave arrival picks that could be analyzed and used for locating. Focal mechanisms were also provided for certain earthquakes from depths of 0 to 30 km if sufficient data were available (Figure 14). Focal mechanisms were used to determine the orientation of the horizontal maximum stress and to constrain the type of faulting throughout the study area.

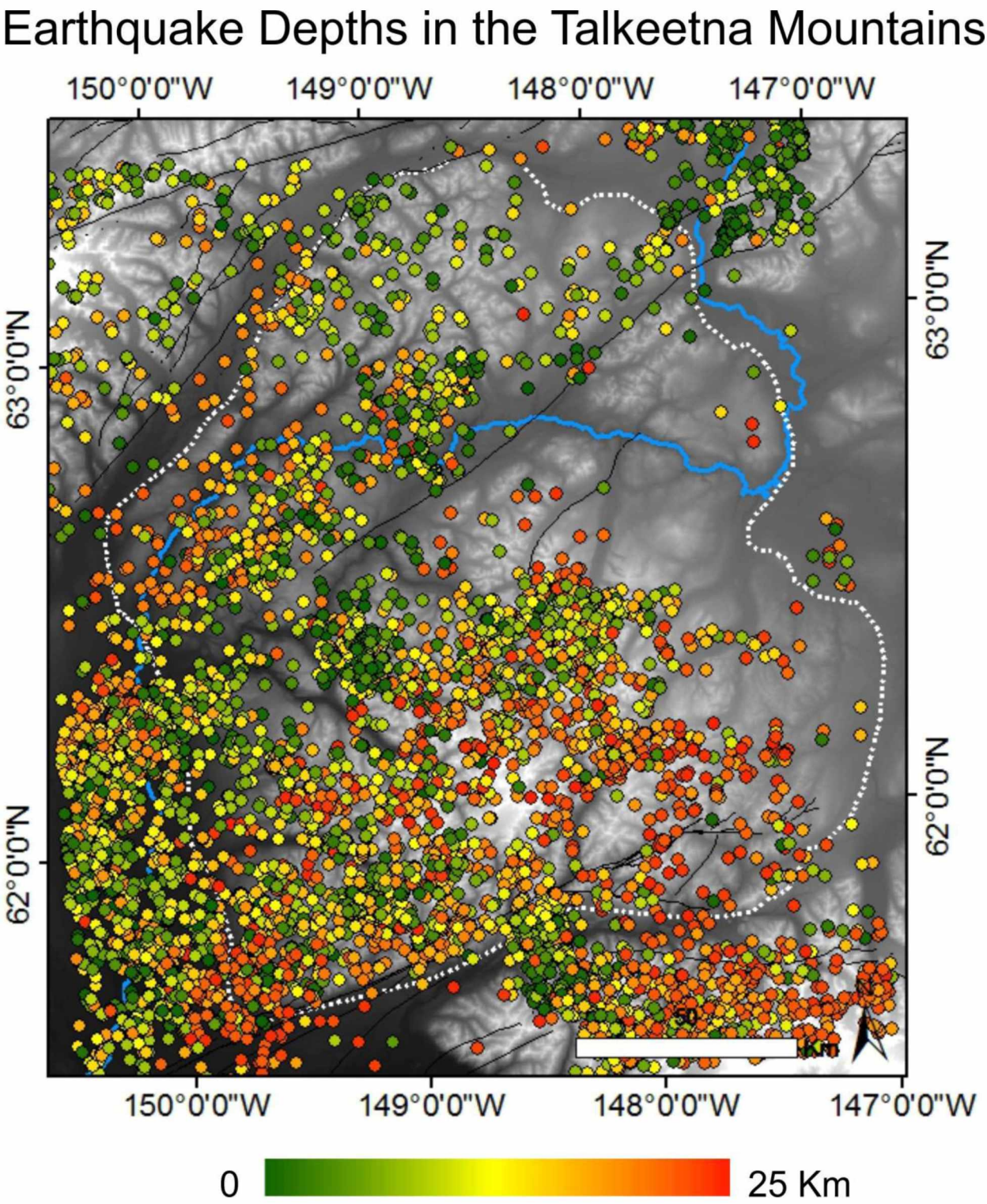

Figure 13. Earthquakes > *M1.5* in the Talkeenta Mountains from 1994 – 2014. The Talkeetna Mountains are outlined by the white dashed line. Mapped faults are shown as black lines; the Susitna River is shown in blue. Earthquakes are color-scaled by depth. The average magnitude in the study area is *M2*. More earthquakes are observed in the southern half of the study area and earthquake depths decrease to the north. (Natasha Ruppert, Personal Communication, 2015).

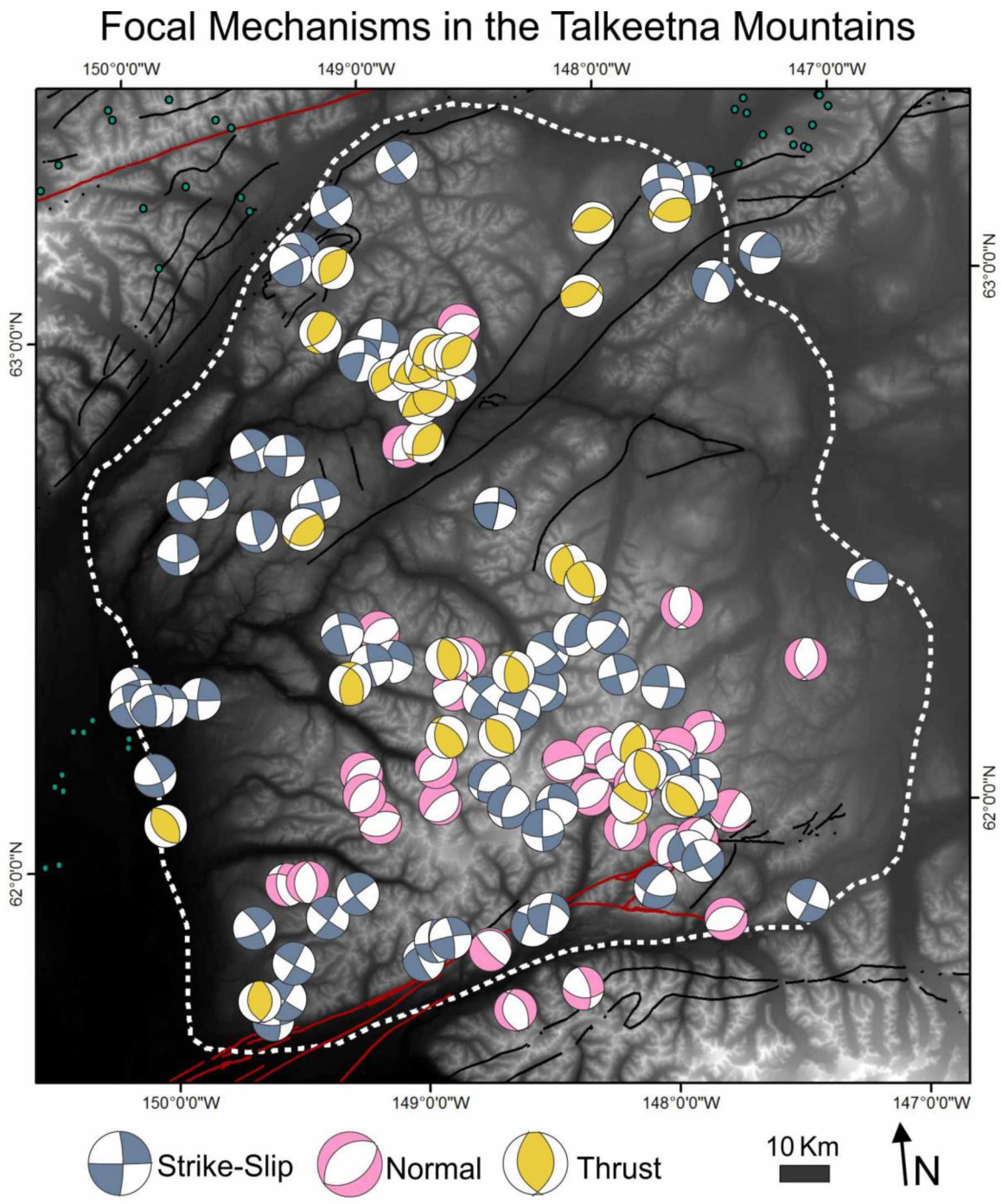

Figure 14. Earthquake focal mechanisms in the Talkeetna Mountains. The Talkeetna Mountains are outlined by the white dashed line. Major faults are shown in black and red. Red faults represent those that are active in Quaternary time. Focal mechanism data were provided by Natasha Ruppert (Personal Communication, 2015).

3.2.3 ArcGIS Geological Maps

Geological maps were obtained from US Geological Survey (USGS) databases for integrative use in ArcGIS for geological and geomorphic analyses. Maps for Talkeetna, the Talkeetna Mountains, Anchorage, and Healy using 1: 250,000-scale quadrangles were imported into ArcGIS. These maps were used along with the geological map by Hampton et al. (2007) to create a simplified geological map of the Talkeetna Mountains and surrounding areas (Figure 3). Geological maps were used in conjunction with DEMs and earthquake hypocenters to compare drainage networks with topographic anomalies and structural trends in order to identify areas of possible tectonic activity.

3.2.4 ArcGIS National Hydrology Dataset (NHD)

Stream network analysis was made possible through the USGS National Hydrology Dataset (NHD). I obtained a stream network map of the study area through the NHD website and imported the data into ArcGIS for geomorphic analysis (Figure 6). The NHD datasets are digital vector datasets designed to be used with geographic information systems (GIS). Streams in and around the Talkeetna Mountains were analyzed, including major drainage networks like the Susitna River, Copper River, Nenana River, Chulitna, and Delta River networks.

3.2.5 ArcGIS Late Wisconsin Glacial Extent Map

To determine the approximate amount of isostatic rebound in the Talkeetna Mountains I obtained a map of the glacial extent during the Late Wisconsin time (also known as the Last Glacial Maximum) in south-central Alaska (Figure 12). It was imported from the Alaska PaleoGlacier

Atlas (Manley and Kaufman, 2002) and used to reconstruct the ice sheet thickness over the Talkeetna Mountains during Late Wisconsin time. The Alaska PaleoGlacier Atlas is in an online database of maps that represent a geospatial summary of Pleistocene glaciation across Alaska (Manley and Kaufman, 2002).

3.2.6 Apatite Fission-Track Thermochronology (AFT)

To identify the age of uplift of the Talkeetna Mountains, I collected a total of five rock samples along a transect in the northwest Talkeetna Mountains and sent them to Paul O'Sullivan of GeoSeps Services for apatite fission-track thermochronology (AFT) analysis (Figure 11). The AFT data was used to determine an approximate age of regional uplift in the Talkeetna Mountains and to identify periods of rapid cooling rates that could be associated with uplift.

CHAPTER 4: RESULTS

4.1 Geomorphic Reconnaissance

The first phase of the geomorphic analysis was a reconnaissance investigation of the topography and drainage network morphology. Patterns and anomalies in topography and drainage networks identified areas in the Talkeetna Mountains that could be tectonically active. I investigated these areas further with quantitative geomorphic analysis.

4.1.1 Topographic Analysis

Examination of DEMs revealed changes in the distribution of elevation across the Talkeetna Mountains. These changes include topographic plateaus, lowlands, and dome-like highs. The north and northwestern Talkeetna Mountains consist of two small plateaus: the Northern Plateau and Chunilna Plateau (Figures 2 and 5). The southern Talkeetna Mountains have a large northeast-trending topographic dome, referred to as the Southern Dome (Figure 2 and 5). Between the plateaus in the north and the Southern Dome is a broad valley commonly referred to as the Fog Lakes Lowland (Figures 2 and 5). The Fog Lakes Lowland is a trapezoidal basin filled with Jurassic to Cretaceous meta-flysch of Kahiltna sequence, filled by Eocene Deadman volcanics, and bounded to the east by an extensional fault trending N30°E (O'Neill et al., 2003).

In a cross-sectional view, topographic profiles A-A', B-B', and C-C' all demonstrated what was observed aerially (Figure 5). Profile A-A', which extends from north to south, displays a slightly southward dipping Northern Plateau, followed to the south by the broad Fog Lakes Lowlands, and then the large Southern Dome, which has a sharp elevation drop near the Castle Mountain fault. Profile B-B' extends across the western Chunilna Plateau through the Fog Lakes Lowlands

and through the east side of the Talkeetna Mountains. The eastern boundary of the Fog Lakes Lowlands in profile B-B' showed a sharp jump in elevation to a topographic high, which represents the eastern edge of the Talkeetna Mountains. Profile C-C' extends across the northeast-trending ridgeline of the Southern Dome. Though these profiles are exaggerated, the slope on the eastern side of the Southern Dome is more gradual than the slope on the western side due to a higher base elevation of the Copper River basin in the east as compared to the Susitna River basin in the west.

4.1.2 Drainage Patterns

Examination of the drainage network morphology revealed several noteworthy patterns including strongly linear drainages, radial drainages, barbed drainages, and a change in river morphology of the Susitna River.

The pronounced linearity of drainages may be evidence of a fault since water tends to preferentially erode more fractured rock in order to find the path of least resistance. Several drainages in the northern half of the Talkeetna Mountains follow a northeast structural fabric; some of these are situated in previously mapped faults (Figure 6).

Radial drainage may indicate the presence of an uplifted dome or antiformal structure. It is common for radial drainage to center on the apex of structures likes this. This particular drainage pattern is dominant in the southern half of the Talkeetna Mountains and includes the topographic Southern Dome, where the drainage divide coincides with a northeast-trending ridgeline (Figure 6).

Barbed drainages or drainages that turn 90° or more downstream into adjacent valleys commonly indicate a stream capture event caused by uplift or faulting. Barbed drainages in the Talkeetna Mountains are circled in Figure 6. Some of these make nearly 180° degree turns into adjacent stream valleys and several of them have produced wind gaps. The largest and most significant of the barbed drainages occurs along the Susitna River. As the river begins to cross the northeastern Talkeetna Mountains, its downstream direction abruptly changes from southward to westward (Figure 6). Most of the barbed drainages are observed in the eastern half of the Talkeetna Mountains.

Changes in river morphology can be related to changes in lithology and/or active uplift. The Susitna River has morphology changes that are characteristic of a river that is flowing through an actively uplifting structure. The stream is wide and braided as it flows south from its headwaters in the Alaska Range on the eastern side of the Talkeetna Mountains. However, once it makes the abrupt westward turn into the mountains, it becomes narrower and begins incision into the bedrock. As the river begins to exit the Talkeetna Mountains in the west, it turns to the south and becomes wide and braided again as it flows toward the Cook Inlet (Figure 6).

Stream incision is an indicator of changes in base level, which are often linked to tectonic uplift. Incision was observed in valley profiles along the Susitna River through the Talkeetna Mountains where valley profiles were narrow and V-shaped (Figure 15).

4.2 Geomorphic Indices

Quantitative geomorphic analysis can identify areas that could be tectonically active. I divided the Talkeetna Mountains into 170 drainage basins and applied several different geomorphic

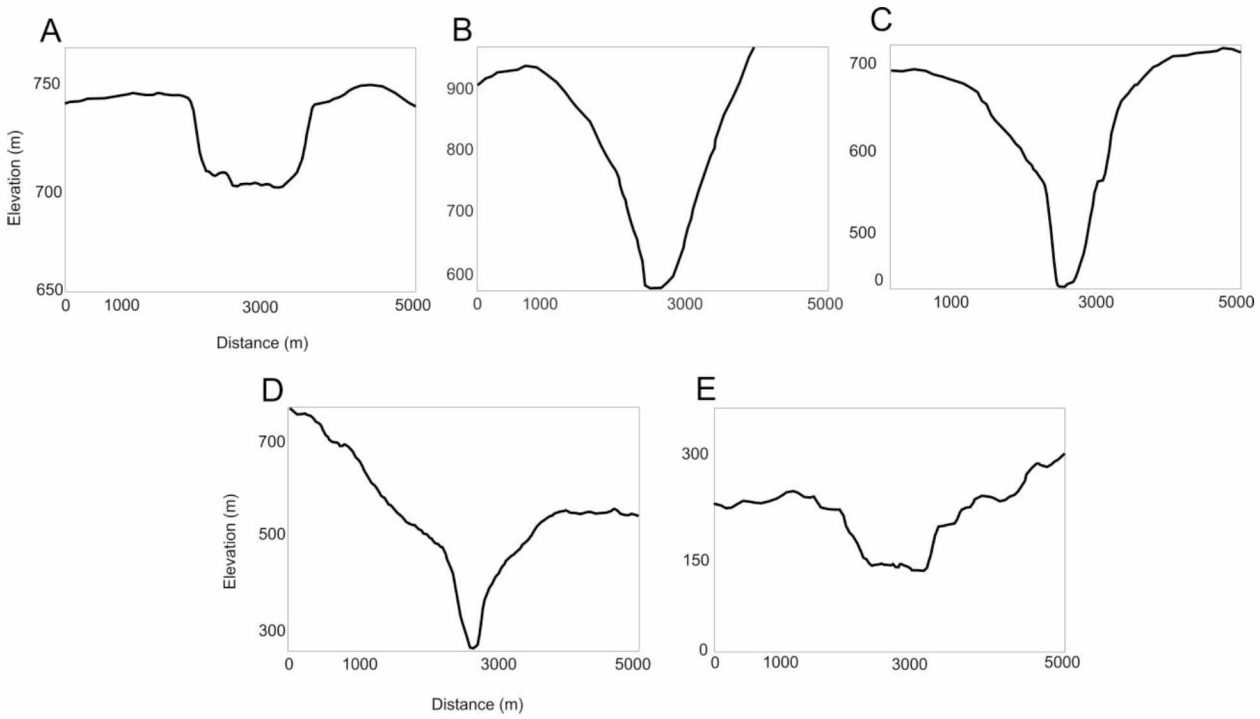

Figure 15. Valley profiles A-E of the Susitna River as marked by the red lines on Figure 6. These profiles show the change in the Susitna River's profile from broad valley floors outside of the Talkeetna Mountains to incision of deep V-shaped valleys within the Talkeetna Mountains.

indices to each basin to develop a regional map of geomorphology that may reflect neotectonic activity.

4.2.1 Hypsometric Integral (HI)

To better analyze the HI distribution throughout the Talkeetna Mountains, I produced a map where each drainage basin was color-scaled based on its HI value; basins with high values are shown as warmer colors (Figure 16). In the 170 drainage basins, HI values ranged from 0.12 to 0.7 (Figure 16). The majority of basins have intermediate HI values, suggesting that they are at a mature state in the cycle of erosion, though some areas have high HI values representing more

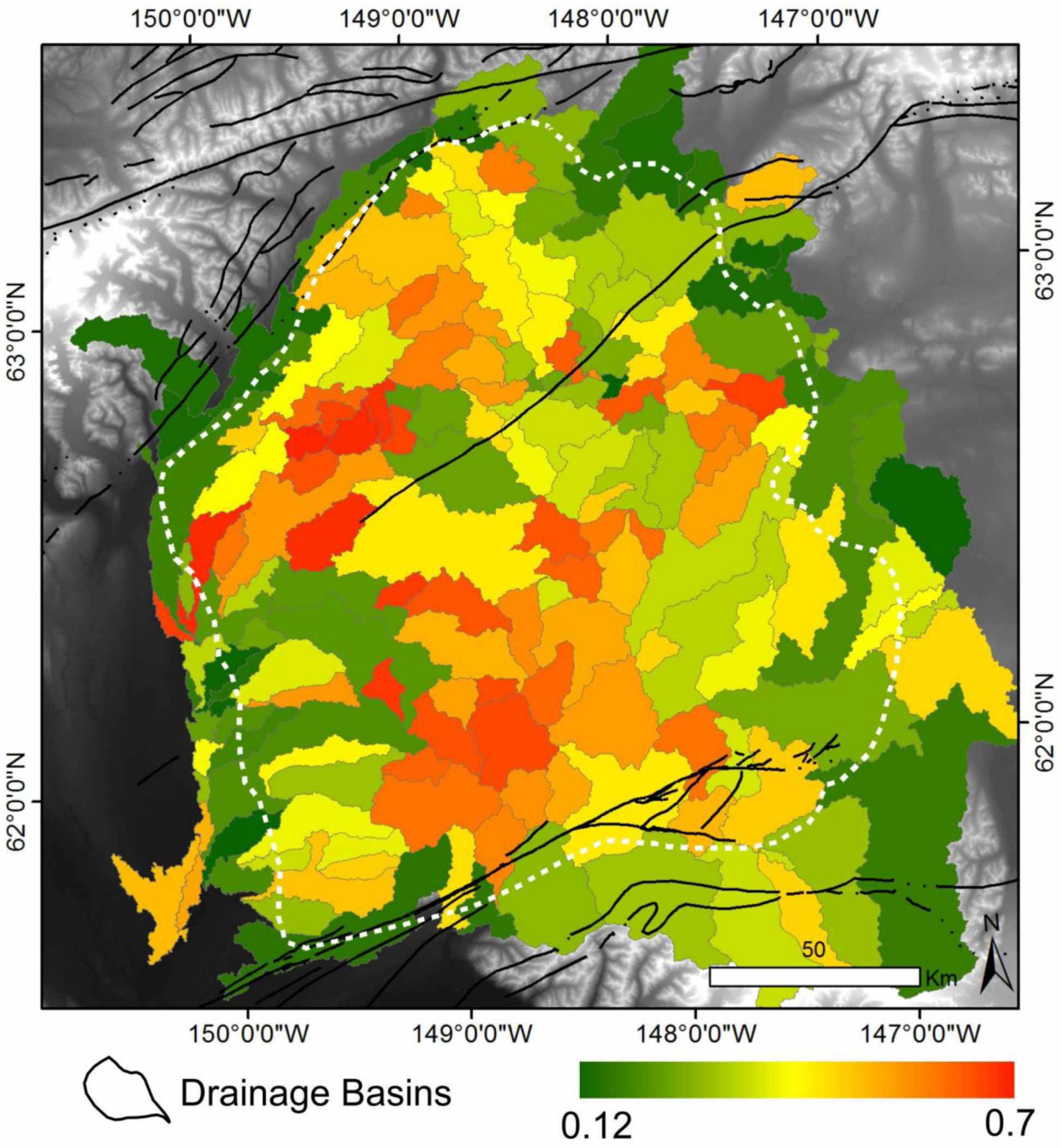

Figure 16. Hypsometric Integral (HI) map of drainage basins in the Talkeetna Mountains. The HI was calculated for 170 drainage basins and are color-scaled from low to high values. High values represent drainage basins that are in a youthful stage of erosion and are interpreted to reflect recent uplift or faulting.

youthful or active states. Drainage basins with the highest values of HI (≥ 0.55) are located along the Chunilna Plateau, the center of the Southern Dome, and near the barbed drainage of the Susitna River in the east. These basins are surrounded by intermediate HI values (0.55 to 0.35). Intermediate values are also observed in the center of the Northern Plateau and near the Castle Mountain fault to the south. Drainage basins with the lowest HI values (<= 0.35) are associated with topographic basins that form the border of the Talkeetna Mountains.

There was no consistent relationship between lithology and HI value. High HI values were found in both hard and soft rock types. Low values were also equally distributed among different rock types.

4.2.2 Drainage Basin Asymmetry Factor (AF)

The drainage basin AF is a measure of stream deflection. Past studies have used this method to infer that values as low as 5 represent significant asymmetry (Mahmood and Gloaguen, 2012). In the Talkeetna Mountains, many basins show evidence of stream deflection to one side or the other, with AF values ranging from 0.17 to 49 (Figure 17). In an effort to be more conservative, only those basins where the value of AF is greater than 10 are considered to represent significant drainage basin asymmetry. To avoid false interpretations, I decreased the AF values of the south facing slope of the southern Talkeetna Mountains by 50%. This way my interpretations in these areas would be less affected by deflection due to climate-controlled erosion. In the resulting AF map where higher values were observed, basins are shown in warmer colors (Figure 17).

Of the 170 basins in the study area, 90 basins have an AF value of greater than 10. These basins are widely distributed throughout the Talkeetna Mountains. Analysis of the direction of drainage

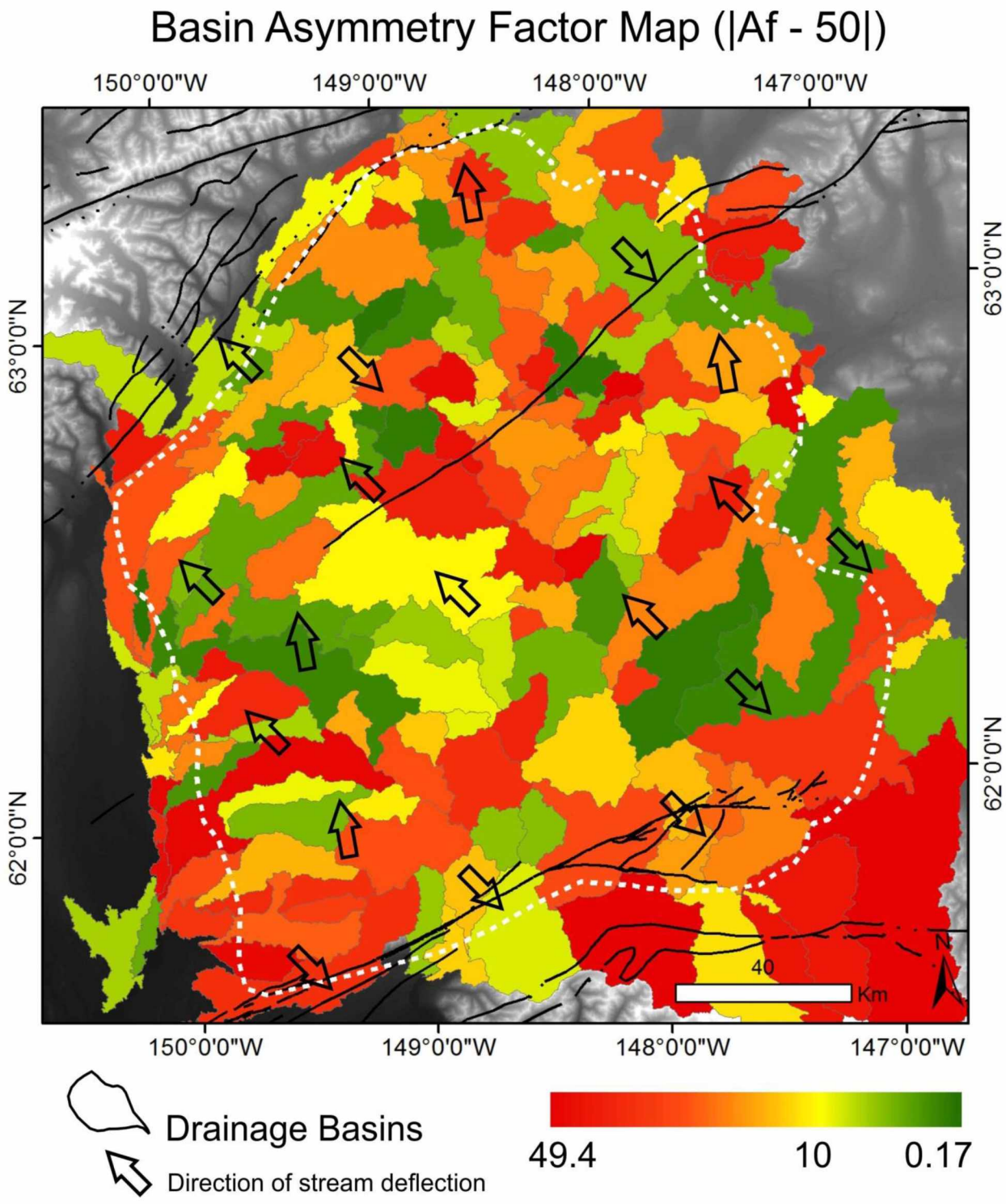

Figure 17. Basin asymmetry map (Af) of the Talkeetna Mountains. High values represent drainage basins with significant drainage asymmetry caused by the deflection of the main river to one direction. The Talkeetna Mountains are outlined by the white dashed line. Black arrows represent the average direction of drainage deflection in the surrounding basins.

deflection in these basins shows that the majority of basins have drainages that deflect to the north-northwest; however, basins on the southern side of the Southern Dome ridgeline have deflected drainage to the southeast (Figure 17).

4.2.3 Valley Floor Width-to-Height Ratio (Vf)

Valley profiles were extracted in each of the 170 drainage basins and elevation values were found following the example in Figure 9. Since this is an area that has experienced extreme glaciation in the past most valleys already have a broad U-shape. To overcome this, I focused on the erosion created by present-day streams within the ancestral U-shaped valleys. This allowed a focus on sites where actively flowing rivers in the Talkeetna Mountains are presently eroding valleys. Where the drainage basin covered a considerable length of the river, a Vf was calculated along multiple spots and averaged together. Values < 1 are associated with V-shaped valleys formed by actively incising rivers in uplifting areas and values > 1 represent broad U-shaped valleys associated with low uplift rates where the stream was able to cut broad valley floors (Keller and Pinter, 2002).

The Vf values range from 0.01 to 161 across the Talkeetna Mountains (Figure 18), suggesting that both V- and U-shaped valleys are present. Higher values associated with broad valley floors are more dominant on the eastern half of the Talkeetna Mountains, with the exception of the area surrounding the barbed drainage of the Susitna River. Lower values associated with incising valleys are more dominant on the western half of the Talkeetna Mountains, with a concentration in the Southern Dome, the Northern Plateau, the Chunilna Plateau, near the Susitna River, and the Castle Mountain fault.

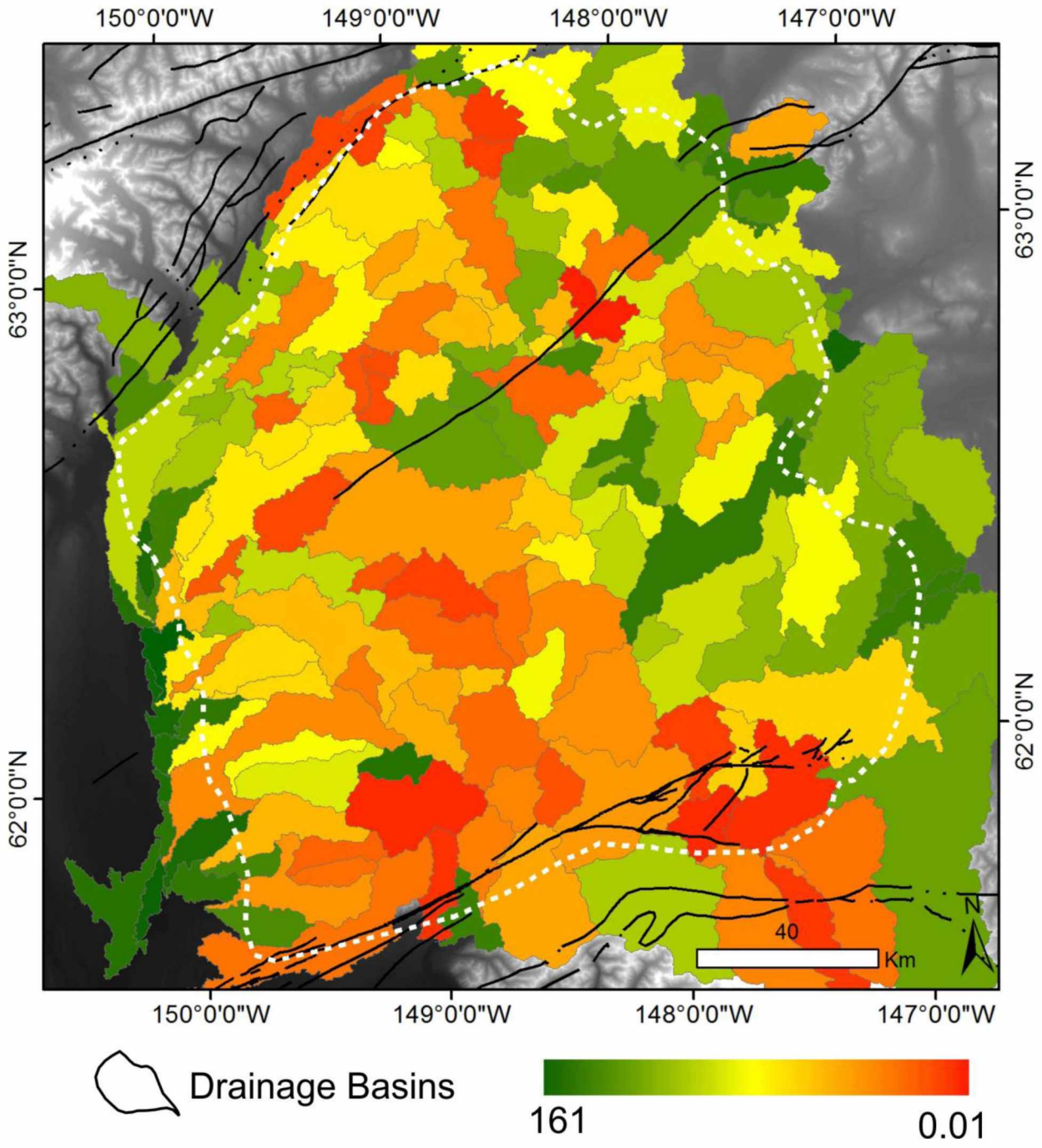

Figure 18. Valley floor width-to-height (Vf) ratio map of drainage basins in the Talkeetna Mountains. High values represent drainage basins whose valley is more narrow, incised, and V-shaped as opposed to those with broadly cut valley floors. The Talkeetna Mountains are outlined by the white dashed line; mapped faults shown in black.

4.2.4 Index of Relative Active Tectonics (IRAT) Map

Individual geomorphic indices are useful indicators of neotectonic activity but they are more effective when used in combination. Therefore, I generated the index of relative active tectonics (IRAT) map based on the averaged geomorphic indices (Figure 19). In the IRAT map, drainage basins range from Class 1 to Class 8, where higher classes represent areas that are more likely to be tectonically active and those with a lower class represent areas that are likely inactive relative to other basins.

The IRAT map shows a similar pattern of high versus low classes of tectonic activity observed in the individual geomorphic index maps. The highest classified basin is located on the Chunilna Plateau in the Kahiltna basin assemblage (Figure 19). Classes 1 to 3 make up 41 of the 170 drainage basins and are located along the stretch of the Susitna River as it flows through the majority of the Talkeetna Mountains, the center of the Southern Dome, and surrounding the Castle Mountain fault and fault splays (Figure 19).

This map shows a west-northwest trending divide between lower class basins to the east and higher class basins to the west, only interrupted by the areas of the Fog Lakes Lowlands, Susitna River barbed drainage, and the Castle Mountain fault splays (Figure 19).

4.2.5 Stream-Length Gradient Index (SL)

I used ArcGIS to generate a SL gradient index map of larger rivers in the Talkeetna Mountains and color-scaled the river reaches according to their SL index value. This map was compared to other geomorphic index maps to better identify areas of possible activity (Figure 20). The SL values in the Talkeetna Mountains range from 3 to 1974. Anomalously high values (>1000) are

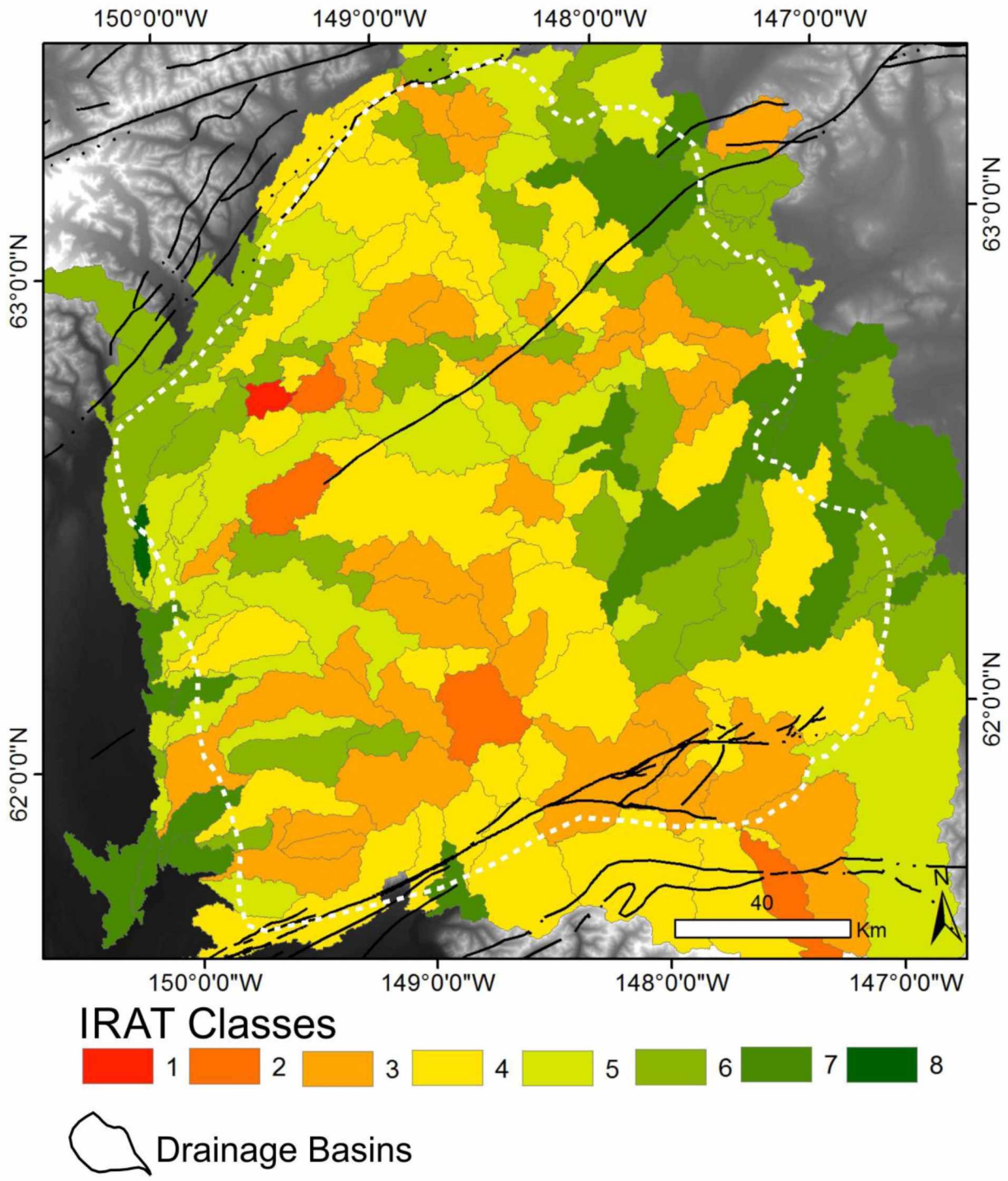

Figure 19. Index of relative active tectonics (IRAT) map. The IRAT index represents the averaged values of the hypsometric integral (HI), drainage basin asymmetry factor (AF), and the valley floor width-to-height ratio (Vf). The IRAT values are subdivided into 8 classes, with class 1 representing drainage basins with the highest likelihood of neotectonic activity relative to the study area. The Talkeetna Mountains are outlined by the white dashed line; major faults are shown in black.

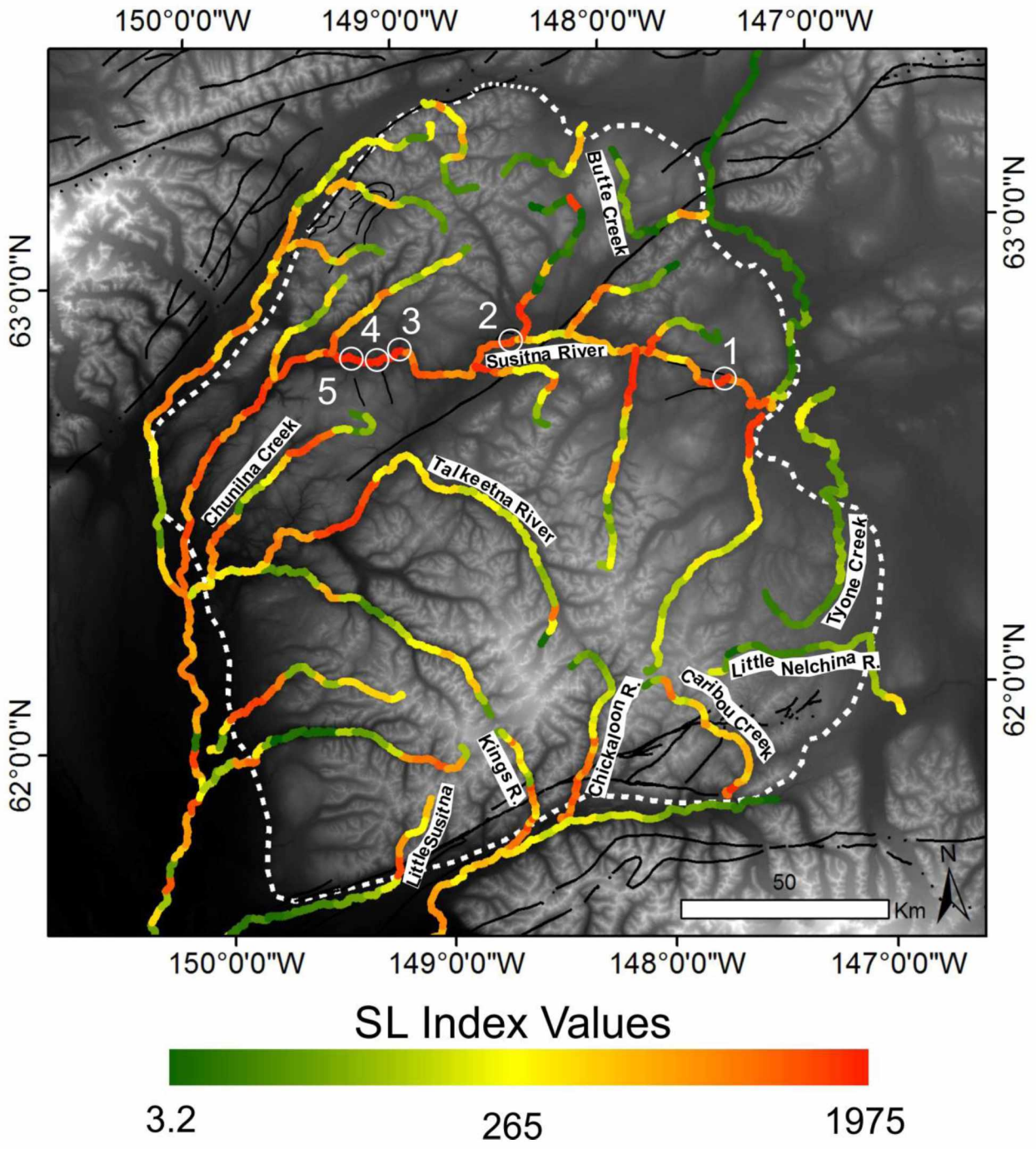

Figure 20. Stream length gradient index map of the drainage network in the Talkeetna Mountains. The Talkeetna Mountains are outlined by the white dashed line and major faults are shown in black. Rivers referenced in text are labeled and knickpoints are numbered and circled in white and correlate to the knickpoints in Figure 21. SL Index values that are anomalously high along a river are indicative of stream reaches that may be tectonically active.

located in the central Talkeetna Mountains along the Susitna River (Figure 20). These high SL values correlate to previously mapped faults along the Susitna River (Figure 20). The SL values remain higher as the river circles the Chunilna Plateau, and values vary from 500 to 813. Middle reaches of the Chunilna Creek and the Talkeetna River, which run through and around the Chunilna Plateau, have moderate to high SL values that range from 300 to 915.

The SL index values across the Southern Dome are moderate to high, ranging from 200 to 600. Tyone Creek and Little Nelchina River are the easternmost rivers flowing out from the Southern Dome and have notably low SL values from 3 to 249 within the boundaries of the Talkeetna Mountains. Rivers on the south side of the Southern Dome have high SL values from 249 to 1186. The rivers from west to east are the Little Susitna River, Kings River, Chickaloon River, and Caribou Creek. These rivers have higher SL values where they cross the Castle Mountain fault and Caribou fault splays (Figure 20).

Overall, lower SL values are observed on the eastern edge of the Talkeetna Mountains and higher values are observed near the Castle Mountain fault and Caribou fault splays, near some previously mapped faults along the Susitna River, along the Chunilna Plateau, and along the northwest edges of the Talkeetna Mountains (Figure 20).

4.2.6 Susitna River Longitudinal Stream Profile

The Susitna River was ideal for longitudinal stream profile analysis because it is the largest river in the study area, has an interesting change in morphology, and cuts through the entire range of the Talkeetna Mountains. I have evaluated a longitudinal stream profile for the Susitna River for anomalous profile characteristics (Figure 21). In the areas where profiles deviated from a graded

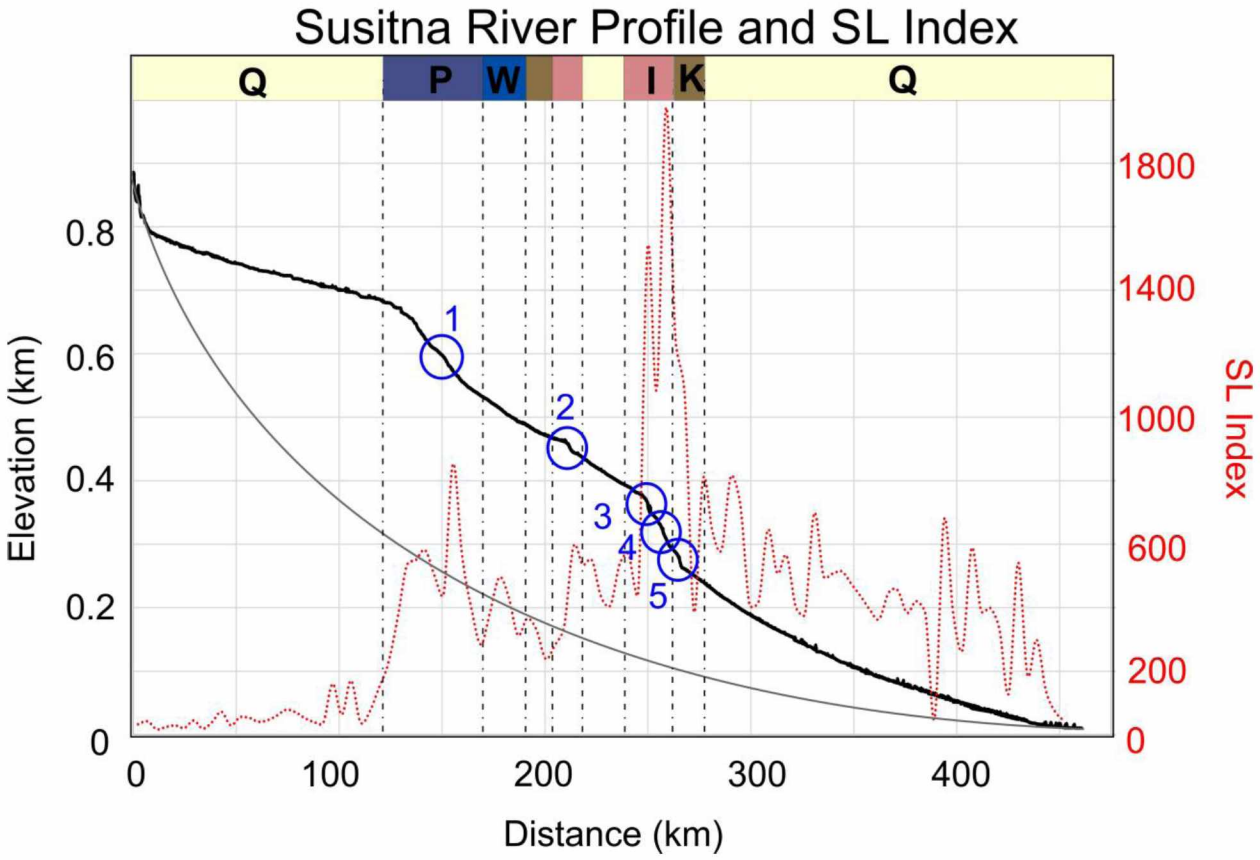

Figure 21. Longitudinal stream profile and SL for the Susitna River. The bold black line represents the longitudinal profile of the Susitna River. The thin gray line represents a profile that would be expected of a graded river in equilibrium. The red dashed line represents the stream-length gradient index (SL Index) along individual reaches of the Susitna River. Knickpoints are circled by in blue and are also identified on the SL Index map in Figure 20 as white circles. The simplified geology along the rivers path is shown at the top of the graph and correlates with the colors shown in the regional geology figure (Figure 3).

Q = Quaternary sediments, P = Peninsular terrane, W = Wrangellia terrane, K = the Kahiltna basin, I = Igneous intrusions.

river profile, I checked the rock types associated with that reach along the stream. If the deviation was not obviously caused by a lithological change, I compared the location with mapped faults in the area. This analysis helped to identify evidence of active faulting and uplift.

The longitudinal stream profile of the Susitna River is quite different than that of a graded river that has reached equilibrium and is in an area of tectonic quiescence (Keller and Pinter, 2002). A typical graded profile is concave with a steep gradient near the headwaters that gradually decreases as the river reaches base level. The Susitna River's profile is convex in comparison, with multiple deviations from a graded river profile (Figure 21). The convex curvature of the Susitna River profile occurs where the stream begins to enter the Talkeetna Mountains and gradually subsides as the stream is exiting the Talkeetna Mountains.

A knickpoint is a pronounced break in slope of a river's longitudinal profile. Along the Susitna River profile, three areas that have the most pronounced knickpoints are circled on Figure 21. These knickpoints correspond with mapped faults or prominent lineations and with high SL values. The first knickpoint observed is in the eastern Talkeetna Mountains and lies along a previously mapped fault. The second knickpoint is near locally mapped thrust faults and is also just upstream of the proposed site for the Susitna-Watana hydroelectric dam. The last three knickpoints are located along the north side of the Chunilna Plateau and are observed as three consecutive stair-stepping knickpoints in the longitudinal profile (Figure 21). These knickpoints are just north of mapped northwest-trending strike-slip faults in the Chunilna Plateau (Figure 20). Lineations related to the strike-slip faults extend toward the Susitna River near the knickpoints and are associated with the highest SL values in the Talkeetna Mountains (Figure 20).

There does not appear to be any relationship between lithologic contacts and knickpoints. The Susitna River crosses many different rock types, including sedimentary and plutonic rocks. All

knickpoints occur within individual rock units rather than at contacts with adjacent units (Figure 21).

4.3 Apatite Fission-Track Thermochronology (AFT)

Table 2 summarizes details of the apatite fission-track samples collected during this study and the initial analytical results, including sample name, collection elevation, pooled age, number of grains used, number of spontaneous tracks found, average track length, and Dpar of tracks. The Dpar is the diameter of the fission track parallel to the apatite crystal c-axis and is a kinetic proxy for how fast a sample went through the PAZ (Ketcham et al., 1999). Samples were collected from the northwest Talkeetna Mountains, and their locations can be found in Figure 11 along with their pooled ages.

4.3.1 AFT Age Results

Table 2. Summary of AFT results from the northwest Talkeetna Mountains.

Sample	Elevation (m)	AFT Age, 1 SD (Ma)	Number of Grains	Spontaneous Tracks	Track Length, 1 SD (µm)	Dpar (µm)
DCM01	1456	34.38 ± 0.23	39	117	12.58 ± 1.75	1.92
DCM02	1342	35.28 ± 0.23	39	57	13.14 ± 1.62	1.85
DCM03	1306	36.71 ± 0.23	39	114	12.61 ± 1.74	2.02
DCM05	1260	37.71 ± 0.23	27	55	12.13 ± 2.02	1.99
DCM06	1360	55.35 ± 0.23	37	128	13.37 ± 1.64	2.07

The AFT pooled ages range from ca. 55 to 34 Ma; four samples have a clustered age range from 37 to 34 Ma. One sample is clearly older at 55 Ma and was located just south of sample DCM05 (Figure 11). Track-length distribution was tight and mean track lengths ranged from 12.13 μm to 13.37 μm. Dpar ranged from 1.85 to 2.07, which suggests fast-annealing grains (Ketcham et al., 1999).

4.3.2 HeFTy Modeling Results

The HeFTy inverse models for all five samples display similar time-temperature uplift paths (Figure 22a-e). Based on the time-temperature curves and the weighted-mean path of all samples, a faster cooling rate is modeled from ca. 45 to 30 Ma (~3.5°/Ma), followed by a period of slower cooling rates (~1.25°/Mya) until approximately 10 Ma where the cooling rate increases to present day (~6°/Mya). The goodness of fit (GOF) of the time-temperature curves ranges from 94% to 97%, and the GOF for the track-length distribution ranges from 77% to 100% (Figure 22a-e). This indicates that the modeled data matches well with the measured AFT data.

The HeFTy models can be used to calculate averaged uplift rates for the study area by analyzing the slope of the weighted-mean curve using the standard geothermal gradient of 25°C/km. The first period of rapid cooling from 45 to 30 Ma has an averaged uplift rate of 0.14 mm/yr, while the following period from 30 to 10 Ma has an uplift rate of 0.05 mm/yr, and the final period of rapid cooling from 10 Ma to present has an uplift rate of 0.24 mm/yr (Figures 22a – e).

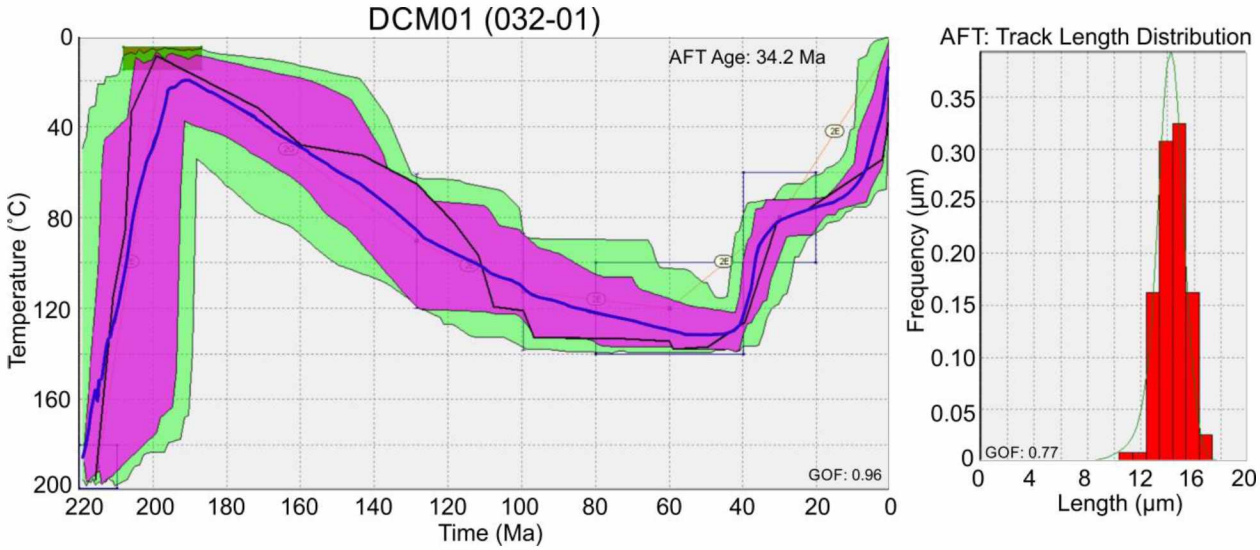

Figure 22a. HeFTy model and track length distribution sample DCM01 (032-01). Location of sample shown on Figure 7. Purple and green areas represent good and acceptable path envelopes, respectively. Black and dark blue lines represent the best fit curve and the weighted mean path, respectively.

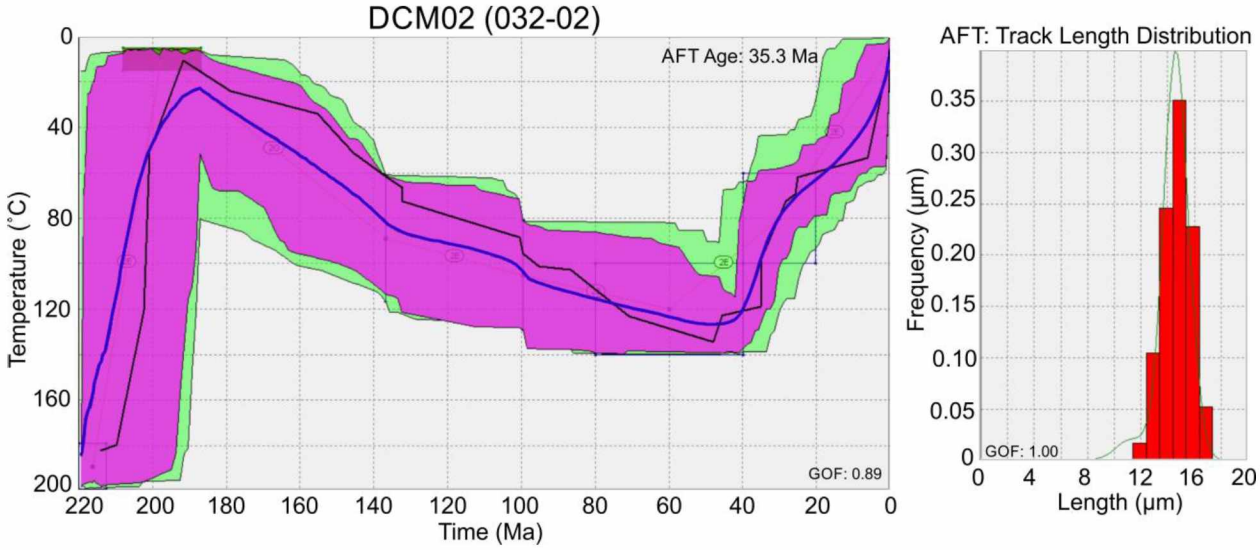

Figure 22b. HeFTy model and track length distribution sample DCM02 (032-02). Location of sample shown on Figure 7. Purple and green areas represent good and acceptable path envelopes, respectively. Black and dark blue lines represent the best fit curve and the weighted mean path, respectively.

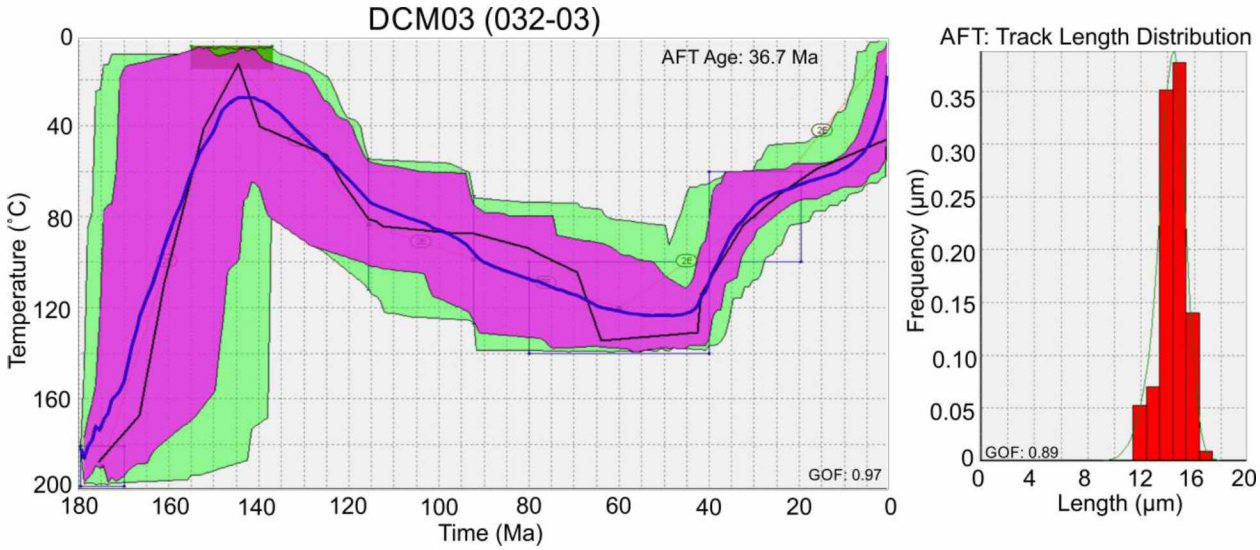

Figure 22c. HeFTy model and track length distribution sample DCM03 (032-03). Location of sample shown on Figure 7. Purple and green areas represent good and acceptable path envelopes, respectively. Black and dark blue lines represent the best fit curve and the weighted mean path, respectively.

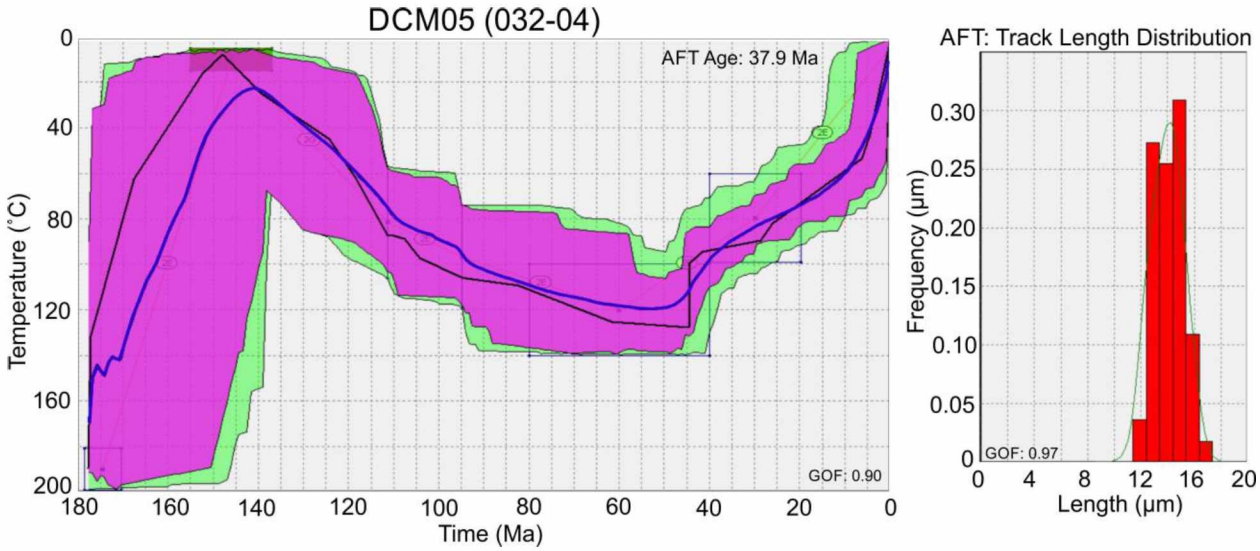

Figure 22d. HeFTy model and track length distribution sample DCM05 (032-04). Location of sample shown on Figure 7. Purple and green areas represent good and acceptable path envelopes, respectively. Black and dark blue lines represent the best fit curve and the weighted mean path, respectively.

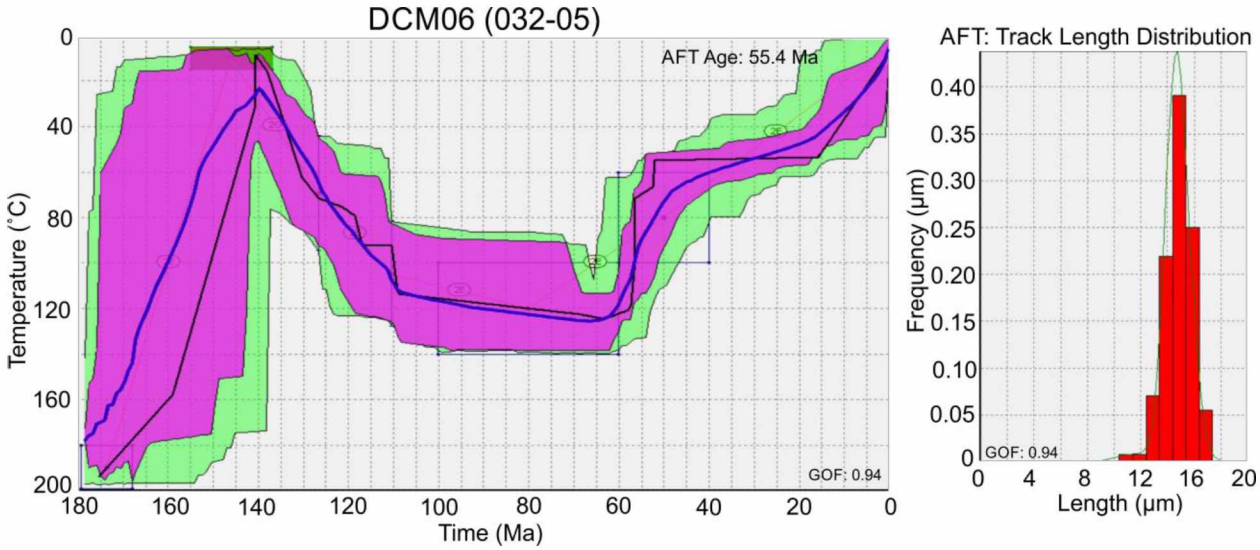

Figure 22e. HeFTy model and track length distribution sample DCM06 (032-05). Location of sample shown on Figure 7. Purple and green areas represent good and acceptable path envelopes, respectively. Black and dark blue lines represent the best fit curve and the weighted mean path, respectively.

4.3.3 Distribution of Other Published Thermochronology Data

I compiled thermochronology data from two other studies in the area and observed the differences in interpreted uplift ages. Their locations and ages are shown in Figure 10. The two ages found from samples in the middle of the Talkeetna Mountains have pooled AFT ages of 44.45 and 107.12 Ma. These samples were collected as part of the detailed mapping of the Talkeetna Mountains C-4 quadrangle (Twelker et al., 2015). The second set of samples in the southwest corner of the Talkeetna Mountains consists of apatite (U-TH)/He (AHe) samples from Hoffman (2005). Their ages range from 16.36 to 70.38 Ma, with a cluster of ages from 16 to 20 Ma (Figure 11).

4.4 Glacial Isostasy

In order to determine the amount of rebound and uplift due to glacial loading, I determined the thickness of the Late Wisconsin ice sheet over the Talkeetna Mountains and calculated the amount of uplift due to glacial isostasy. I then used a simple isostatic rebound equation to approximate the amount of rebound due to glacial loading (Middleton and Wilcock, 1994; Nye, 1952).

The generated theoretical ice sheet thickness profile based on Nye's 1952 calculations was compared to the reconstructed ice sheet profiles (Figure 23). The close match between the two profiles suggests that the ice sheet over the study area did indeed match the behavior of the theoretical profile (Figure 23). Therefore, I could use the theoretical profile to determine the maximum thickness of the Late Wisconsin ice sheet.

The average ice sheet thickness determined using this method was 1.15 km. Using this thickness in the isostatic rebound equation indicates that approximately 0.32 km of asthenosphere displacement would have occurred due to glacial loading during the Late Wisconsin glacial event. Since glacial extent was greater than it was at the Last Glacial Maximum over the study area, this is likely a conservative estimate but represents the minimum amount of glacial rebound that would have occurred after the onset of glacial melting.

4.5 Structural Analysis

Most of the structural studies done in the Talkeetna Mountains have focused on particular structures or on site-specific areas in relation to the Susitna-Watana hydroelectric dam project or mineral exploration (Acres, 1982; Hampton et al., 2010, 2007; Twelker et al., 2015). I conducted

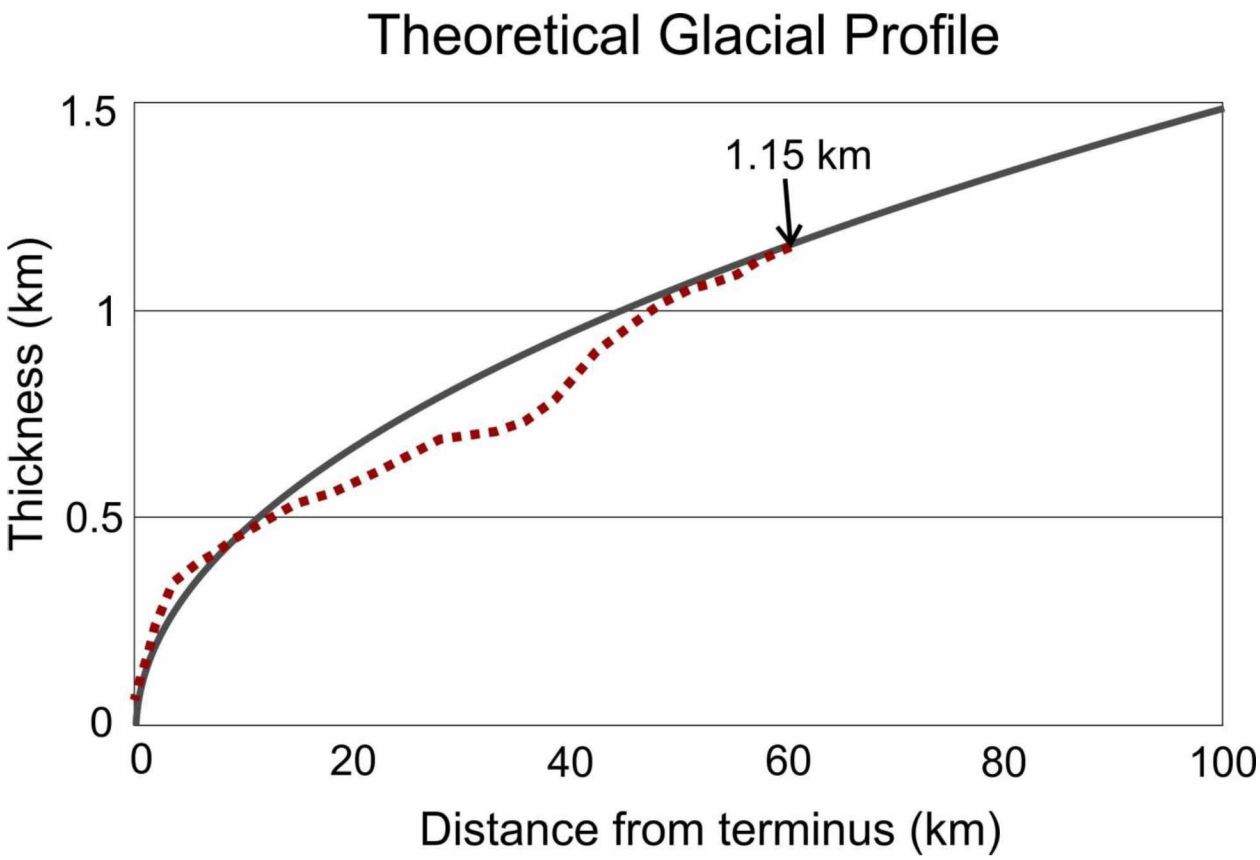

Figure 23. Theoretical glacial profile and the reconstructed ice sheet thickness over the Talkeetna Mountains during Late Wisconsin. Theoretical profile of ice sheet thickness is shown in gray and is based on Nye's 1952 calculations. The red dashed line represents the ice sheet profile over the Talkeetna Mountains based on the glacial extent during the Late Wisconsin time. This comparison suggests that the minimum ice sheet thickness over the Talkeetna Mountains during Late Wisconsin was 1.15 km.

a regional-scale structural analysis using earthquake hypocenter and focal mechanism data. This study found many significant variations in the depths and concentrations of earthquakes across the Talkeetna Mountains and changes in stress regimes laterally and vertically across the study area.

The average magnitude of earthquakes in the Talkeetna Mountains is M2. Earthquake hypocenter data shows that hypocenter depths decrease from south to north across the Talkeetna Mountains (Figure 13). Hypocenters are more abundant in the southern Talkeetna Mountains

around the Southern Dome and decrease in abundance toward the north. Hypocenters are clustered near the Chunilna Plateau and north of the U-shaped bend in the Susitna River in the Northern Plateau (Figure 13). The eastern Talkeetna Mountains shows a distinct lack of seismicity compared to the surrounding areas.

Focal mechanism data shows a variation in fault types and in horizontal maximum stress orientation across the Talkeetna Mountains (Figure 14). Strike-slip and thrust fault stress regimes are present in all areas. Strike-slip faults dominate the Chunilna Plateau, and strike-slip and thrust faults dominate the Northern Plateau. These areas are under a northwest to southeast horizontal maximum stress according to the fault mechanisms. Strike-slip and thrust fault focal mechanisms in the Southern Dome and around the Castle Mountain fault suggest an approximate east to west maximum horizontal stress orientation over most of the area. This area is also defined by an abundance of normal fault solutions oriented east to west; however, these are found only at depths below 25 km. Above 25 km in this area, no normal faults are observed in the focal mechanism data. The area around the Castle Mountain fault at the southern edge of the Talkeetna Mountains is almost entirely dominated by strike-slip fault regimes.

CHAPTER 5: ANALYSIS AND DISCUSSION

In this chapter, I will subdivide the Talkeetna Mountains based on the integration of geomorphology, thermochronology, and structural analysis and discuss how and why the Talkeetnas have deformed heterogeneously. I will then present models that explain the variation in deformation in the context of regional structure and tectonics in order to better understand how the Talkeetna Mountains fit into the tectonic framework of south-central Alaska.

5.1 Structural Domains of the Talkeetna Mountains

It is evident that the Talkeetna Mountains are accommodating deformation heterogeneously based on spatial variations in topography and drainage patterns, geomorphic indices, the location of seismicity, the orientation of horizontal maximum stresses, and fault types across the study area. In order to better understand this heterogeneity, I divided the Talkeetna Mountains into four different structural domains. The characteristics of each domain are summarized in Table 3 and Figure 24.

5.1.1 Domain 1

Domain 1 is located in the northern Talkeetna Mountains and generally lies north of the Talkeetna thrust fault trace. This domain includes the Northern Plateau, the Chunilna Plateau, Fog Lakes Lowlands, and the Kahiltna sequence. Topographically, this domain is defined by plateaus and lowlands, northeast-trending drainages, and barbed drainages. This domain is characterized by relatively shallow seismicity compared to the rest of the study area with the majority of earthquakes at depths between 5 and 15 km (Figure 24). It is within a strike-slip and

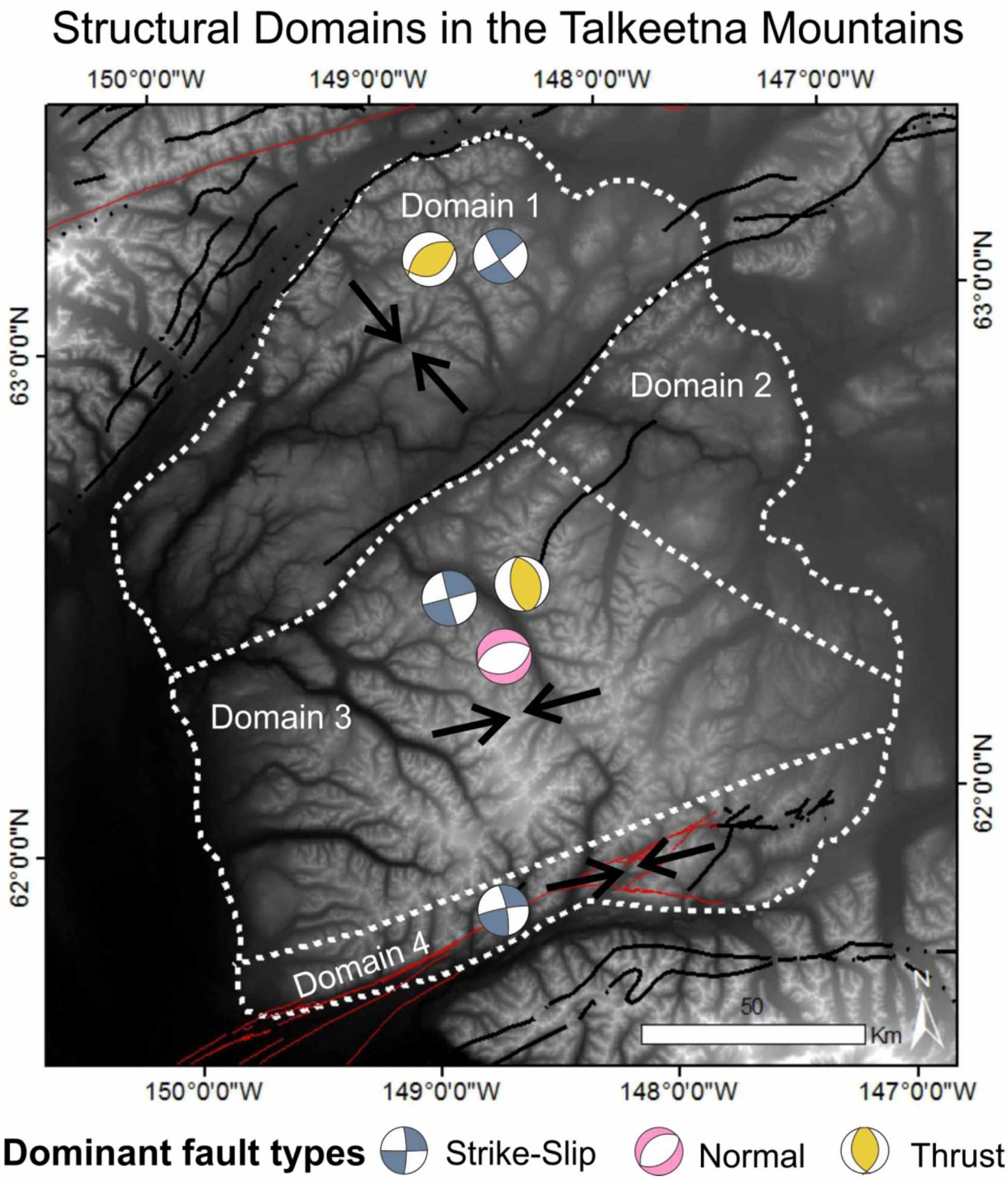

Figure 24. Structural domains of the Talkeetna Mountains. Domains are outlined with white dashed lines and are based on the presence or absence of seismicity, the dominant fault types, and the orientations of horizontal maximum stress (black arrows). Characteristics of the domains are described in Table 3.

thrust fault stress regime, and the average orientation of maximum horizontal stress is northwest to southeast, based on the orientations of fault mechanisms (Figure 14).

Quantitative geomorphic analyses, including the HI, AF, Vf, IRAT, and SL gradient index, revealed multiple areas of possible tectonic activity in Domain 1. These areas included the Chunilna Plateau and the center of the Northern Plateau which had high classes of likely tectonic activity according to the HI, Af, Vf, and IRAT maps (Figures 16 – 19). Geomorphic indices suggest that the Chunilna Plateau and the center of the Northern Plateau have youthful landscapes, incised V-shaped valleys, and strong evidence for north-northwest stream deflection or valley tilt. All geomorphic indices support that these areas have experienced neotectonic activity. The eastern half of domain 1 is less neotectonically active relative to the Chunilna Plateau and the center of the Northern Plateau, with moderate to old aged landscapes and more broadly cut valley floors.

The AFT samples from the northwest Talkeetna Mountains in Domain 1 have clustered ages from 34.38 to 37.71 Ma and an outlier age of 55.35 Ma (Table 2; Figure 11). Their age distribution along a northwest to southeast transect suggests that uplift in this area began in the southeast and progressed to the northwest, along a series of Tertiary northwest vergent thrust faults (Hampton et al., 2007; Figure 11). Uplift was rapid through the PAZ as indicated by a high frequency of long mean lengths ($\geq$ 15 μm), narrow track-length distributions, and Dpar values between 1.85 and 2.07 μm (Figure 22a-e).

The HeFTy model of the samples from the northwest Talkeetna Mountains shows two episodes of increased uplift rate, the first at approximately 45 to 30 Ma and the second from around 10 Ma to present, with cooling rates of ~3.5°/Ma and ~6°/Ma, respectively (Figure 22a-e). This

indicates that the northwest Talkeetna Mountains experienced two major episodes of rapid cooling, suggesting uplift at these times.

5.1.2 Domain 2

Domain 2 is located in the eastern Talkeetna Mountains, where seismicity is absent (Figure 24). This domain also contains prominent barbed drainage patterns including the Susitna River barbed drainage and the eastern slope of the Talkeetna Mountains.

Geomorphic indices including the HI, AF, Vf, IRAT, and SL suggest that Domain 2 is tectonically inactive relative to the surrounding domains. The majority of the domain, with the exception of those areas located along the Susitna River, shows geomorphic evidence for mature to old age landscapes and broadly cut valley floors and lower classes (5-8) of relative active tectonics, all indicating the domain is the most tectonically inactive (Figures 16-19). Those drainage basins that do provide geomorphic evidence for neotectonic activity are located along the barbed drainage of the Susitna River, suggesting that the river is cutting through an area that is actively experiencing neotectonic activity, but this signature may not be reflected in the majority of the surrounding basins (Figures 16-19).

Of all the areas studied in the Talkeetna Mountains, this domain has had the least amount of detailed geologic mapping or thermochronology data. Therefore, any determined age of uplift for this study is based on the thermochronology work conducted in other domains.

5.1.3 Domain 3

Domain 3 is south of Domains 1 and 2 and consists of the majority of the northeast-trending Southern Dome (Figure 24). This domain has a distinct radial drainage pattern not seen elsewhere. Domain 3 is characterized by frequent deep earthquakes, strike-slip and thrust fault regimes at depths above 25 km, and a normal fault regime below 25 km (Figures 13 and 14). The orientation of maximum horizontal stress is approximately east to west, which is notably different from the orientation in Domain 1, suggesting that there is a structural boundary between these two domains that allows for partitioning of the direction of horizontal maximum stress.

Geomorphic indices revealed that the most neotectonically active area of Domain 3 was in drainage basins centrally located along the northeast-trending Southern Dome (Figures 16-19). Geomorphic indices show that the center of the Southern Dome contains more youthful landscapes, more deeply incised valleys, higher classes of relative tectonic activity (Classes 2-4) than surrounding drainage basins, suggesting that the center is experiencing more neotectonic activity. Drainage basins on the eastern half of Domain 3 show little evidence for neotectonic activity based on geomorphic indices that indicated that the area has mature to old age landscapes and broadly cut valley floors; however, prominent barbed drainage is occurring along the eastern edge (Figure 6). This suggests that the eastern half of Domain 3 may not be as neotectonically active relative to the central Southern Dome, but drainage patterns do provide evidence for uplift along the eastern edge.

Previous thermochronology studies in Domain 3 show that the southwestern area of the domain underwent exhumation from 15 to 20 Ma (Hoffman and Armstrong, 2005; Figure 11) while the central area was uplifted between 45 and 65 Ma (Twelker et al., 2015; Figure 11). These contrasting ages suggest differential uplift throughout this domain.

5.1.4 Domain 4

Domain 4 is the southernmost edge of the Talkeetna Mountains and includes the active Castle Mountain fault and fault splays (Figure 24). It contains the southernmost edge of the Southern Dome and is characterized by earthquake depths from 15 to 30 km, a strike-slip stress regime, and an average east to west orientation of maximum horizontal stress.

In Domain 4, geomorphic indices show that areas around the eastern Castle Mountain fault splays have more youthful landscapes than areas to the east and that the entire domain has deeply incised valleys and strong evidence of stream deflection or valley tilt in the southeastern direction (Figures 16-19). This evidence suggests that Domain 4 is moderately neotectonically active (Figure 19).

Domain 4 includes three (U-TH)/He data points from the Hoffman and Armstrong (2005) study (Figure 11). The interpreted cooling ages from the samples in this domain are 17 to 20 Ma.

5.2 Heterogeneous Deformation

I propose that deformation is being accommodated differently across the Talkeetna Mountains, with the scale and character of deformation changes correlating to changes in the dominant lithology and to regional tectonic influences by the Yakutat microplate. I also suggest that there is a strain partitioning structure (or structures) that aides in the separation of northwest-southeast oriented horizontal maximum stresses in the north from east-west oriented horizontal maximum stresses in the south. In the following discussion, I will support these interpretations based on the observations in the structural domains.

5.2.1 Change in Scale of Deformation

There are significant differences in the scale and frequency of mapped faults between the domains. Domain 1 has more evidence of faulting based on the higher abundance of linear drainages that are likely following fault surfaces. In contrast, Domain 3 is dominated by a single large antiformal structure, the Southern Dome. This difference in deformation between the two domains may be partially due to a difference in rock type. Domain 1 is dominantly composed of the sedimentary Kahiltna flysch, whereas Domains 3 and 4 are primarily composed of harder plutonic, volcanic, metamorphic, and metasedimentary rocks of the Wrangellia and Peninsular terranes. This change in lithology from weaker layered rocks in the north to harder, mechanically homogeneous rocks in the south results in more deformation by smaller-scale faulting and folding in the north and in larger structures like the Southern Dome antiform in the south.

Table 3. Domain characteristics in the Talkeetna Mountains. SHmax refers to horizontal maximum stress

Domain	Topographic Features	Drainage Patterns	Geomorphic Indices	Seismicity	SHmax Orientation	Dominant Fault Regime	AFT/AHe Data
1	Chunilna Plateau Northern Plateau Fog Lakes Lowlands NE and NNW trending lineation	NE linear drainage 	HI, AF, Vf, SL; tectonically active – moderately active IRAT class = 1-7	Average *M2* Majority at depths ≤ 15 km	NW-SE 	Strike-Slip Thrust	34.38 – 37.71 Ma *This study *Rapid uplift after 10 Ma
2		Major barbed drainage of Susitna River	IRAT class = 5-8	Lack of frequent seismicity	Not enough data	Not enough data	No data
3	NE trending Southern Dome	Radial drainage about NE drainage divide 	HI, AF, Vf, SL; moderately active IRAT class = 2-6	Abundant seismicity Average *M2* More frequent earthquakes from 15-30 km	E-W 	Strike-slip Thrust Normal	38.35, 60.38, 73.38 Ma *AHe, Hoffman, 2005 107 Ma *Twelker et al., 2015
4		Southern portion of radial drainage	HI, AF, Vf, SL; tectonically active – moderately active IRAT class = 2-4	Abundant seismicity Average *M2* More frequent earthquakes from 15-30 km	E-W 	Strike-Slip	16.36 – 20.46 Ma *AHe, Hoffman, 2005

5.2.2 Change in SHmax Orientation

The change in the orientation of maximum horizontal stress from northwest to southeast in Domain 1 to approximately east to west in Domains 3 and 4 suggests heterogeneous deformation. The change in the orientation of SHmax correlates with the southern edge of Domain 1 near the Chunilna Plateau, the Fog Lakes Lowlands and, approximately, with the trace of the Talkeetna thrust fault. I suggest that this abrupt change in SHmax orientation indicates the presence of a strain partitioning structure or structures between the northern Domain 1 and the southern domains.

Geophysical studies across this boundary indicate there is a deep vertical crustal break between oceanic Wrangellia terrane crust to the south and transitional Kahiltna basin crust to the north (Glen et al., 2007a; Figure 4). Rather than being expressed by a single structure at the surface, this crustal break correlates with a wide zone of deformation, including the Fog Lakes Lowland trapezoidal basin and bounding extensional faults (Glen et al., 2007a, 2007b; O'Neill et al., 2005, 2003). This may also be the cause of the clustered zones of shallow seismicity along the Chunilna Plateau and north of the Fog Lake Lowlands where deformation has exploited a zone of structural weakness above the crustal break.

This deep crustal break may also contribute to strain partitioning, resulting in the variations in SHmax between the northern and southern domains. Changes in stress orientations across large structures are predicted by fault models and observed in other areas around the world (Lin et al., 2010; Liu et al., 2014).

5.3 Timing and Causes of Uplift and Deformation

The uplift history of the Talkeetna Mountains is complex. The AFT ages determined in this study are remarkably consistent, but thermochronology studies from other areas of the Talkeetna Mountains indicate a wider range of uplift ages. However, two things can be said based on the data provided in this study: 1) isostatic rebound does not play a significant role in recent uplift, and 2) the Talkeetna Mountains have undergone two episodes of rapid uplift from 45 to 30 Ma and from 10 Ma to present (Figures 22a-e).

5.3.1 Effect of Glacial Isostasy

A conservative estimate of the amount of isostatic rebound experienced in the Talkeetna Mountains after glacial melting in the Late Wisconsin is approximately 0.32 km. According to the typical uplift curve, the initial rebound would have been extremely rapid with almost 40% of the uplift occurring within the first 2,000 years, with the remaining uplift taking place within 10,000 years (Andrews, 1967). The Last Glacial Maximum during the Late Wisconsin was about 21 to 25 thousand years ago. Consequently, isostatic rebound from deglaciation would be complete by now. This suggests that isostatic rebound due to glacial isostasy most likely does not play a significant role in uplift in the Talkeetna Mountains in the Late Neogene time.

However, there are still modern glaciers at the highest elevations of the Southern Dome. It is likely that the presence of these glaciers has aided in the local maintenance of high elevation atop the highest peaks in this area. However, the regional neotectonic uplift seen throughout the Talkeetna Mountains is too recent to be solely driven by isostatic rebound.

5.3.2 Tectonic Causes of Uplift and Deformation

With the effect of regional glacial isostasy eliminated, tectonics is the remaining candidate for regional uplift and neotectonic activity. Modeled AFT data collected for this study indicate that two periods of rapid uplift occurred in the Talkeetna Mountains: the first from 45 to 30 Ma, and the second from approximately 10 Ma to present (Figures 22a-e). These two periods correspond to distinct tectonic events in southern Alaska.

5.3.2.1 First Period of Rapid Uplift (45 to 30 Ma)

The first period of rapid uplift from 45 to 30 Ma, with an uplift rate of 0.14 mm/yr, coincided with significant plate reorganization that took place between 56 and 43 Ma and led to the start of a new tectonic environment in Alaska (Engebretson et al., 1984; Wallace et al., 1989). Plate reorganization resulted in the direction of the Pacific plate motion shifting from north-directed to northwestward-directed and a significant decrease in the convergence rate between the Pacific and North American plates (Engebretson et al., 1984). This shift in direction of the Pacific plate motion changed the western Canada and southeastern Alaska margin from primarily a convergent margin to a left-lateral transform margin, resulting in translation of terranes like the Wrangellia and Peninsular terranes northward along dextral fault systems (Trop and Ridgway, 2007; Wallace et al., 1989). The Wrangellia and Peninsular terranes were likely near or at their present locations by 45.5 to 36.8 Ma (Nokleberg et al., 1994; Trop et al., 2003).

These unroofing ages also correlate with the 40 Ma AFT age found by O'Sullivan and Currie (1996) in the Chugach-St. Elias Mountains and with one AFT age found by Haeussler (2008) of 36 Ma in the Tordrillo Mountains of the western Alaska Range. It would be premature to link

these ages by any interpretation, but for the area of the Talkeetna Mountains, this period of uplift may represent when the Wrangellia composite terrane settled into its present position in south-central Alaska in the Late Eocene (Nokleberg et al., 1985).

5.3.2.2 Second Period of Rapid Uplift (10 Ma to Present)

The second phase of rapid uplift in Neogene time occurred during the subduction and collision of the Yakutat microplate. Far-field deformation seen throughout south-central Alaska is a suggested consequence of the flat-slab subduction and collision of the Yakutat microplate (Haeussler, 2008; Table 1). I suggest that an additional consequence of the subduction and collision of the Yakutat microplate is the second period of rapid uplift from 10 Ma to present seen in the Talkeetna Mountains.

Deformation and uplift driven by the Yakutat microplate in the Talkeetna Mountains could be facilitated by three mechanisms: 1) underplating or coupling of the downgoing Yakutat flat-slab with the overlying plate; 2) northwest compression in the overlying plate driven by the collision of the Yakutat microplate; and/or 3) translation of the overlying crust through dextral fault systems driven by Yakutat collision. All of these mechanisms are ultimately driven by the subduction and/or collision of the Yakutat microplate.

The second period of uplift from around 10 Ma to present in the Talkeetna Mountains corresponds with the suggested location of the leading edge of flat-slab subduction of the Yakutat microplate beneath the Talkeetna Mountains at this time (Eberhart-Phillips et al., 2006; Figure 1). This correlation suggests that a major mechanism of uplift in Neogene time was the underplating of the buoyant Yakutat crust beneath the Talkeetna Mountains beginning

approximately 10 Ma. South of the Talkeetna and Chugach Mountains, elastic dislocation models provide evidence for coupling to the subducting Yakutat slab below Prince William Sound and indicate that the area is locked at the megathrust interface (Zweck et al., 2002). A cross section through the Talkeetna Mountains study area (Figure 4) shows that the crust beneath Domains 3 and 4 (velocities <7 km/sec) is located just above the downgoing Yakutat slab; however, the occurrence of earthquakes in both the overlying crust and the downgoing slab with an aseismic zone in between suggests that there is not significant plate coupling underlying the southern Talkeetna Mountains. In the same crustal scale cross section, it is also evident that the downgoing Yakutat slab is in no way coupled to the northern Talkeetna Mountains beneath Domain 1, as the angle of subduction has increased greatly, and a mantle wedge is observed in velocity models (Figure 4). Therefore, there is not sufficient evidence to propose coupling or underplating as the tectonic driver of deformation in the Talkeetna Mountains.

If the rocks of the Talkeetna Mountains are not coupled to the underlying downgoing slab, I suggest that crustal deformation is driven by northwest-directed compression in the upper plate, or by translation of the upper plate northwestward through dextral fault systems, which are both consequences of the collision and subduction of the Yakutat Microplate. Either mechanism would explain the heterogeneous deformation observed in the Talkeetna Mountains (Figure 24; Table 3).

The relationship between the upper crust and the downgoing slab is very different from north to south and correlates with the separate structural domains (Figure 4). Beneath Domains 3 and 4, the slab is at its shallowest depths in the study area, between 35 and 40 km, and is dipping approximately 10° to the north (Figure 4). In these southern domains, Shmax is oriented primarily east-west and structures are dominated by broad regional folding.

In contrast, beneath Domain 1, the angle of subduction changes to approximately 25 to 30°, and an asthenosphere wedge is present between the overlying and subducting crust (Figure 4). The location in which the change in subduction angle and presence of a mantle wedge occurs coincides with the southern boundary of Domain 1. In Domain 1, SHmax orientation changes to northwest-southeast, and structures are dominated by small scale folding and thrust faulting.

A tomographic cross section from southwest to northeast suggests that the interpreted northeastern edge of the Yakutat microplate coincides with the northeastern boundary of seismicity in the Talkeetna Mountains (D-D', Figure 4). This is also the western boundary of Domain 2. According to the tomographic cross section by Eberhart-Phillips et al. (2006), Domain 2 has a thicker crust (velocities < 7 km/sec) and is similar to the thickened crust underlying the Copper River basin to the east of the Talkeetna Mountains (Figure 4). This area of thickened crust, which is nearly 10 km thicker than the surrounding areas (Eberhart-Phillips et al., 2006), may be allowing the area of Domain 2 and the seismically inactive regions to the east of the Talkeetna Mountains to act as a rigid block that is resisting deformation.

Based on these observations, I suggest that changes in the character of the overlying plate and changes in dip of the subducting slab of the Yakutat microplate causes fundamental differences in deformation of the overlying crust. In the north, the Kahiltna basin in the upper plate is experiencing primarily north-directed folding and thrust-faulting while in the south, the Wrangellia/Peninsular Super Terrane is experiencing east-west compression and warping probably related to right-lateral translation of the upper plate. The Talkeetna thrust is a major crustal discontinuity that facilitates this change in deformational character, Deformation is driven by the actively-accreting Yakutat microplate.

5.4 The Susitna River: Geomorphic Evidence for Neotectonic Activity

The Susitna River is an area of interest that I have evaluated separately from the individual domains because it crosses more than one domain and reaches across the entire Talkeetna Mountains. The change in the morphology of the Susitna River from braided and wide northeast of the mountains to sinuous, incising, and narrow within the mountains and then back to braided and wide where it exits the mountains in the west suggests that the Talkeetna Mountains are actively uplifting (Figure 6). This interpretation is further supported by the longitudinal profile of the Susitna River. The convex curvature of this profile suggests that the Susitna River has not yet reached equilibrium, suggesting that it is flowing through an uplifting structure (Figure 21; Keller and Pinter, 2002).

The highest change in SL values occurs along the middle reaches of the Susitna River as it passes previously mapped faults and topographic lineation. These SL values correlate to observed knickpoints in the SL gradient profile of the river identified in Figures 20 and 21. The presence of knickpoints along the river and deep incision into the bedrocksmay result from active faulting in the Talkeetna Mountains.

The most prominent barbed drainage occurs along the Susitna River where flow direction abruptly changes from flowing southward to approximately west by 90° as the river begins to flow through the Talkeetna Mountains. This area correlates with the change in river morphology from wide to narrow, sinuous, and incising, with a change from low to high SL values, and with a change from U-shaped to V-shaped valley incision, as observed by Vf and valley profiles.

The geomorphology of the Susitna River suggests that it is an antecedent stream that predates the rise of the Talkeetna Mountains, and during uplift, the Upper Susitna migrated along its northern reaches toward the southeast, avoiding the growing edge of the mountain range while the middle

reaches of the river incised into the uplifting surface. It is possible that the Susitna River originally had a more direct route through the Talkeetna Mountains through the northeast-trending valley where Butte Creek is situated today (Figure 6). Butte Creek has a sharp barbed drainage where its flow direction changes from south to eastward where it connects to the present-day Upper Susitna River outside of the Talkeetna Mountains. The river may have originally connected to the proto-Upper Susitna as it was flowing south-southwest through this valley into the present-day Fog Lakes Lowlands. During uplift, the proto-Upper Susitna drainage may have been deflected to the southeast toward its present-day course as the Talkeetna Mountains were uplifting. This kind of river deflection is typically seen in response to an uplifting anticline (Keller and Pinter, 2002). The drainage pattern and frequency of barbed drainage along the eastern half of the Talkeetna Mountains and the uplifted longitudinal profile of the Susitna River are interpreted here as evidence that the Talkeetna Mountains are an actively uplifting antiform.

5.5 Sources of Uncertainty in this Analysis

The influence of lithological change could be considered a caveat to the type of geomorphic indices used in this study. However, in all quantitative geomorphic analyses (HI, AF, Vf, IRAT, SL) the distribution of values and classes of activity does not clearly correlate with the diverse lithology in the Talkeetna Mountains. Therefore, the clusters of high IRAT classes likely correspond to areas that are the most neotectonically active relative to the rest of the study area.

Knickpoints in longitudinal stream profiles can also be affected by lithology and sea level drops. As previously mentioned, the knickpoints observed along the Susitna River occur within

lithologic units rather than at contacts between units, suggesting that knickpoints are not caused by lithological change.

Changes in base level caused by climate or sea level change can also create knickpoints. However, in south-central Alaska the last major sea level change would have been due to deglaciation in the Pleistocene age, culminating around 11,000 years ago, and any knickpoints caused by this would have likely been adjusted by now and not visible in the longitudinal stream profiles. Therefore, the presence of knickpoints along the Susitna River can be likely attributed to fault-related activity.

Base level changes from rivers flowing to the Copper River basin versus the Susitna River basin may account for some of the difference in high versus low classes of relative tectonic activity observed from the western side of the Talkeetna Mountains to the eastern side (Figures 16, 18 and 19). The Copper River basin is topographically higher than the Susitna River basin, which presumably has experienced more tectonic subsidence over time. Therefore, rivers that flow into the Copper River basin have a higher base level and do not incise as greatly into the landscape as rivers flowing into the Susitna River basin. This difference in the amount of incision may be reflected in the division of Vf and HI values from east to west (Figures 16 and 18). The west side would have experienced more incision due to a lower base level, creating narrower V-shaped valleys with lower valley floor elevations relative to valley height, resulting in lower valley floor width-to-height ratio values. Lower Vf value would likely cause higher HI values, as there would be a greater incision in the landscape relative to mean elevation. The change in base level was not taken into account for the purposes of this study but could be further addressed in future studies.

CHAPTER 6: CONCLUSION

There is abundant geomorphic, structural, seismic, and thermochronologic evidence for neotectonic activity in the Talkeetna Mountains. This evidence includes areas of anomalous drainage patterns, high classifications of tectonic activity based on geomorphic indices, active seismicity, and rapid uplift rates in the Neogene period.

Geomorphic indices, such as the HI, basin AF, Vf, and SL gradient index, and anomalies like barbed drainages, incised valleys, knickpoints, and a change in the Susitna River morphology all suggest recent tectonic activity and uplift. Areas that are the most relatively active are the Chunilna Plateau, the center of the Southern Dome, and the drainage basins surrounding the Castle Mountain fault. Geomorphic evidence of active faulting also exists along the length of the Susitna River, most notably on the Chunilna Plateau and near the proposed site of the Susitna-Watana hydroelectric dam.

The Talkeetna Mountains can be divided into 4 different structural domains based on geomorphic indices, river morphology, seismicity, and SHmax orientations. Each domain accommodates deformation differently. Differences between Domain 1 and Domains 3 and 4 are in the scale and frequency of structures, drainage patterns, dominant fault types, and orientation of horizontal maximum stress. Domain 2 is characterized by the lack of noticeable seismicity.

The change of SHmax orientation from northwest-southeast in Domain 1 to east-west in Domains 3 and 4 implies the presence of a strain partitioning structure between Domain 1 and the southern domains. In this study, partitioning of SHmax orientation is suggested to be due to the Talkeetna thrust crustal break, exposed at the surface as a wide zone of deformation.

Thermochronology data from the Kahiltna basin suggest that the Talkeetna Mountains have undergone two distinct periods of uplift: one from 45 to 30 Ma and another from approximately 10 Ma to present, with uplift rates of 0.14 mm/yr and 0.24 mm/yr, respectively. The first phase of rapid uplift could be related to significant plate reorganization that took place between 56 and 43 Ma, leading to a new tectonic environment in Alaska, and northwestward translation of the Wrangellia and Peninsular terranes.

The second period of rapid uplift coincides with the continued subduction and collision of the Yakutat microplate. Deformation in the Talkeetna Mountains could be a result of underplating, or coupling, of the subducting slab, northwest compression from the south, or translation of the crust through dextral fault systems, which are all driven by the collision and subduction of the Yakutat microplate. However, I identified little evidence to support the idea of coupling in the Talkeetna Mountains; therefore, I suggest that the ultimate mechanism of deformation caused by collision and subduction of the Yakutat microplate is northwest compression in the northern Talkeetna Mountains, and northwestward translation/strike-slip in the southern Talkeetna Mountains between the Talkeetna Thrust fault and the Castle Mountain fault.

A hydroelectric dam has been proposed for the Susitna River, which is located, in part, above the Talkeetna Thrust Fault. This study suggests that the Talkeetna Thrust fault could be a major crustal boundary that is accommodating strain partitioning between the northern and southern Talkeetna Mountains. I suggest that this structure should be further studied in order to confirm or disprove this hypothesis.

REFERENCES

Acres, 1982. Susitna Hydroelectric Project Feasibility Report. Prep. Alaska Power Auth.

American Energy Authority, 2015. Susitna-Watana Hydroelectric Project Site-Specific Hazard Study Summary Report. Prep. Fed. Energy Regul. Commision by Alaska Energy Authority, Anchorage, Alaska.

Andrews, J.T., 1967. Postglacial rebound in Arctic Canada: similarity and prediction of uplift curves. Can. J. Earth Sci. 5, 39–47. doi:10.1139/e68-004

Armstrong, P.A., Haeussler, P.J., Arkle, J.C., 2007. Rapid Quaternary exhumation of the Eastern Alaska Range, Geol. Soc. Am. Abstr. Programs, 39(4), 71.

Bemis, S.P., Wallace, W.K., 2007. Neotectonic framework of the north-central Alaska Range foothills, *in* Tectonic Growth of a Collisional Continental Margin: Crustal Evolution of Southern Alaska, Geol. Soc. Am. Spec. Pap. vol 431, edited by K.D. Ridgway et al., p 549–572. doi:10.1130/2007.2431

Benowitz, J.A., Fowell, S.J., Addison, J., Layer, P., 2007. Tectonic and paleoclimatic significance of early Pliocene palynofloras from the southeastern Alaska Range, Geol. Soc. Am. Abstr. Programs, 39(4), paper 29-7.

Brocher, T.M., Fuis, G.S., Fisher, M.A., Plafker, G., Moses, J., Survey, U.S.G., Park, M., Taber, J.J., Christensen, N.I., 1994. Mapping the megathrust beneath the northern Gulf of Alaska using wide-angle seismic data, J. Geophys. Res., 99, 11,663-11,685.

Bruhn, R.L., Pavlis, T.L., Plafker, G., Serpa, L., 2004. Deformation during terrane accretion in the Saint Elias orogen, Alaska, Geol. Soc. Am. Bull., 116, 771–787. doi:10.1130/B25182.1

Chapman, J.B., Pavlis, T.L., Gulick, S., Berger, A., Lowe, L., Spotila, J., Bruhn, R., Vorkink, M., Koons, P., Barker, A., Picornell, C., Ridgway, K., Hallet, B., Jaeger, J., McCalpin, J., 2008. Neotectonics of the Yakutat Collision: Changes in Deformation Driven by Mass Redistribution. Act. Tectonics Seism. Potential Alaska 65–81. doi:10.1029/179GM04

Coney, P.J., Jones, D.L., Monger, W.H., 1980. Cordilleran suspect terranes. Nat. Geosci.

Csejtey, B., Nelson, W.H., Jones, D.L., Siberling, N.J., Dean, R.M., Morris, M.S., Lanphere, M.A., Smith, J.G., Silberman, M.L., 1978. Reconnaissance geologic map and geochronology, Talkeetna Mountains Quadrangle, northern part of Anchorage Quadrangle, and southwest corner of Healy Quadrangle, Alaska. PhD Propos. doi:10.1017/CBO9781107415324.004

Csejtey, B.B., 1982. Discrepancies Between Geologic Evidence and Rotational Models-Tal keetna Mountains and Adjacent Areas of South-Central Alaska. Geol. Stud. Alaska by U.S. Geol. Surv. 1990 71–80.

Curran, C.A., Magirl, C.S., Duda, J.J., 2014. Suspended-Sediment Concentrations during Dam Decommissioning in the Elwha River, Washington: U. S. Geolgoical Survey Data Set. doi:10.5066/F7M043DB

Detterman, R.L., Case, J.E., Miller, J.W., Wilson, F.H., Yount, M.E., 1996. Stratigraphic framework of the Alaska Peinsula: U.S. Geologic Survey Bulletin 1969-A, 74 p.

Detterman, R.L., Plafker, G., Hudson, T., Tysdal, R.G., Pavoni, N., 1974. Surface geology and Holocene braks along the Susitna segment of the Castle Mountain fault, Alaska: U.S. Geological Survey Map MF-618, scale 1:24,000.

Donelick, R.A., O'Sullivan, P.B., Ketcham, R.A., 2005. Apatite Fission-Track Analysis. Rev. Mineral. Geochemistry 58, 49–94. doi:10.2138/rmg.2005.58.3

Eberhart-Phillips, D., Christensen, D.H., Brocher, T.M., Hansen, R., Ruppert, N.A., Haeussler, P.J., Abers, G.A., 2006. Imaging the transition from Aleutian subduction to Yakutat collision in central Alaska, with local earthquakes and active source data. J. Geophys. Res. Solid Earth 111, 1–31. doi:10.1029/2005JB004240

El Hamdouni, R., Irigaray, C., Fernández, T., Chacón, J., Keller, E.A., 2008. Assessment of relative active tectonics, southwest border of the Sierra Nevada (southern Spain). Geomorphology 96, 150–173. doi:10.1016/j.geomorph.2007.08.004

Elliott, J., 2011. Active Tectonics in Southern Alaska and the Role of the Yakutat Block Constrained by GPS Measurements.

Engebretson, D.C., Cox, A., Gordon, R.G., 1984. Relative motions between oceanic plates of the Pacific Basin. J. Geophys. Res. Solid Earth 89, 10291–10310. doi:10.1029/JB089iB12p10291

Ferris, A., Abers, G.A., Christensen, D.H., Veenstra, E., 2003. High resolution image of the subducted Pacific (?) plate beneath central Alaska, 50-150 km depth. Earth Planet. Sci. Lett. 214, 575–588. doi:10.1016/S0012-821X(03)00403-5

Finzel, E.S., Trop, J.M., Ridgway, K.D., Enkelmann, E., 2011. Upper plate proxies for flat-slab subduction processes in southern Alaska. Earth Planet. Sci. Lett. 303, 348–360. doi:10.1016/j.epsl.2011.01.014

Fitzgerald, P.G., Sorkhabi, R.B., Redfield, T.F., Stump, E., 1995. Uplift and denudation of the central Alaska Range: A case study in the use of apatite fission track thermochronology to determine absolute uplift parameters. J. Geophys. Res. 100, 20175. doi:10.1029/95JB02150

Fletcher, H.J., 2002. Crustal deformation in Alaska measured using the Global Positioning System, Ph.D. thesis, 135 pp., University of Alaska Fairbanks.

Freymueller, J.T., Woodard, H., Cohen, S.C., Cross, R., Elliott, J., Larsen, C.F., Hreinsdóttir, S., Zweck, C., 2008. Active Deformation Processes in Alaska, Based on 15 Years of GPS Measurements. Act. Tectonics Seism. Potential Alaska 1–42. doi:10.1029/179GM02

Fuis, G.S., Moore, T.E., Plafker, G., Brocher, T.M., Fisher, M.A., Mooney, W.D., Nokleberg, W.J., Page, R.A., Beaudoin, B.C., Christensen, N.I., Levander, A.R., Lutter, W.J., Saltus, R.W., Ruppert, N.A., 2008. Trans-Alaska Crustal Transect and continental evolution involving subduction underplating and synchronous foreland thrusting. Geology 36, 267–270. doi:10.1130/G24257A.1

Glen, J.M.G., 2004. A kinematic model for the southern Alaska orocline based on regional fault patterns, *in* Orogenic Curvature: Integrating Paleomagnetic and Structural Analysis, Geol. Soc. Am. Spec. Pap., 383, 161–172. doi:10.1130/0-8137-2383-3(2004)383[161:AKMFTS]2.0.CO

Glen, J.M.G., Morin, R., Schmidt, J., 2007a. Gravity and magnetic character of south-central Alaska : Constraints on geologic and tectonic interpretations , and implications for mineral exploration. Geol. Soc. Am. Spec. Pap. 431, 593–622. doi:10.1130/2007.2431(23).

Glen, J.M.G., Schmidt, J., Pellerin, L., McPhee, D.K., O'Neill, J.M., 2007b. Crustal structure of Wrangellia and adjacent terranes inferred from geophysical studies along a transect through the northern Talkeetna Mountains. Geol. Soc. Am. Spec. Pap. 431, 21–41. doi:10.1130/2007.2431

Grantz, A., Jones, D.L., Lanphere, M.A., 1966. Stratigraphy, paleontology, and isotopic ages of Upper Mesozoic rocks in teh southwestern Wrangell Mountains, Alaska: U.S. Geological Survey Professional Paper 550-C 39–47.

Green, P., Duddy, I., Gleadow, A.J., Tingate, P., Laslett, G., 1986. Thermal annealing of fission tracks in apatite. Chem. Geol. Isot. Geosci. Sect. 59, 237–253. doi:10.1016/0168-9622(86)90074-6

Gutscher, M.-A., Peacock, S.M., 2009. Thermal models of flat subduction and the rupture zone of great subduction earthquakes. J. Geophys. Res. 108, 1–16. doi:10.1029/2001JB000787

Hack, J.T., 1973. Stream-profile analysis and stream-gradient index. J. Res. U.S. Geol. Surv. 1, 9.

Haeussler, P.J., 2008. An Overview of the Neotectonics of Interior Alaska : Far-Field Deformation From the Yakutat Microplate Collision. Act. Tectonics Seism. Potential Alaska 83-108.

Haeussler, P.J., O'Sullivan, P., Berger, A.L., Spotila, J.A., 2008. Neogene Exhumation of the Tordrillo Mountains, Alaska, and Correlations With Denali (Mount Mckinley). Act. Tectonics Seism. Potential Alaska 269–285. doi:10.1029/179GM15

Hampton, B.A., Ridgway, K.D., Gehrels, G.E., 2010. A detrital record of Mesozoic island arc accretion and exhumation in the North American Cordillera: U-Pb geochronology of the Kahiltna basin, southern Alaska. Tectonics 29, 1–21. doi:10.1029/2009TC002544

Hampton, B.A., Ridgway, K.D., Gehrels, G.E., Schmidt, J., Blodgett, R.B., 2007. Pre- , syn- , and postcollisional stratigraphic framework and provenance of Upper Triassic-Upper Cretaceous strata in the northwestern Talkeetna Mountains , Alaska. Geol. Soc. Am. Spec. Pap. 431, 401–438. doi:10.1130/2007.2431(16).

Hoffman, M.D., Armstrong, P.A., 2005. Miocene exhumation of the southern Talkeetna Mountains, south central Alaska, based on apatite (U/Th)/He thermochronology. Geol. Soc. Am. Abstr. with Programs, 38(5), 9.

Jacques, P.D., Salvador, E.D., Machado, R., Grohmann, C.H., Nummer, A.R., 2014. Application of morphometry in neotectonic studies at the eastern edge of the Paraná Basin, Santa Catarina State, Brazil. Geomorphology 213, 13–23. doi:10.1016/j.geomorph.2013.12.037

Keller, E.A., Pinter, N., 2002. Active Tectonics, 2nd ed. Prentice-Hall, Inc, Upper Saddle River, New Jersey.

Ketcham, R. A., 2005. Forward and Inverse Modeling of Low-Temperature Thermochronometry Data. Rev. Mineral. Geochemistry 58, 275–314. doi:10.2138/rmg.2005.58.11

Ketcham, R.A., Donelick, R.A., Donelick, M.B., 1999. AFTSolve: A program for multi-kinetic modeling of apatite fission-track data. Am. Mineral. 88, 929.

Laslett, G.M., Green, P.F., Duddy, I.R., Gleadow, A.J.W., 1987. Thermal annealing of fission tracks in apatite 2. A quantitative analysis. Chem. Geol. Isot. Geosci. Sect. 65, 1–13. doi:10.1016/0168-9622(87)90057-1

Lin, W., Yeh, E.C., Hung, J.H., Haimson, B., Hirono, T., 2010. Localized rotation of principal stress around faults and fractures determined from borehole breakouts in hole B of the Taiwan Chelungpu-fault Drilling Project (TCDP). Tectonophysics 482, 82–91. doi:10.1016/j.tecto.2009.06.020

Liu, Q.Y., Hilst, R.D. Van Der, Li, Y., Yao, H.J., Chen, J.H., Guo, B., Qi, S.H., 2014. Eastward expansion of the Tibetan Plateau by crustal flow and strain partitioning across faults. Nat. Geosci. 7, 361–366. doi:10.1038/NGEO2130

Mahmood, S.A., Gloaguen, R., 2012. Appraisal of active tectonics in Hindu Kush: Insights from DEM derived geomorphic indices and drainage analysis. Geosci. Front. 3, 407–428. doi:10.1016/j.gsf.2011.12.002

Manley, W.F., Kaufman, D.S., 2002. Alaska PaleoGlacier Atlas: Institute of Arctic and Alpine Research (INSTAAR), University of Colorado.

Matmon, A., Schwartz, D.P., Haeussler, P.J., Finkel, R., Lienkaemper, J.J., Stenner, H.D., Dawson, T., 2006. Denali fault slip rates and Holocene–late Pleistocene kinematics of central Alaska. Geology 34, 645. doi:10.1130/G22361.1

Middleton, G.V., Wilcock, P.R., 1994. Mechanics in Earth and Environmental Sciences. Cambridge University Press, Cambridge.

Monger, W.H., Nokleberg, W.J., 1996. Evolution of the northern North American Cordillera; generation, fragmentation, displacement and accretion of successive North American plate-margin arcs. Geol. ore Depos. Am. Cordillera.

Naeser, C.W., 1976. Fission track dating. US Geol. Surv. Open-File Rep. 76-190.

Nokleberg, W.J., Jones, D.L., Silberling, N.J., 1985. Origin and tectonic evolution of the Maclaren and Wrangellia terranes, eastern Alaska Range, Alaska.

Nokleberg, W.J., Plafker, G., Wilson, F.H., 1994. Geology of south-central Alaska.

Nye, J.F., 1952. The mechanics of a glacier flow. J. Glaciol. 2, 52–23. doi:10.3189/2015JoG15J164

O'Neill, J.M., Ridgway, K.D., Eastham, K.R., 2003. Mesozoic and Tertiary structural history of the northern Talkeetna Mountains. in Galloweay, J.P., ed., Studies by the U.S. Geological Survey in Alaska, 2001: U.S. Geol. Surv. Prof. Pap., 1678, 83-92.

O'Neill, J.M., Schmidt, J.M., Cole, R.B., 2005. Cenozoic intraplate tectonics - lithospheric right-lateral bulk shear deformation in the northern Talkeetna Mountains, south-central Alaska. Geo. Soc. Am. Abs. Prog., 37(7), 79.

O'Sullivan, P.B., Currie, L.D., 1996. Thermotectonic history of Mt Logan, Yukon Territory, Canada: implications of multiple episodes of middle to late Cenozoic denudation. Earth Planet. Sci. Lett. 144, 251–261. doi:10.1016/0012-821X(96)00161-6

Plafker, G., 1987. Regional geology and petroleum potential of the northern Gulf of Alaska continental margin. Earth Sci. Ser. 6, 229–268.

Plafker, G., Berg, H.C., 1994. Overview of the geology and tectonic evolution of Alaska, 1068 p.

Plafker, G., Moore, J.C., Winkler, G.R., 1994. Geology of the southern Alaska margin, The Geology of Alaska, The Geology of North America, vol. G-1, plate 12, edited by G. Plafker, and H.C. Berg, pp. 989–1082, GSA, Boulder, Colo.

Plafker, G., Naeser, C.W., Zimmermann, R.A., Lull, J.S., Hudson, T., 1992. Cenozoic uplift history of the Mount McKinley area in the central Alaska Range based on fission-track dating, *in* U.S. Geol. Surv. Bull. 2041:202-2.

Poulos, M.J., Pierce, J.L., Flores, A.N., Benner, S.G., 2012. Hillslope asymmetry maps reveal widespread, multi-scale organization. Geophys. Res. Lett. 39, n/a–n/a. doi:10.1029/2012GL051283

Richter, D.H., Smith, J.G., Lanphere, M.A., Dalrymple, G.B., Reed, B.L., Shew, N., 1990. Age and progression of volcanism, Wrangell volcanic field, Alaska. Bullet. Volcanol. 29–44.

Ridgway, K.D., Flesch, L.M., 2007. Cenozoic tectonic processes along the southern Alaska convergent margin. Geology 35, 1055. doi:10.1130/focus112007.1

Ridgway, K.D., Skulski, T., Sweet, A.R., 1996. Cenozoic strike-slip tectonics along the Duke River fault, St. Elias Mountains: Intracontinental transform fault response to terrane accretion. Geol. Soc. Am. Abstr. with Programs 28, 313.

Schumm, S.A., Dumont, J.F., Holbrook, J.M., 2000. Active tectonics and alluvial rivers: Cambridge, Cambridge University Press, 276 p.

Silva, P.G., Goy, J.L., Zazo, C., Bardaji, T., 2003. Faulth-generated mountain fronts in southeast Spain: Geomorphologic assessment of tectonic and seismic activity. Geomorphology 50, 203–225. doi:10.1016/S0169-555X(02)00215-5

Strahler, A.N., 1952. Hypsometric (Area - Altitude) Analysis of Erosional Topography. Geol. Soc. Am. Bull. 63, 1117–1142. doi:10.1130/0016-7606(1952)63

Trop, J.M., Ridgway, K.D., 2007. Mesozoic and Cenozoic tectonic growth of southern Alaska : A sedimentary basin perspective. Tecton. growth a collisional Cont. margin Crustal Evol. south-central Alaska 431, 55–94. doi:10.1130/2007.2431(04).

Trop, J.M., Ridgway, K.D., Spell, T.L., 2003. Sedimentary record of transpressional tectonics and ridge subduction in the Tertiary Matanuska Valley - Talkeetna Mountains forearc basin, southern Alaska 89–118.

Twelker, E., Hubbard, T.D., Wypych, A., Sicard, K.R., Newberry, R.J., Reioux, D.A., Freeman, L.K., Lande, L.L., 2015. Geologic map of the Talkeetna Mountains C-4 Quadrangle and adjoining areas, central Alaska. doi:10.14509/29470

Wallace, W.K., Hanks, C.L., Rogers, J.F., 1989. The southern Kahiltna terrane: Implications for the tectonic evolution of southwestern Alaska. Geol. Soc. Am. Bull. 101, 1389–1407.

Wells, D.L., Coppersmith, K.J., 1994. New Empirical Relationships among Magnitude, Rupture Length, Rupture Width, Rupture Area, and Surface Displacement. Bull. Seismol. Soc. Am. 84, 974–1002. doi:

Willis, J.B., Bruhn, R.L., 2006. Active tectonics of the Susitna River basin, Alaska - intraplate deformation drivenby microplate collision and subduction. Geol. Soc. Am. Abstr. with Programs 38, 96.

Willis, J.B., Haeussler, P.J., Bruhn, R.L., Willis, G.C., 2007. Holocene Slip Rate for the Western Segment of the Castle Mountain Fault, Alaska. Bull. Seismol. Soc. Am. 97, 1019–1024. doi:10.1785/0120060109

Zweck, C., Freymueller, J.T., Cohen, S.C., 2002. Three-dimensional elastic dislocation modeling of the postseismic response to the 1964 Alaska earthquake. J. Geophys. Res. Solid Earth 107, ECV 1–1–ECV 1–11. doi:10.1029/2001JB000409

Appendix A

Apatite fission-track age data table

Sample Name	DCM01TM	DCM02TM	DCM03TM	DCM05TM	DCM06TM
GeoSeps Sample Name	032-01	032-02	032-03	032-04	032-05
Pooled age (Ma)	34.38	35.28	36.71	37.71	55.35
95%-CI (Ma)	4.6	6.77	5.82	4.25	4.73
95%+CI (Ma)	5.3	8.37	6.92	4.79	5.17
wmean pz:sz UCa	0.836	0.8404	0.8453	0.8539	0.8627
wmean pz:unk Ca	1.0182	1.0182	1.0181	1.0181	1.0181
relerr pz:sz	0.0182	0.0182	0.0182	0.0182	0.0182
relerr analyst	0	0	0	0	0
relerr deficit	1	1	1	1	0.898
relerr Ca apfu	0	0	0	0	0
Primary Zeta	12.357	12.357	12.357	12.357	12.357
+/- 1 sigma	0.2251	0.2251	0.2251	0.2251	0.2251
Number of Spots	36	38	39	27	37
Number of Tracks	282	109	191	309	617
Rho	0.000101	0.0000381	0.0000641	0.000101	0.000137
+/- 1 sigma	0.00000364	0.00000165	0.00000282	0.000000525	0.00000106
Cation Isotope	43Ca	43Ca	43Ca	43Ca	43Ca
chi-squared	2093.3066	1235.4199	594.8626	1823.339	734.0925
Q(chi-squared)	0	0	0	0	0
Mean Dpar (um)	2.14	2.16	2.11	2.05	2.07
Mean Dper (um)	0.46	0.48	0.45	0.46	0.46
Mean [U] (ppm)	33.98	16.11	24.41	95.95	105.35
Mean [Th] (ppm)	49.53	52.23	99.42	51.83	68.74
Mean [Sm] (ppm)	294.94	231.44	168.02	229.53	214.17

Appendix B

Apatite fission-track length data table

Sample Name	DCM01TM	DCM02TM	DCM03TM	DCM05TM	DCM06TM
GeoSeps Sample Name	032-01	032-02	032-03	032-04	032-05
Mean (um)	12.58	13.14	12.61	12.13	13.37
Std. error (um)	0.16	0.22	0.16	0.28	0.15
Std. dev (um)	1.75	1.62	1.74	2.02	1.64
Skewness	-0.0147	-0.356	-0.8972	-0.5087	-0.8658
Kurtosis	-0.5706	-0.377	1.0445	0.3484	1.5568
Number tracks	117	57	114	55	128
Mean Dpar (um)	1.92	1.85	2.02	1.99	2.03
Mean Dper (um)	0.39	0.38	0.39	0.37	0.43
Mean [U] (ppm)	1.96	2	3.42	18.09	101.5
Mean [Th] (ppm)	7.63	9.24	18.75	5.25	700.88
Mean [Sm] (ppm)	58.1	280.01	69.18	319.84	335.2